

Surprisal Driven k -NN for Robust and Interpretable Nonparametric Learning

Amartya Banerjee¹ Christopher J. Hazard² Jacob Beel² Cade Mack² Jack Xia² Michael Resnick²
Will Goddin²

Abstract

Nonparametric learning is a fundamental concept in machine learning that aims to capture complex patterns and relationships in data without making strong assumptions about the underlying data distribution. Owing to simplicity and familiarity, one of the most well-known algorithms under this paradigm is the k -nearest neighbors (k -NN) algorithm. Driven by the usage of machine learning in safety-critical applications, in this work, we shed new light on the traditional nearest neighbors algorithm from the perspective of information theory and propose a robust and interpretable framework for tasks such as classification, regression, density estimation, and anomaly detection using a single model. We can determine data point weights as well as feature contributions by calculating the conditional entropy for adding a feature without the need for explicit model training. This allows us to compute feature contributions by providing detailed data point influence weights with perfect attribution and can be used to query counterfactuals. Instead of using a traditional distance measure which needs to be scaled and contextualized, we use a novel formulation of *surprisal* (amount of information required to explain the difference between the observed and expected result). Finally, our work showcases the architecture’s versatility by achieving state-of-the-art results in classification and anomaly detection, while also attaining competitive results for regression across a statistically significant number of datasets.

1. Introduction

Nonparametric methods, such as k -Nearest Neighbors (k -NN), have been studied and applied in various domains of statistics and machine learning. Unlike parametric models,

nonparametric methods do not rely on a fixed number of parameters or make strict distributional assumptions about the underlying data. This allows for algorithms to flexibly adapt to different types of data and capture intricate structures. First proposed by (Fix & Hodges, 1951), and (Cover & Hart, 1967), k -NN has seen several modifications and evolutions over the past decades (Aha et al., 1991; Wang et al., 2009; Hastie et al., 2009; Alpaydin, 1999). Despite these advancements, k -NN still has some disadvantages. For example, the curse of dimensionality (Hastie et al., 2009; Indyk & Motwani, 1998; Schuh et al., 2013; Tao et al., 2009), the selection of a distance metric (Prasath et al., 2017), and imbalanced datasets (He & Garcia, 2009) all present significant challenges to k -NN.

In this work, we propose methods to enhance k -NN to address these issues, derive new concepts driven by entropy, and then demonstrate the performance of this enhanced k -NN on various applications. Using our methodology, we are able to improve the performance of k -NN while retaining its natural interpretability. Additionally, these improvements allow us to understand the importance of features and weigh them accordingly in the model’s decision making, thereby improving interpretability further. First, we derive the Łukaszyk–Karmowski (LK) distance (Łukaszyk, 2003; 2004) for Laplace distributions to prevent distances of zero based on uncertainty. To our knowledge, this is the first published derivation of that result. Second, we show how Inverse Residual Weighting (IRW) can be used to move our distance measurements into surprisal space. Then, we introduce the concept of *conviction*: a ratio of expected surprisal to observed surprisal. This is further broken down into *familiarity conviction*, *similarity conviction*, and *residual conviction*. Finally, we show how these methods and concepts can be used to achieve near or above state-of-the-art results on classification, regression, and anomaly detection tasks.

2. Related Work

In recent years, k -NN based methods have grown in popularity in Natural Language Processing (NLP) and Computer Vision (CV). In NLP, variants of k -NN have been used on machine translation tasks (Khandelwal et al., 2021), (Jiang

¹Department of Computer Science, UNC-Chapel Hill, NC, USA ²Howso Incorporated. Correspondence to: Howso Incorporated <info@howso.com>.

et al., 2022), (Meng et al., 2022). In (Khandelwal et al., 2021), the authors propose carrying out translation using a large database of pre-translated sentences or phrases as a reference, and during translation, the system searches for the most similar sentences in the database as the translation output. (Meng et al., 2022) built on top of this work by proposing an efficient indexing scheme to organize the reference database, enabling faster search and retrieval of the nearest neighbors. This indexing scheme reduces the computational complexity of the translation process and improves overall efficiency. Another line of work that has gained attention in the recent past focuses on low resource text classification using k -NN on compressed text data (Jiang et al., 2023). Other methods use k -NN as an auxiliary model on intermediate representations of neural networks for filtering samples. (Bahri et al., 2020) proposed a version of the k -NN algorithm called Deep k -NN. This algorithm incorporates the principles of k -NN into deep learning architectures, specifically convolutional neural networks (CNNs), to effectively handle noisy labels. The work (Papernot & McDaniel, 2018) proposes a new layer, referred to as the confidence layer, which captures the confidence of the network’s predictions. This layer measures the agreement of the predictions of the deep neural network based on the k nearest neighbors to detect nonconformal, out-of-distribution instances. (Papernot & McDaniel, 2018) highlights the need for interpretable deep learning models, especially in domains where model transparency, explainability, and robustness are critical. Beyond the popularity in CV and NLP, k -NN continues to be a favored approach for classification and regression tasks in tabular and categorical datasets.

2.1. Anomaly Detection

Anomaly detection, also known as outlier detection, is a field in data analysis and machine learning that focuses on identifying instances that deviate significantly from the expected behavior of a given dataset. In recent years, the utilization of anomaly detection techniques has expanded across a diverse range of domains. These methods have found application in detecting fraudulent activities within credit cards, insurance, and healthcare sectors, as well as identifying intrusions in cyber-security, pinpointing faults in safety-critical systems, etc. Some of the well known methods for anomaly detection for tabular data include (Liu et al., 2008; Li et al., 2022; He et al., 2003; Li et al., 2003; Breunig et al., 2000) and (Ruff et al., 2018). Traditional methods like Isolation Forests randomly select features and split points to recursively partition data points into subsets, marking path lengths that effectively ‘isolate’ a datapoint as anomalies. This approach is an ensemble method. Isolation Forests assume that anomalies are sparse and can be isolated easily. If the dataset contains clusters of anomalies that are not well-separated from normal instances, the

algorithm’s performance may suffer. There are probabilistic methods such as ECOD (Unsupervised Outlier Detection Using Empirical Cumulative Distribution Functions) uses empirical distribution functions to sort the data points and assigns probabilities based on their order. CBLOF (Clustering-Based Local Outlier Factor) assesses the local density deviation of a data point with respect to its neighbors to identify outliers and is a proximity based outlier detection method. While ECOD performs well with unimodal distribution data, it is sensitive to feature dimension noise and may encounter difficulties in accurately identifying outliers in datasets with multiple modes. Additionally, it may face challenges in high-dimensional scenarios, as it focuses on one-dimensional projections. CBLOF on the other hand focuses on local clusters, potentially missing the global context of the dataset. It necessitates a priori specification of the cluster number, posing a challenge. Unevenly sized clusters may impede its ability to distinguish between normal and outlier instances, particularly within smaller clusters. Recently there have been deep learning based approaches such as DeepSVDD which projects high-dimensional data into a latent space using an autoencoder architecture. Anomalies are detected by measuring the distance of data points to the center of a constructed hypersphere in the latent space, employing a threshold to flag anomalous cases based on this distance. These methods relying on training deep neural networks may exhibit sensitivity to noisy labels when mislabeled instances are present in the training data. This sensitivity can have adverse effects on the model’s generalization and its accuracy in detecting outliers. Additionally, these approaches often lack interpretability, making it challenging to understand the rationale behind classifying certain instances as outliers. Furthermore, their performance is often contingent on the careful tuning of hyperparameters within the neural network.

3. Methods

In this section, we introduce the methods through which we enhance k -NN, incorporating a novel distance measure and a feature weighting approach, enabling the utilization of innovative techniques and contributing to enhanced performance. Through the application of these methods to an instance-based k -NN base, we leverage the inherent interpretability of the architecture, augmenting it with the following methods and concepts. For instance, using the formulae that are to be provided, each decision that a model makes can be traced to the individual cases that influenced it. Additionally, the concepts that are introduced are human oriented in terms of both the simplicity of the math involved and the relationship of the various measures to the model itself.

3.1. Distance Metric

Like many other approaches to k -NN, we use Minkowski distance as a starting point

$$d_p(x, y) = \sqrt[p]{\sum_{i \in \Xi} w_i |x_i - y_i|^p}, \quad (1)$$

where p is the parameter for the Lebesgue space, Ξ is the feature set, and w_i is the weight for each feature. One problem with this distance metric, however, is that distinguishing points becomes more and more difficult in higher dimensions. One proposed solution is to use a fractional norm heading towards zero to enable points to be distinguished more easily in high dimensional space (Aggarwal et al., 2001). Motivated by this, we derived the Minkowski distance as $p \rightarrow 0$ expressed over the feature set Ξ

$$\lim_{p \rightarrow 0} d_p(x, y) = \sqrt[\|\Xi\|]{\prod_{i \in \Xi} |x_i - y_i|^{w_i}}, \quad (2)$$

assuming that the weights w sum to 1.

The above is a geometric mean, which has the useful property of being scale invariant. This derivation presents a problem, however. If any of the differences are zero, the entire distance metric will become zero. In order to solve this problem, we use the Łukaszyk–Karmowski metric as a distance term rather than absolute error. Given two random variables X and Y with probability density functions $f(x)$ and $g(x)$ respectively, the LK metric is defined as

$$d_{LK}(X, Y) = \int_{-\infty}^{\infty} \int_{-\infty}^{\infty} |x - y| f(x) g(y) dx dy. \quad (3)$$

We assume that if both points (say x and y) are near enough to be worth determining the distance between them, then the distributions and parameters for the probability density functions should represent the local data. The two simple maximum entropy distributions on $(-\infty, \infty)$ given a point and a distance around the point are the Laplace distribution (double exponential), where the distance is represented as mean absolute error (MAE), and the Gaussian distribution (normal), where the distance is represented as the standard deviation. We choose the Laplace distribution and derive a closed-form solution of equation 3 for it. Letting $\mu \equiv |x - y|$ and with b being the expected deviation,

$$d_{LK}(\mu, b) = \mu + \frac{1}{2} e^{-\frac{\mu}{b}} (3b + \mu), \quad (4)$$

the full derivation of which can be found in the appendix.

In order to employ this measure for our method, we need a value for b . Measurement error may not always be readily available, and it does not take into account the additional error among the relationships within the model. Hence, residuals are calculated for each prediction. The MAE is be calculated for each observation using a leave-one-out approach, where instances are removed from the model and each of the held out instance's features are predicted using the rest of the data. (The idea is to quantify the uncertainty in the model). These errors can be locally aggregated or can be aggregated across the entire model to obtain the expected residual, r , for predicting each feature, i , as r_i . This results in a Minkowski distance metric which uses the derived distance term of

$$\begin{cases} d_0(x, y) = \sqrt[\|\Xi\|]{\prod_{i \in \Xi} d_{LK}(|x_i - y_i|, r_i)^{w_i}}, & \text{for } p = 0 \\ d_p(x, y) = \sqrt[p]{\sum_{i \in \Xi} w_i d_{LK}(|x_i - y_i|, r_i)^p}, & \text{otherwise.} \end{cases} \quad (5)$$

We have found that using the residuals in the k -NN system with the above distance metric, calculating new residuals, and then feeding these back in, generally yields convergence of the residual values with notable convergence after only 3 or 4 iterations. Measuring a distance value for each feature further enables parameterization regarding the type of data a feature holds. For example, nominal data can result in a distance of 1 if the values are not equal and 0 if they are equal. Thus, one-hot encoding, the expansion of nominal values into multiple features, is not needed. Ordinal data can use a distance of 1 between each ordinal type.

3.2. Inverse Residual Weighting

Having established a distance metric, we can determine distances between points, but the units of measurement and scales of each feature may be entirely different. We propose Inverse Residual Weighting (IRW), a maximum entropy method of transforming these each feature difference into surprisal space so that the entire distance itself becomes expected surprisal.

Using our assumption that absolute prediction residuals follow the exponential distribution where the mean value is the feature residual, we can describe the probability a single prediction residual, v , being within the feature residual, r as

$$P(v \leq r) = 1 - e^{-\frac{1}{r}v}. \quad (6)$$

It then follows that the probability of the prediction residual being outside the feature residual is

$$P(v > r) = e^{-\frac{v}{r}}, \quad (7)$$

and the surprisal of observing the prediction residual larger than the feature residual is

$$I(v > r) = -\ln(P(v > r)), \quad (8)$$

expanded as

$$I(v > r) = -\ln(e^{-\frac{v}{r}}) = \frac{v}{r}.$$

In light of this, we observe that to find the surprisal of an observed residual, we can simply divide by the feature residual. This is the motivation for using IRW, where the inverse of feature residuals are used for feature weights when computing distances.

As previously described, we are able to compute a residual for each feature as the mean absolute deviation between the observed values and predicted values for the feature. We can express the feature residual r_i as

$$r_i = \frac{1}{|X|} \sum_{x_j \in X} |x_{i,j} - \hat{x}_{i,j}|, \quad (9)$$

where $x_{i,j}$ represents the i^{th} feature value of case x_j and $\hat{x}_{i,j}$ represents the prediction for that specific value. Then this feature residual can be used to determine feature weights, w_i , which can then be expressed as

$$w_i = \frac{1}{r_i^p}. \quad (10)$$

Using the inverse of the residual as the weight for each feature allows the distance contributed by each feature to be in the same space as one another. This gives the distance function scale invariance across varying feature types and scales, which solves one common challenge of using nearest neighbors approaches. Additionally, using IRW allows the model to emphasize features with strong relationships and reduce the influence features that appear to be significantly noisy or generally unpredictable. For models with a designated target feature, feature weights can further augmented using Mean Decrease in Accuracy (MDA) or similar techniques that attempt to capture the predictive power of a feature. Additionally, we are actively researching methods of incorporating MDA techniques alongside IRW in targetless applications of our methods.

Furthermore, scaling by the inverse residual feature weights enables the system to interpret distances in surprisal space.

Being in surprisal space allows us to utilize a maximum entropy assumption and the Laplace distribution to measure observed residuals in terms of surprisal. These surprisal values can then be utilized for various metrics and downstream tasks. Specifically we use these surprisal values to compute surprisal ratios that we refer to as convictions, which is covered in detail in the concepts section.

4. Concepts

In this section, we introduce human-oriented concepts which enable or enhance interpretable analyses and applications of the above methods to common tasks including classification, regression, feature selection, and anomaly detection. Many of these concepts are naturally understandable, being ratios. Additionally, they provide insight that lends itself naturally to strong performance on many difficult machine learning tasks.

4.1. Distance Contribution

The distance contribution reflects how much distance a point contributes to a graph connecting the nearest neighbors, which is the inverse of the density of points over a unit of distance in the Lebesgue space. The harmonic mean of the distance contribution reflects the inverse of the inverse distance weighting often employed with k -NN, though other techniques may be substituted if inverse distance weighting is not employed. We define the distance contribution as:

$$\phi(x) = \left(\frac{1}{k} \sum_{x_j \in X_k} \frac{1}{d(x, x_j)} \right)^{-1}, \quad (11)$$

where X_k is the set of nearest neighbors to point x and d is the distance function. This is a harmonic mean over the distances to each nearest neighbor. Note that the properties of the previously defined distance metric are useful here to prevent divisions by zero.

We can quantify the information needed to express a distance contribution $\phi(x)$ by transforming it into a probability. We begin by selecting the exponential distribution to describe the distribution of residuals as it is the maximum entropy distribution constrained by the first moment. We represent this in typical nomenclature for the exponential distribution using p norms.

$$\frac{1}{\lambda} = \|r(x)\|_p. \quad (12)$$

We can directly compare the distance contribution and p -normed magnitude of the residual. This is because the distance contribution and the norm of the residual are both on the same scale, with the distance contribution being the

expected distance of new information that the point adds to the model, and the norm of the residual is the expected distance of deviation. Given the entropy maximizing assumption of the exponential distribution of the distances, we can then determine the probability that a distance contribution is greater than or equal to the magnitude of the residual $\|r(x)\|_p$ in the form of cumulative residual entropy (Rao et al., 2004) as

$$P(\phi(x) \geq \|r(x)\|_p) = e^{-\frac{1}{\|r(x)\|_p} \cdot \phi(x)}. \quad (13)$$

We then convert the probability to self-information as

$$I(x) = -\ln P(\phi(x) \geq \|r(x)\|_p), \quad (14)$$

which simplifies to

$$I(x) = \frac{\phi(x)}{\|r(x)\|_p}. \quad (15)$$

4.2. Conviction

If we have some form of prior distribution of data given all of the information observed up to that point, the surprisal is the amount of information gained when we observe a new sample, event, case, or state change and update the prior distribution to form a new posterior distribution after the event. The surprisal of an event of observing a random variable $x \sim X$ is defined as $I(x) = -\ln p(x)$. Thus, the conviction, π , can be expressed as

$$\pi(x) = \frac{\mathbb{E}[I(X)]}{I(x)}. \quad (16)$$

By computing this ratio for different types of information, we derive several different types of *conviction* with different uses in various applications: *familiarity conviction*, *similarity conviction*, and *residual conviction*.

4.2.1. FAMILIARITY CONVICTION

Familiarity conviction is a metric for describing surprisal of points in a model relative to the training data. Consider a data set that has data points at regular intervals, such as a data point for each corner in a grid. Now consider a new point is added that is very close to one of the existing corner points. This new point should be quite easy to predict as it is close to an existing point, making it unsurprising. However, given this grid data, familiarity conviction would indicate a higher surprisal for such a point even though it is easy to label because the point is unusual with regard to the even distribution of the rest of the data points. This new point does not form another corner of the grid. These properties make familiarity conviction valuable for sanitizing data and reducing data as well as extracting patterns and anomalies, as is discussed in other sections.

Familiarity conviction is based on the distance metric described previously. As long as a low or zero value of p is used in L_p space metrics for similarity, familiarity conviction is independent of the scale of the data provided and does not overreact to feature dominance based on feature scale and range. Given a set of points $X \subset \mathbb{R}^z$, $\forall x \in \mathbb{X}$ and an integer $1 \leq k < |X|$ we define the distance contribution probability distribution, C of X to be the set

$$C = \left\{ \frac{\phi(x_1)}{\sum_{j=1}^n \phi(x_j)}, \frac{\phi(x_2)}{\sum_{j=1}^n \phi(x_j)}, \dots, \frac{\phi(x_n)}{\sum_{j=1}^n \phi(x_j)} \right\}, \quad (17)$$

for a function $\phi : X \rightarrow \mathbb{R}$ that returns the distance contribution. Note that because $\phi(0) = \infty$ may be true under some circumstances, multiple identical points may need special consideration, such as splitting the distance contribution among those points. Clearly C is a valid probability distribution. We will use this fact to compute the amount of information in C . The point probability of a point $x_i, j = 1, 2, \dots, n$ is

$$l(i) = \frac{\phi(x_i)}{\sum_{j=1}^n \phi(x_j)}, \quad (18)$$

where we see the index j is assigned the probability of the indexed point's distance contribution.

We assume the set of random variables that characterize the discrete distribution of point probabilities, L , is the set of $L = \{l(1), l(2), \dots, l(n)\}$. Because we have no additional knowledge of the distribution of points other than they follow the distribution of the data, we assume L is uniform as the distance probabilities have no trend or correlation. Then, the familiarity conviction of a point $x_j \in X$ is defined as

$$\pi_f(x_j) = \frac{\frac{1}{|X|} \sum_j D_{KL}(L||L - \{j\} \cup \mathbb{E}l(j))}{D_{KL}(L||L - \{x_j\} \cup \mathbb{E}l(j))}, \quad (19)$$

where D_{KL} is the Kullback-Leibler divergence. Since we assume L is uniform, we have that the expected probability $\mathbb{E}l(j) = \frac{1}{n}$.

Familiarity conviction is well suited for anomaly detection, particularly at detecting inliers, which would have familiarity conviction significantly smaller than 1. This performance comes at the cost of computational complexity.

4.2.2. SIMILARITY CONVICTION

Similarity Conviction is another method to evaluate the surprisal of a point in the data relative to the distribution of data that make up the point's nearest neighbors. Similarity conviction is defined as the expected distance contribution

of the point divided by the point’s observed distance contribution. To get the expected distance contribution of a point, the distance contributions of its nearest k neighbors are computed and then averaged. Using the local model of the point to get an expected distance contribution gives us a measure of conviction that leverages the contextual information about the sparsity in the local model.

Similarity conviction can be used as a tool to identify anomalies in the data, whether looking for inliers or outliers. Inliers will have uncharacteristically low distance contribution, and consequently have high values for similarity conviction. Similarly, outliers should have higher distance contributions than their local model which gives them low values for similarity conviction. Non-anomalous data should be expected to have similarity conviction values around 1.0, since the expected distance contribution is to be expected. Similarity conviction is less computationally expensive than familiarity conviction, but may not perform as well at identifying certain inliers.

Similarity conviction, π_s , can be expressed as:

$$\pi_s(x) = \frac{\mathbb{E}[\phi(x)]}{\phi(x)}. \quad (20)$$

Using the average distance contribution of the local model as the expected distance contribution, $\mathbb{E}[\phi(x)]$ can be expressed by:

$$\mathbb{E}[\phi(x)] = \left(\frac{1}{k} \sum_{x_j \in X_k} \phi(x_j) \right). \quad (21)$$

4.2.3. RESIDUAL CONVICTION

Examining *residual conviction* provides insight into the model’s uncertainty for a feature prediction. Residual conviction is calculated as the expected model residual for a feature divided by the computed prediction residual for that feature. The expected model residual is calculated by taking the mean of the residuals in the local model of its nearest k neighbors around the predicted feature, thus the residual conviction for feature i of point x is

$$\pi_r(x, \hat{x}, i) = \frac{\frac{1}{k} \sum_{x_i \in X_k} |x_i - \hat{x}_i|}{|x - \hat{x}|}, \quad (22)$$

where X_k is the set of points in the local model around point x . This ratio quantifies the difficulty of individual case’s feature prediction, with prediction certainty decreasing as the conviction approaches 0. In more practical terms, residual conviction serves to characterize how uncertain one or more predictions are relative to how uncertain they are expected

to be. This can be used to explain model decisions. If a decision is incorrect but has a residual conviction ≈ 1 , then this uncertainty is likely due to uncertainty in the data rather than the model.

5. Applications

In this section we demonstrate the performance of the above methods and concepts on various machine learning tasks. Namely, classification, regression, and anomaly detection. In general, we see that k -NN using these enhancements consistently performs near or above state of the art while maintaining strong interpretability and flexibility.

5.1. Classification and Regression

We conducted a comprehensive series of experimental comparisons on a diverse set of algorithms. We first perform classification and regression across 308 PMLB datasets (Romano et al., 2021). (146 for classification and 162 for regression)¹. and compare our approach across gradient boosted trees, traditional k -nearest neighbors, logistic regression (for classification), regularized least squares (for regression), neural networks, random forests and Light-GBM. A stratified sampling of data having cells $N \cdot d \leq 400000$ was chosen. To ensure robustness and reliability, each classification and regression experiment was iterated 30 times with varying random seeds, and the resulting metric averages were computed for statistical significance. For classification tasks, we present mean, precision, recall, and Matthews Correlation Coefficient (MCC) as evaluation metrics. In regression, Mean R^2 , mean absolute error (MAE), mean square error (MSE) and Spearman coefficient were calculated. The consolidated results are detailed in Table 1 and Table 2, providing a comparative perspective against a diverse set of algorithms. It is worth noting that our proposed method consistently outperforms all other classification algorithms in terms of accuracy and precision, while also demonstrating competitive results in regression.

5.2. Anomaly Detection

Using the defined conviction metrics, we can judge whether or not a data point is an anomaly on a standardized scale. To evaluate the the accuracy of this method, we present results on anomaly detection on 20 datasets from Outlier Detection Datasets (ODDS)² (Rayana, 2016). These datasets have ground truth labels indicating which data points are anomalous, which makes them ideal for this analysis. We utilize the previously established method of evaluating the conviction values of each point and compare to the results

¹Kindly refer to the appendix for more information on the datasets used and for additional experiments and details.

²Kindly refer to the appendix for dataset related details.

Table 1. Classification Results across 146 PMLB Datasets
 (Blue values indicate the best performance; Brown values indicate the second-best performance)

CLASSIFICATION	OURS	GB	KNN	LR	NN	RF	LGBM
MEAN ACCURACY (%) ↑	82.2278	81.9668	79.3017	79.0799	79.7512	81.4218	81.9154
MEAN PRECISION ↑	0.786554	0.774766	0.746573	0.743946	0.732757	0.772808	0.782817
MEAN RECALL ↑	0.770464	0.764163	0.719889	0.731404	0.736894	0.756036	0.779027
MEAN MCC ↑	0.644526	0.628351	0.562876	0.575105	0.584838	0.618480	0.653397

Table 2. Regression Results across 162 PMLB Datasets
 (Blue values indicate the best performance; Brown values indicate the second-best performance)

REGRESSION	OURS	GB	KNN	LINEAR	NN	RF	LGBM
R^2 MEAN ↑	0.857244	0.864342	0.724857	0.509989	0.727337	0.855368	0.818680
MAE ↓	0.841702	0.851328	1.038063	1.975748	1.008824	0.827424	1.069768
MSE ↓	10.168815	10.459248	12.222883	36.569369	11.598598	9.640429	20.453173
SPEARMAN COEFF. ↑	0.916272	0.925263	0.832777	0.719865	0.821594	0.917626	0.913498

of using many of the popular anomaly detection methods as shown in Table 3. Specifically, we trained our model by splitting our dataset into two parts (train and test). The training set comprised solely of inliers, and a test set encompassing both inliers and outliers, with a notable prevalence of inliers. Since the ODDS dataset has ground truth labels for both inliers and outliers, we used the ground truth labels to compute F1 scores to measure the performance of the anomaly detection benchmark routine. For our methods, we simply computed the conviction (similarity conviction or familiarity conviction) and compared it to a threshold of 0.7. If the conviction fell below the threshold, then it was classified as an anomaly. In practice we would recommend tuning this threshold per dataset, but here we show that picking a conviction level of 0.7 for all datasets (without choosing it in a dataset specific manner), our method achieves the highest $F1$ scores in 12 of the 20 datasets, surpassing the performance of all other outlier detection methods.

In Table 3, we show the average $F1$ score for each method across the 20 ODDS datasets. To see the results per dataset, please refer to the appendix.

It is worth noting that certain methodologies, such as CBLOF (Clustering-Based Local Outlier Factor), LOF (Local Outlier Factor), and ECOD (Extended Connectivity-Based Outlier Detection) usually incorporate a distinct partition exclusively composed of inliers during the training phase. Though this is not necessary, these methods can benefit from inlier-based training partitions. In contrast, our approach which harnesses the notion of familiarity conviction, allows us the capability to identify anomalies without necessitating an explicit ‘inlier’ dataset. This innovation enables us to gauge the uncertainty inherent in our model and promptly identify anomalous instances in a real-time

manner.

We demonstrate this on a toy dataset as shown in Figure 1. Consider a toy training dataset D in Figure 1 which is

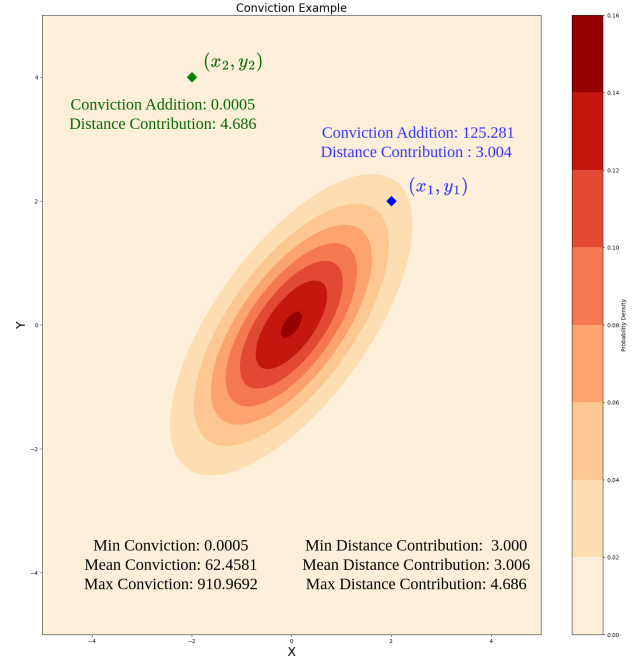


Figure 1. Depiction of familiarity conviction addition and distance contribution of two given points (x_1, y_1) and (x_2, y_2) given data distributed normally.

sampled from a random variable $X \sim \mathcal{N}(0, \Sigma^2)$ and we observe two points (x_1, y_1) (blue) and (x_2, y_2) (green) within the data. Given this data, familiarity conviction allows us to measure how close a point is to existing data. Using

Table 3. Mean F1 scores for Anomaly detection across 20 ODDS datasets
(Bold values indicate the best performance)

METHOD	MEAN F1 SCORE ↑
OURS (FAMILIARITY CONVICTION)	0.32
OURS (SIMILARITY CONVICTION)	0.49
ONE CLASS SVM (LI ET AL., 2003)	0.22
ISOLATION FOREST (LIU ET AL., 2008)	0.38
CBLOF (HE ET AL., 2003)	0.37
LOCAL OUTLIER FACTOR (BREUNIG ET AL., 2000)	0.19
ECOD (LI ET AL., 2022)	0.32
DEEPSVDD (RUFF ET AL., 2018)	0.45

our notion of surprisal, we can observe that (x_2, y_2) has high surprisal and therefore low conviction. Moreover, the distance contribution is higher than the mean distance contribution of the entire dataset. This allows for us to detect it as anomalous without having requirement of a separate inlier partition.

6. Limitations and Future Work

The present methodology, while promising, exhibits certain limitations in terms of the scale of data it can effectively handle. As an extension of the foundational k -Nearest Neighbors framework, this approach necessitates that the data used for model fitting is constrained to the memory capacity of the a machine. Secondly, the challenge lies in determining the conviction threshold beforehand, as it depends on factors such as the contamination level within the anomalous dataset or the absence of an inlier training set (for similarity conviction). Furthermore, placing additional emphasis on interpretability may introduce a trade-off in classification and regression performance, as the model becomes less reliant on spurious correlations within the data. To address the issue of scale we have implemented techniques that make querying the dataset more efficient than many standard methods. Specifically, in practice we use an efficient branch-and-bound implementation that combines efficient use of bit vectors to reduce the total compute required for all but the most pathological datasets. Furthermore, we are looking into sampling strategies of best representing the variance of our original data as well as data ablation techniques which could allow us to store more information in less space by intelligently adjusting weights of trained cases. We have also begun to probe the robustness of our method against inference-time adversarial attacks. Owing to the lack of gradient-based optimization in our approach and the adeptness at outlier detection tasks, early results have shown significant promise of our method’s robustness to out of distribution data across tabular as well as image datasets. Although this facet remains part of our future work, early indications of its resilience against such challenges substantiate the potential for our approach to thrive in safety-critical

contexts.

7. Discussion and Conclusion

In summary, we propose several enhancements to the traditional k -NN algorithm from the perspective of information theory. In particular, our method utilizes the Łukaszyk–Karmowski (LK) distance tailored to Laplace distributions, effectively mitigating the problem of zero distances predicated on data uncertainty. Furthermore, by leveraging Inverse Residual Weighting (IRW), we convert our distance measurements into the realm of surprisal space. Using the notion of surprisal, we define a new concept of conviction with which we are able to compute interpretable measures of the importance and surprisal for each data point. Finally, these enhancements have increased the effectiveness of k -NN while maintaining its natural interpretability. Since our method utilizes nearest-neighbors, it can effectively estimate the underlying density of the data, contributing to its versatility in various statistical and machine learning applications. Unlike traditional methods that rely on post-model interpretability tools, our approach directly addresses data and feature uncertainty. By leveraging the aforementioned tools, we can determine data point weights as well as feature contributions by calculating the conditional entropy for adding a feature without the need for explicit model training. This also allows us to compute MDA and MAE along with feature contributions. Our method provides detailed data point influence weights with perfect attribution and can be used to query counterfactuals. Moreover, by calculating SHAP over feature sets sampled from the entire feature space, we can obtain a more reliable estimate of SHAP that is robust to multicollinearity and feature order. Lastly, we conducted an extensive analysis on 308 datasets for classification and regression, alongside an additional 20 ODDS datasets for anomaly detection. In conclusion, we see that this approach aligns with human understanding of decision-making from data, such as similarity, differences and causality and facilitates a clearer understanding of a model’s decision-making process.

References

- Aggarwal, C. C., Hinneburg, A., and Keim, D. A. On the surprising behavior of distance metrics in high dimensional space. In *Database Theory—ICDT 2001: 8th International Conference London, UK, January 4–6, 2001 Proceedings* 8, pp. 420–434. Springer, 2001.
- Aha, D. W., Kibler, D. F., and Albert, M. K. Instance-based learning algorithms. *Mach. Learn.*, 6:37–66, 1991. doi: 10.1023/A:1022689900470. URL <https://doi.org/10.1023/A:1022689900470>.
- Alpaydin, E. Voting over multiple condensed nearest neighbors. *Artificial Intelligence Review*, 11, 09 1999. doi: 10.1023/A:1006563312922.
- Bahri, D., Jiang, H., and Gupta, M. Deep k-nn for noisy labels, 2020.
- Breunig, M. M., Kriegel, H.-P., Ng, R. T., and Sander, J. Lof: identifying density-based local outliers. In *Proceedings of the 2000 ACM SIGMOD international conference on Management of data*, pp. 93–104, 2000.
- Cover, T. and Hart, P. Nearest neighbor pattern classification. *IEEE Transactions on Information Theory*, 13(1):21–27, 1967. doi: 10.1109/TIT.1967.1053964.
- Fix, E. and Hodges, J. *Discriminatory Analysis: Nonparametric Discrimination: Consistency Properties*. USAF School of Aviation Medicine, 1951.
- Hastie, T., Tibshirani, R., and Friedman, J. *The Elements of Statistical Learning: Data Mining, Inference, and Prediction, Second Edition (Springer Series in Statistics)*. 02 2009. ISBN 0387848576.
- He, H. and Garcia, E. A. Learning from imbalanced data. *IEEE Transactions on Knowledge and Data Engineering*, 21(9):1263–1284, 2009. doi: 10.1109/TKDE.2008.239.
- He, Z., Xu, X., and Deng, S. Discovering cluster-based local outliers. *Pattern recognition letters*, 24(9-10):1641–1650, 2003.
- Indyk, P. and Motwani, R. Approximate nearest neighbors: Towards removing the curse of dimensionality. In *Proceedings of the Thirtieth Annual ACM Symposium on Theory of Computing*, STOC ’98, pp. 604–613, New York, NY, USA, 1998. Association for Computing Machinery. ISBN 0897919629. doi: 10.1145/276698.276876. URL <https://doi.org/10.1145/276698.276876>.
- Jiang, H., Lu, Z., Meng, F., Zhou, C., Zhou, J., Huang, D., and Su, J. Towards robust k-nearest-neighbor machine translation. In *Proceedings of the 2022 Conference on Empirical Methods in Natural Language Processing*, pp. 5468–5477, Abu Dhabi, United Arab Emirates, December 2022. Association for Computational Linguistics. URL <https://aclanthology.org/2022.emnlp-main.367>.
- Jiang, Z., Yang, M., Tsirlin, M., Tang, R., Dai, Y., and Lin, J. “low-resource” text classification: A parameter-free classification method with compressors. In *Findings of the Association for Computational Linguistics: ACL 2023*, pp. 6810–6828, Toronto, Canada, July 2023. Association for Computational Linguistics. doi: 10.18653/v1/2023.findings-acl.426. URL <https://aclanthology.org/2023.findings-acl.426>.
- Khandelwal, U., Fan, A., Jurafsky, D., Zettlemoyer, L., and Lewis, M. Nearest neighbor machine translation. In *International Conference on Learning Representations*, 2021. URL <https://openreview.net/forum?id=7wCBOfJ8hJM>.
- Li, K.-L., Huang, H.-K., Tian, S.-F., and Xu, W. Improving one-class svm for anomaly detection. In *Proceedings of the 2003 international conference on machine learning and cybernetics (IEEE Cat. No. 03EX693)*, volume 5, pp. 3077–3081. IEEE, 2003.
- Li, Z., Zhao, Y., Hu, X., Botta, N., Ionescu, C., and Chen, G. Ecod: Unsupervised outlier detection using empirical cumulative distribution functions. *IEEE Transactions on Knowledge and Data Engineering*, 2022.
- Liu, F. T., Ting, K. M., and Zhou, Z.-H. Isolation forest. In *2008 eighth ieee international conference on data mining*, pp. 413–422. IEEE, 2008.
- Meng, Y., Li, X., Zheng, X., Wu, F., Sun, X., Zhang, T., and Li, J. Fast nearest neighbor machine translation. In *Findings of the Association for Computational Linguistics: ACL 2022*, pp. 555–565, Dublin, Ireland, May 2022. Association for Computational Linguistics. doi: 10.18653/v1/2022.findings-acl.47. URL <https://aclanthology.org/2022.findings-acl.47>.
- Papernot, N. and McDaniel, P. Deep k-nearest neighbors: Towards confident, interpretable and robust deep learning, 2018.
- Prasath, V. B. S., Alfeilat, H. A. A., Lasassmeh, O., and Hassanat, A. B. A. Distance and similarity measures effect on the performance of k-nearest neighbor classifier - A review. *CoRR*, abs/1708.04321, 2017. URL <http://arxiv.org/abs/1708.04321>.
- Rao, M., Chen, Y., Vemuri, B., and Wang, F. Cumulative residual entropy: a new measure of information. *IEEE Transactions on Information Theory*, 50(6):1220–1228, 2004. doi: 10.1109/TIT.2004.828057.

Rayana, S. Odds library, 2016. URL <https://odds.cs.stonybrook.edu>.

Romano, J. D., Le, T. T., La Cava, W., Gregg, J. T., Goldberg, D. J., Chakraborty, P., Ray, N. L., Himmelstein, D., Fu, W., and Moore, J. H. Pmlb v1.0: an open source dataset collection for benchmarking machine learning methods. *arXiv preprint arXiv:2012.00058v2*, 2021.

Ruff, L., Vandermeulen, R., Goernitz, N., Deecke, L., Sidqui, S. A., Binder, A., Müller, E., and Kloft, M. Deep one-class classification. In *International conference on machine learning*, pp. 4393–4402. PMLR, 2018.

Schuh, M. A., Wylie, T., and Angryk, R. A. Improving the performance of high-dimensional knn retrieval through localized dataspace segmentation and hybrid indexing. In Catania, B., Guerrini, G., and Pokorný, J. (eds.), *Advances in Databases and Information Systems*, pp. 344–357, Berlin, Heidelberg, 2013. Springer Berlin Heidelberg.

Tao, Y., Yi, K., Sheng, C., and Kalnis, P. Quality and efficiency in high dimensional nearest neighbor search. In *Proceedings of the 2009 ACM SIGMOD International Conference on Management of Data*, SIGMOD ’09, pp. 563–576, New York, NY, USA, 2009. Association for Computing Machinery. ISBN 9781605585512. doi: 10.1145/1559845.1559905. URL <https://doi.org/10.1145/1559845.1559905>.

Wang, Q., Kulkarni, S., and Verdú, S. Divergence estimation for multidimensional densities via -nearest-neighbor distances. *Information Theory, IEEE Transactions on*, 55:2392 – 2405, 06 2009. doi: 10.1109/TIT.2009.2016060.

Łukaszyk, S. *Probability metric, examples of approximation applications in experimental mechanics*. PhD thesis, 01 2003.

Łukaszyk, S. A new concept of probability metric and its applications in approximation of scattered data sets. *Computational Mechanics*, 33:299–304, 03 2004. doi: 10.1007/s00466-003-0532-2.

A. Derivation of Łukaszyk–Karmowski (LK) with Laplace Distributions

To prove Equation 4 of our work, we begin with the expected distance between two random variables X and Y given two probability density functions, $f(x)$ and $g(y)$ as

$$d(X, Y) = \int_{-\infty}^{\infty} \int_{-\infty}^{\infty} |x - y| f(x) g(y) dx dy. \quad (23)$$

Using two Laplace distributions with means μ_1 and μ_2 and expected distance from the mean b_1 and b_2 , we can express the probability density functions as

$$f(x) = \frac{1}{2b_1} e^{-\frac{|x-\mu_1|}{b_1}} \quad (24)$$

and

$$g(y) = \frac{1}{2b_2} e^{-\frac{|y-\mu_2|}{b_2}} \quad (25)$$

respectively.

Substituting in the Laplace distributions into the expected distance, we can simplify this slightly as

$$\begin{aligned} d(X, Y) &= \int_{-\infty}^{\infty} \int_{-\infty}^{\infty} |x - y| \cdot \frac{1}{2b_1} e^{-\frac{|x-\mu_1|}{b_1}} \cdot \frac{1}{2b_2} e^{-\frac{|y-\mu_2|}{b_2}} dx dy \\ &= \frac{1}{4b_1 b_2} \int_{-\infty}^{\infty} \int_{-\infty}^{\infty} |x - y| \cdot e^{-\frac{|x-\mu_1|}{b_1}} \cdot e^{-\frac{|y-\mu_2|}{b_2}} dx dy. \end{aligned}$$

We further assume that $b_1 = b_2$, and use b in place of both, which assumes that the error is the same throughout the space and simplify further as

$$d(X, Y) = \frac{1}{4b^2} \int_{-\infty}^{\infty} \int_{-\infty}^{\infty} |x - y| \cdot e^{-\frac{|\mu_1-x|}{b}} \cdot e^{-\frac{|\mu_2-y|}{b}} dx dy. \quad (26)$$

Because we only have one value for b , we can assume that $\mu_1 \leq \mu_2$ without loss of generality because we can just exchange the values if this is not true, and in the end we will adjust the formula to remove this assumption. There exist 3 regions of the space for x which are $x \leq \mu_1$, $\mu_1 < x \leq \mu_2$, and $\mu_2 < x$.

A.1. $x \leq \mu_1, y \leq \mu_1$

Rewriting Equation 26 for the part of the space where $x < \mu_1, y < \mu_1$ is

$$\begin{aligned} d_{x \leq \mu_1, y \leq \mu_1}(X, Y) &= \frac{1}{4b^2} \int_{-\infty}^{\mu_1} \int_{-\infty}^{\mu_1} |y - x| \cdot e^{-\frac{(\mu_1-x)}{b}} \cdot e^{-\frac{(\mu_2-y)}{b}} dx dy \\ &= \frac{1}{4b^2} \int_{-\infty}^{\mu_1} \left(\int_{-\infty}^{\mu_1} |y - x| \cdot e^{-\frac{(\mu_1-x)}{b}} dx \right) \cdot e^{-\frac{(\mu_2-y)}{b}} dy \\ &= \frac{1}{4b^2} \int_{-\infty}^{\mu_1} \left(\int_{-\infty}^y (y - x) \cdot e^{-\frac{(\mu_1-x)}{b}} dx + \int_y^{\mu_1} (x - y) \cdot e^{-\frac{(\mu_1-x)}{b}} dx \right) \cdot e^{-\frac{(\mu_2-y)}{b}} dy \\ &= \frac{1}{4b^2} \int_{-\infty}^{\mu_1} \left(b^2 e^{\frac{y-\mu_1}{b}} + b^2 e^{\frac{y-\mu_1}{b}} - by + b\mu_1 - b^2 \right) \cdot e^{-\frac{(\mu_2-y)}{b}} dy \\ &= \frac{1}{4b} \int_{-\infty}^{\mu_1} \left(2be^{\frac{y-\mu_1}{b}} - y + \mu_1 - b \right) \cdot e^{-\frac{(\mu_2-y)}{b}} dy \\ &= \frac{1}{4b} b^2 e^{\frac{-(\mu_2-\mu_1)}{b}} \\ &= \frac{1}{4} be^{\frac{-(\mu_2-\mu_1)}{b}}. \end{aligned}$$

A.2. $x \leq \mu_1, \mu_1 < y \leq \mu_2$

Rewriting Equation 26 for the part of the space where $x < \mu_1, \mu_1 < y < \mu_2$ is

$$\begin{aligned} d_{x \leq \mu_1, \mu_1 < y \leq \mu_2}(X, Y) &= \frac{1}{4b^2} \int_{\mu_1}^{\mu_2} \int_{-\infty}^{\mu_1} (y - x) \cdot e^{\frac{-(\mu_1-x)}{b}} \cdot e^{\frac{-(\mu_2-y)}{b}} dx dy \\ &= \frac{1}{4b^2} \int_{\mu_1}^{\mu_2} (by - b\mu_1 + b^2) \cdot e^{\frac{-(\mu_2-y)}{b}} dy \\ &= \frac{1}{4b} \int_{\mu_1}^{\mu_2} (y - \mu_1 + b) \cdot e^{\frac{-(\mu_2-y)}{b}} dy \\ &= \frac{1}{4b} (b\mu_2 - b\mu_1) \\ &= \frac{1}{4} (\mu_2 - \mu_1). \end{aligned}$$

A.3. $x \leq \mu_1, \mu_2 < y$

Rewriting Equation 26 for the part of the space where $x < \mu_1, \mu_2 < y$ is

$$\begin{aligned} d_{x \leq \mu_1, \mu_2 < y}(X, Y) &= \frac{1}{4b^2} \int_{\mu_2}^{\infty} \int_{-\infty}^{\mu_1} (y - x) \cdot e^{\frac{-(\mu_1-x)}{b}} \cdot e^{\frac{-(y-\mu_2)}{b}} dx dy \\ &= \frac{1}{4b^2} \int_{\mu_2}^{\infty} \left(\int_{-\infty}^{\mu_1} (y - x) \cdot e^{\frac{-(\mu_1-x)}{b}} dx \right) \cdot e^{\frac{-(y-\mu_2)}{b}} dy \\ &= \frac{1}{4b^2} \int_{\mu_2}^{\infty} (by - b\mu_1 + b^2) \cdot e^{\frac{-(y-\mu_2)}{b}} dy \\ &= \frac{1}{4b} \int_{\mu_2}^{\infty} (y - \mu_1 + b) \cdot e^{\frac{-(y-\mu_2)}{b}} dy \\ &= \frac{1}{4b} (b\mu_2 - b\mu_1 + 2b^2) \\ &= \frac{1}{4} (\mu_2 - \mu_1 + 2b). \end{aligned}$$

A.4. $\mu_1 < x \leq \mu_2, y \leq \mu_1$

Rewriting Equation 26 for the part of the space where $\mu_1 < x < \mu_2, y < \mu_1$ is

$$\begin{aligned} d_{\mu_1 < x \leq \mu_2, y \leq \mu_1}(X, Y) &= \frac{1}{4b^2} \int_{-\infty}^{\mu_1} \int_{\mu_1}^{\mu_2} (x - y) \cdot e^{\frac{-(x-\mu_1)}{b}} \cdot e^{\frac{-(\mu_2-y)}{b}} dx dy \\ &= \frac{1}{4b^2} \int_{-\infty}^{\mu_1} \left(\int_{\mu_1}^{\mu_2} (x - y) \cdot e^{\frac{-(x-\mu_1)}{b}} dx \right) \cdot e^{\frac{-(\mu_2-y)}{b}} dy \\ &= \frac{1}{4b^2} \int_{-\infty}^{\mu_1} \left(e^{\frac{\mu_1-\mu_2}{b}} (by - b\mu_2 - b^2) - by + b\mu_1 + b^2 \right) \cdot e^{\frac{-(\mu_2-y)}{b}} dy \\ &= \frac{1}{4b} \int_{-\infty}^{\mu_1} \left(e^{\frac{\mu_1-\mu_2}{b}} (y - \mu_2 - b) - y + \mu_1 + b \right) \cdot e^{\frac{-(\mu_2-y)}{b}} dy \\ &= \frac{1}{4b} \left(2b^2 e^{\frac{\mu_1-\mu_2}{b}} + e^{\frac{2\mu_1-2\mu_2}{b}} (-b\mu_2 + b\mu_1 - 2b^2) \right) \\ &= \frac{1}{4} \left(2be^{\frac{\mu_1-\mu_2}{b}} + e^{\frac{2\mu_1-2\mu_2}{b}} (\mu_1 - \mu_2 - 2b) \right). \end{aligned}$$

A.5. $\mu_1 < x \leq \mu_2, \mu_1 < y \leq \mu_2$

Rewriting Equation 26 for the part of the space where $\mu_1 < x < \mu_2, \mu_1 < y < \mu_2$ is

$$\begin{aligned}
 d_{\mu_1 < x \leq \mu_2, \mu_1 < y \leq \mu_2}(X, Y) &= \frac{1}{4b^2} \int_{\mu_1}^{\mu_2} \int_{\mu_1}^{\mu_2} |y - x| \cdot e^{-\frac{(x-\mu_1)}{b}} \cdot e^{-\frac{(\mu_2-y)}{b}} dx dy \\
 &= \frac{1}{4b^2} \int_{\mu_1}^{\mu_2} \left(\int_{\mu_1}^{\mu_2} |y - x| \cdot e^{-\frac{(x-\mu_1)}{b}} dx \right) \cdot e^{-\frac{(\mu_2-y)}{b}} dy \\
 &= \frac{1}{4b^2} \int_{\mu_1}^{\mu_2} \left(\int_{\mu_1}^y (y - x) \cdot e^{-\frac{(x-\mu_1)}{b}} dx + \int_y^{\mu_2} (x - y) \cdot e^{-\frac{(x-\mu_1)}{b}} dx \right) \cdot e^{-\frac{(\mu_2-y)}{b}} dy \\
 &= \frac{1}{4b^2} \int_{\mu_1}^{\mu_2} \left(\left(b^2 e^{\frac{\mu_1-y}{b}} + by - b\mu_1 - b^2 \right) \right. \\
 &\quad \left. + \left(b^2 e^{\frac{\mu_1-y}{b}} + e^{\frac{\mu_1-\mu_2}{b}} (by - b\mu_2 - b^2) \right) \right) \cdot e^{-\frac{(\mu_2-y)}{b}} dy \\
 &= \frac{1}{4b} \int_{\mu_1}^{\mu_2} \left(2be^{\frac{\mu_1-y}{b}} + y - \mu_1 - b + e^{\frac{\mu_1-\mu_2}{b}} (y - \mu_2 - b) \right) \cdot e^{-\frac{(\mu_2-y)}{b}} dy \\
 &= \frac{1}{4b} \left(b\mu_2 - b\mu_1 - 2b^2 + e^{\frac{\mu_1-\mu_2}{b}} (2b\mu_2 - 2b^2) \right. \\
 &\quad \left. + e^{\frac{\mu_1-\mu_2}{b}} (-2b\mu_1 + 2b^2) + e^{\frac{2\mu_1-2\mu_2}{b}} (b\mu_2 - b\mu_1 + 2b^2) \right) \\
 &= \frac{1}{4} \left(\mu_2 - \mu_1 - 2b + e^{\frac{\mu_1-\mu_2}{b}} (2\mu_2 - 2\mu_1) + e^{\frac{2\mu_1-2\mu_2}{b}} (\mu_2 - \mu_1 + 2b) \right).
 \end{aligned}$$

A.6. $\mu_1 < x \leq \mu_2, \mu_2 < y$

Rewriting Equation 26 for the part of the space where $\mu_1 < x < \mu_2, \mu_2 < y$ is

$$\begin{aligned}
 d_{\mu_1 < x \leq \mu_2, \mu_2 < y}(X, Y) &= \frac{1}{4b^2} \int_{\mu_2}^{\infty} \int_{\mu_1}^{\mu_2} (y - x) \cdot e^{-\frac{(x-\mu_1)}{b}} \cdot e^{-\frac{(y-\mu_2)}{b}} dx dy \\
 &= \frac{1}{4b^2} \int_{\mu_2}^{\infty} \left(\int_{\mu_1}^{\mu_2} (y - x) \cdot e^{-\frac{(x-\mu_1)}{b}} dx \right) \cdot e^{-\frac{(y-\mu_2)}{b}} dy \\
 &= \frac{1}{4b^2} \int_{\mu_2}^{\infty} \left(by - b\mu_1 - b^2 - e^{\frac{\mu_1-\mu_2}{b}} (by - b\mu_2 - b^2) \right) \cdot e^{-\frac{(y-\mu_2)}{b}} dy \\
 &= \frac{1}{4b} \int_{\mu_2}^{\infty} \left(y - \mu_1 - b - e^{\frac{\mu_1-\mu_2}{b}} (y - \mu_2 - b) \right) \cdot e^{-\frac{(y-\mu_2)}{b}} dy \\
 &= \frac{1}{4b} (b\mu_2 - b\mu_1) \\
 &= \frac{1}{4} (\mu_2 - \mu_1)
 \end{aligned}$$

A.7. $\mu_2 < x, y \leq \mu_1$

Rewriting Equation 26 for the part of the space where $\mu_2 < x, y < \mu_1$ is

$$\begin{aligned}
 d_{\mu_2 < x, y \leq \mu_1}(X, Y) &= \frac{1}{4b^2} \int_{-\infty}^{\mu_1} \int_{\mu_2}^{\infty} (x - y) \cdot e^{-\frac{(x-\mu_1)}{b}} \cdot e^{-\frac{(\mu_2-y)}{b}} dx dy \\
 &= \frac{1}{4b^2} \int_{-\infty}^{\mu_1} \left(\int_{\mu_2}^{\infty} (x - y) \cdot e^{-\frac{(x-\mu_1)}{b}} dx \right) \cdot e^{-\frac{(\mu_2-y)}{b}} dy \\
 &= \frac{1}{4b^2} \int_{-\infty}^{\mu_1} e^{\frac{\mu_1-\mu_2}{b}} (-by + b\mu_2 + b^2) \cdot e^{-\frac{(\mu_2-y)}{b}} dy \\
 &= \frac{1}{4b} \int_{-\infty}^{\mu_1} e^{\frac{\mu_1-\mu_2}{b}} (-y + \mu_2 + b) \cdot e^{-\frac{(\mu_2-y)}{b}} dy \\
 &= \frac{1}{4b} e^{\frac{2\mu_1-2\mu_2}{b}} (b\mu_2 + 2b^2 - b\mu_1) \\
 &= \frac{1}{4} e^{\frac{2\mu_1-2\mu_2}{b}} (\mu_2 + 2b - \mu_1) \\
 &= \frac{1}{4} e^{\frac{-2(\mu_2-\mu_1)}{b}} (2b + \mu_2 - \mu_1)
 \end{aligned}$$

A.8. $\mu_2 < x, \mu_1 < y \leq \mu_2$

Rewriting Equation 26 for the part of the space where $\mu_2 < x, \mu_1 < y < \mu_2$ is

$$\begin{aligned}
 d_{\mu_2 < x, \mu_1 < y \leq \mu_2}(X, Y) &= \frac{1}{4b^2} \int_{\mu_1}^{\mu_2} \int_{\mu_2}^{\infty} (x - y) \cdot e^{-\frac{(x-\mu_1)}{b}} \cdot e^{-\frac{(\mu_2-y)}{b}} dx dy \\
 &= \frac{1}{4b^2} \int_{\mu_1}^{\mu_2} \left(\int_{\mu_2}^{\infty} (x - y) \cdot e^{-\frac{(x-\mu_1)}{b}} dx \right) \cdot e^{-\frac{(\mu_2-y)}{b}} dy \\
 &= \frac{1}{4b^2} \int_{\mu_1}^{\mu_2} \left(e^{\frac{\mu_1-\mu_2}{b}} (-by + b\mu_2 + b^2) \right) \cdot e^{-\frac{(\mu_2-y)}{b}} dy \\
 &= \frac{1}{4b} \int_{\mu_1}^{\mu_2} \left(e^{\frac{\mu_1-\mu_2}{b}} (-y + \mu_2 + b) \right) \cdot e^{-\frac{(\mu_2-y)}{b}} dy \\
 &= \frac{1}{4b} \left(2b^2 e^{\frac{\mu_1-\mu_2}{b}} - e^{\frac{2\mu_1-2\mu_2}{b}} (b\mu_2 - b\mu_1 + 2b^2) \right) \\
 &= \frac{1}{4} \left(2be^{\frac{\mu_1-\mu_2}{b}} + e^{\frac{2\mu_1-2\mu_2}{b}} (\mu_1 - \mu_2 - 2b) \right)
 \end{aligned}$$

Rewriting Equation 26 for the part of the space where $\mu_2 < x, \mu_2 < y$ is

$$\begin{aligned}
 d_{\mu_2 < x, \mu_2 < y}(X, Y) &= \frac{1}{4b^2} \int_{\mu_2}^{\infty} \int_{\mu_2}^{\infty} |x - y| \cdot e^{-\frac{(x-\mu_1)}{b}} \cdot e^{-\frac{(y-\mu_2)}{b}} dx dy \\
 &= \frac{1}{4b^2} \int_{\mu_2}^{\infty} \left(\int_{\mu_2}^{\infty} |x - y| \cdot e^{-\frac{(x-\mu_1)}{b}} dx \right) \cdot e^{-\frac{(y-\mu_2)}{b}} dy \\
 &= \frac{1}{4b^2} \int_{\mu_2}^{\infty} \left(\int_{\mu_2}^y (y - x) \cdot e^{-\frac{(x-\mu_1)}{b}} dx + \int_y^{\infty} (x - y) \cdot e^{-\frac{(x-\mu_1)}{b}} dx \right) \cdot e^{-\frac{(y-\mu_2)}{b}} dy \\
 &= \frac{1}{4b^2} \int_{\mu_2}^{\infty} \left(\left(b^2 e^{\frac{\mu_1-y}{b}} + e^{\frac{\mu_1-\mu_2}{b}} (by - b\mu_2 - b^2) \right) + \left(b^2 e^{\frac{\mu_1-y}{b}} \right) \right) \cdot e^{-\frac{(y-\mu_2)}{b}} dy \\
 &= \frac{1}{4b} \int_{\mu_2}^{\infty} \left(2be^{\frac{\mu_1-y}{b}} + e^{\frac{\mu_1-\mu_2}{b}} (y - \mu_2 - b) \right) \cdot e^{-\frac{(y-\mu_2)}{b}} dy \\
 &= \frac{1}{4b} b^2 e^{\frac{\mu_1-\mu_2}{b}} \\
 &= \frac{1}{4} be^{\frac{-(\mu_2-\mu_1)}{b}}.
 \end{aligned}$$

A.9. Combining the Parts

We can combine each of the probability weighted distances as

$$\begin{aligned}
 d(X, Y) &= d_{x \leq \mu_1, y \leq \mu_1}(X, Y) + d_{x \leq \mu_1, \mu_1 < y \leq \mu_2}(X, Y) + d_{x \leq \mu_1, \mu_2 < y}(X, Y) + d_{\mu_1 < x \leq \mu_2, y \leq \mu_1}(X, Y) \\
 &\quad + d_{\mu_1 < x \leq \mu_2, \mu_1 < y \leq \mu_2}(X, Y) + d_{\mu_1 < x \leq \mu_2, \mu_2 < y}(X, Y) + d_{\mu_2 < x, y \leq \mu_1}(X, Y) + d_{\mu_2 < x, \mu_1 < y \leq \mu_2}(X, Y) \\
 &\quad + d_{\mu_2 < x, \mu_2 < y}(X, Y) \\
 &= \frac{1}{4}be^{\frac{-(\mu_2-\mu_1)}{b}} \\
 &\quad + \frac{1}{4}(\mu_2 - \mu_1) \\
 &\quad + \frac{1}{4}(\mu_2 - \mu_1 + 2b) \\
 &\quad + \frac{1}{4}\left(2be^{\frac{\mu_1-\mu_2}{b}} + e^{\frac{2\mu_1-2\mu_2}{b}}(\mu_1 - \mu_2 - 2b)\right) \\
 &\quad + \frac{1}{4}\left(\mu_2 - \mu_1 - 2b + e^{\frac{\mu_1-\mu_2}{b}}(2\mu_2 - 2\mu_1) + e^{\frac{2\mu_1-2\mu_2}{b}}(\mu_2 - \mu_1 + 2b)\right) \\
 &\quad + \frac{1}{4}(\mu_2 - \mu_1) \\
 &\quad + \frac{1}{4}e^{\frac{-2(\mu_2-\mu_1)}{b}}(2b + \mu_2 - \mu_1) \\
 &\quad + \frac{1}{4}\left(2be^{\frac{\mu_1-\mu_2}{b}} + e^{\frac{2\mu_1-2\mu_2}{b}}(\mu_1 - \mu_2 - 2b)\right) \\
 &\quad + \frac{1}{4}be^{\frac{-(\mu_2-\mu_1)}{b}} \\
 &= be^{\frac{-(\mu_2-\mu_1)}{b}} \\
 &\quad + \frac{1}{2}(\mu_2 - \mu_1 + b) \\
 &\quad + \frac{1}{4}\left(2be^{\frac{\mu_1-\mu_2}{b}} + e^{\frac{2\mu_1-2\mu_2}{b}}(\mu_1 - \mu_2 - 2b)\right) \\
 &\quad + \frac{1}{4}\left(\mu_2 - \mu_1 - 2b + e^{\frac{\mu_1-\mu_2}{b}}(2\mu_2 - 2\mu_1) + e^{\frac{2\mu_1-2\mu_2}{b}}(\mu_2 - \mu_1 + 2b)\right) \\
 &\quad + \frac{1}{4}(\mu_2 - \mu_1) \\
 &= be^{\frac{-(\mu_2-\mu_1)}{b}} \\
 &\quad + (\mu_2 - \mu_1) \\
 &\quad + \frac{1}{4}\left(2be^{\frac{\mu_1-\mu_2}{b}}\right) \\
 &\quad + \frac{1}{4}\left(e^{\frac{\mu_1-\mu_2}{b}}(2\mu_2 - 2\mu_1)\right) \\
 &= be^{\frac{-(\mu_2-\mu_1)}{b}} + (\mu_2 - \mu_1) + \frac{1}{2}be^{\frac{\mu_1-\mu_2}{b}} + \frac{1}{2}e^{\frac{\mu_1-\mu_2}{b}}(\mu_2 - \mu_1) \\
 d(X, Y) &= \mu_2 - \mu_1 + \frac{1}{2}e^{\frac{-(\mu_2-\mu_1)}{b}}(3b + \mu_2 - \mu_1).
 \end{aligned}$$

To remove the assumption that $\mu_1 \leq \mu_2$, we can rewrite this result as

$$d(X, Y) = |\mu_2 - \mu_1| + \frac{1}{2}e^{\frac{-|\mu_2-\mu_1|}{b}}(3b + |\mu_2 - \mu_1|). \quad (27)$$

This completes the derivation of LK distance with Laplace Distributions.

B. Information about the Benchmarked Algorithms

- Gradient Boosted Trees

K-fold cross-validation was carried out with $K = 6$. Grid search was carried out on the number of estimators (N_{est}) such that $N_{\text{est}} \in \{\lceil e^i \rceil\}_{i=1}^8$.

- Traditional KNN

K-fold cross-validation was carried out with $K = 6$. Grid search was carried out on the number of neighbors (k_n) and the value of p in l_p norms such that $k_n \in [1, 2, 3, 5, 8, 13, 21, 34, 55, 89, 144]$ and $p \in [1, 2]$. Note that the search space of neighbors are picked according to the Fibonacci sequence since it grows at a slower rate than some other sequences (e.g. exponential), which is advantageous when exploring hyperparameter values. It provides a versatile set of values that can adapt to different datasets and problem characteristics leading to a more diverse exploration of the search space, helping to identify a wider range of potential optimal k_n values.

- Regularized Least Squares

Elastic Net was used in the case of regression. K-fold cross-validation was carried out with $K = 6$. Grid search was carried out on the scaling ration of the l_1 and l_2 penalties ranging from values $[0.1, 0.5, 0.7, 0.9, 0.95, 0.99, 1.0]$

- Logistic Regression

K-fold cross-validation was carried out with $K = 6$. Grid search was carried out on the inverse of regularization strength C in the logarithmic scale such that

$$C \in [0.0001, 0.0008, 0.006, 0.0464, 0.3594, 2.7826, 21.5443, 166.8101, 1291.5497, 10000.0]$$

The optimization problem was solved using stochastic average gradient with l_2 penalty.

- Neural Network

For both classification and regression datasets, Adam Optimizer was used with batch size 128 and learning rate of 0.001. An internal validation set of 10% was used from the training data for an early stopping criteria, with maximum epochs set to 1000 using swish activation for each hidden layer. A dropout rate of 10% with Layer Norm was used after each hidden layer. The details of the architecture can be found in the table below.

Layer #	Parameter Type	Parameter Size
layers 1	0.weight	(512, Input Size)
layers 1	0.bias	(512,)
dropout 1	1.weight	(512,)
dropout 1	1.bias	(512,)
layers 2	4.weight	(512, 512)
layers 2	4.bias	(512,)
dropout 2	5.weight	(512,)
dropout 2	5.bias	(512,)
layers 3	8.weight	(512, 512)
layers 3	8.bias	(512,)
dropout 3	9.weight	(512,)
dropout 3	9.bias	(512,)
Output Layer	weight	(Output Size, 512)
Output Layer	bias	(Output Size,)

- Random Forests

K-fold cross-validation was carried out with $K = 6$. Grid search was carried out on the number of estimators (N_{est}) such that $N_{\text{est}} \in \{\lceil e^i \rceil\}_{i=1}^8$.

- Light-GBM

K-fold cross-validation was carried out with $K = 6$. The number of estimators used was 100 with number of leaves = 31

C. Detailed Information about the PMLB Classification Datasets

	Dataset Name	Rows	Columns	Rows × Columns
1	GAMETES_Epistasis_2_Way_20atts_0.1H_EDM_1_1	1600	21	33600
2	GAMETES_Epistasis_2_Way_20atts_0.4H_EDM_1_1	1600	21	33600
3	GAMETES_Epistasis_3_Way_20atts_0.2H_EDM_1_1	1600	21	33600
4	GAMETES_Heterogeneity_20atts_1600_Het_0.4_0.2_...	1600	21	33600
5	GAMETES_Heterogeneity_20atts_1600_Het_0.4_0.2_...	1600	21	33600
6	Hill_Valley_with_noise	1212	101	122412
7	Hill_Valley_without_noise	1212	101	122412
8	agaricus_lepiota	8145	23	187335
9	allbp	3772	30	113160
10	allhyper	3771	30	113130
11	allhypo	3770	30	113100
12	allrep	3772	30	113160
13	analcatdata_aids	50	5	250
14	analcatdata_asbestos	83	4	332
15	analcatdata_authorship	841	71	59711
16	analcatdata_bankruptcy	50	7	350
17	analcatdata_boxing1	120	4	480
18	analcatdata_boxing2	132	4	528
19	analcatdata_creditscore	100	7	700
20	analcatdata_cyyoung892	97	11	1067
21	analcatdata_cyyoung9302	92	11	1012
22	analcatdata_dmft	797	5	3985
23	analcatdata_fraud	42	12	504
24	analcatdata_germangss	400	6	2400
25	analecatdata_happiness	60	4	240
26	analcatdata_japansolvent	52	10	520
27	analcatdata_lawsuit	264	5	1320
28	ann_thyroid	7200	22	158400
29	appendicitis	106	8	848
30	australian	690	15	10350
31	auto	202	26	5252
32	backache	180	33	5940
33	balance_scale	625	5	3125
34	banana	5300	3	15900
35	biomed	209	9	1881
36	breast	699	11	7689
37	breast_cancer	286	10	2860
38	breast_cancer_wisconsin	569	31	17639
39	breast_w	699	10	6990
40	buggyCrx	690	16	11040
41	bupa	345	6	2070
42	calendarDOW	399	33	13167
43	car	1728	7	12096
44	car_evaluation	1728	22	38016
45	cars	392	9	3528
46	chess	3196	37	118252
47	churn	5000	21	105000
48	clean1	476	169	80444
49	cleve	303	14	4242
50	cleveland	303	14	4242
51	cleveland_nominal	303	8	2424
52	cloud	108	8	864
53	cmc	1473	10	14730
54	colic	368	23	8464
55	collins	485	24	11640
56	confidence	72	4	288
57	contraceptive	1473	10	14730
58	corral	160	7	1120
59	credit_a	690	16	11040
60	credit_g	1000	21	21000
61	crx	690	16	11040
62	dermatology	366	35	12810
63	diabetes	768	9	6912
64	dis	3772	30	113160
65	ecoli	327	8	2616
66	flags	178	44	7832
67	flare	1066	11	11726
68	german	1000	21	21000
69	glass	205	10	2050
70	glass2	163	10	1630
71	haberman	306	4	1224
72	hayes_roth	160	5	800
73	heart_c	303	14	4242

	Dataset Name	Rows	Columns	Rows × Columns
74	heart.h	294	14	4116
75	heart_statlog	270	14	3780
76	hepatitis	155	20	3100
77	horse_colic	368	23	8464
78	house_votes_84	435	17	7395
79	hungarian	294	14	4116
80	hypothyroid	3163	26	82238
81	ionosphere	351	35	12285
82	iris	150	5	750
83	irish	500	6	3000
84	kr_vs_kp	3196	37	118252
85	krkopt	28056	7	196392
86	labor	57	17	969
87	led24	3200	25	80000
88	led7	3200	8	25600
89	lupus	87	4	348
90	lymphography	148	19	2812
91	magic	19020	11	209220
92	mfeat_fourier	2000	77	154000
93	mfeat_karhunen	2000	65	130000
94	mfeat_morphological	2000	7	14000
95	mfeat_zernike	2000	48	96000
96	mofn_3_7_10	1324	11	14564
97	molecular_biology_promoters	106	58	6148
98	monk1	556	7	3892
99	monk2	601	7	4207
100	monk3	554	7	3878
101	movement_libras	360	91	32760
102	mushroom	8124	23	186852
103	mux6	128	7	896
104	new_thyroid	215	6	1290
105	nursery	12958	9	116622
106	page_blocks	5473	11	60203
107	parity5	32	6	192
108	parity5+5	1124	11	12364
109	pendigits	10992	17	186864
110	phoneme	5404	6	32424
111	pima	768	9	6912
112	postoperative_patient_data	88	9	792
113	prnn_crabs	200	8	1600
114	prnn_fglass	205	10	2050
115	prnn_synth	250	3	750
116	profb	672	10	6720
117	ring	7400	21	155400
118	saheart	462	10	4620
119	satimage	6435	37	238095
120	schizo	340	15	5100
121	segmentation	2310	20	46200
122	solar_flare_1	315	13	4095
123	solar_flare_2	1066	13	13858
124	sonar	208	61	12688
125	soybean	675	36	24300
126	spambase	4601	58	266858
127	spect	267	23	6141
128	spectf	349	45	15705
129	splice	3188	61	194468
130	tae	151	6	906
131	texture	5500	41	225500
132	threeOf9	512	10	5120
133	tic_tac_toe	958	10	9580
134	tokyo1	959	45	43155
135	twonorm	7400	21	155400
136	vehicle	846	19	16074
137	vote	435	17	7395
138	vowel	990	14	13860
139	waveform_21	5000	22	110000
140	waveform_40	5000	41	205000
141	wdbc	569	31	17639
142	wine_quality_red	1599	12	19188
143	wine_quality_white	4898	12	58776
144	wine_recognition	178	14	2492
145	xdb	973	10	9730
146	yeast	1479	9	13311

D. Detailed Information about the PMLB Regression Datasets

	Dataset Name	Rows	Columns	Rows × Columns
1	1027_ESL	488	5	2440
2	1028_SWD	1000	11	11000
3	1029_LEV	1000	5	5000
4	1030_ERA	1000	5	5000
5	1089_USCrime	47	14	658
6	1096_FacultySalaries	50	5	250
7	1199_BNG_echoMonths	17496	10	174960
8	192_vineyard	52	3	156
9	197_cpu_act	8192	22	180224
10	210_cloud	108	6	648
11	225_puma8NH	8192	9	73728
12	227_cpu_small	8192	13	106496
13	228_elusage	55	3	165
14	229_pwLinear	200	11	2200
15	294_satellite_image	6435	37	238095
16	4544_GeographicalOriginalofMusic	1059	118	124962
17	503_wind	6574	15	98610
18	505_tecator	240	125	30000
19	519_vinnie	380	3	1140
20	522_pm10	500	8	4000
21	523_analcatdata_neavote	100	3	300
22	529_pollen	3848	5	19240
23	547_no2	500	8	4000
24	560_bodyfat	252	15	3780
25	562_cpu_small	8192	13	106496
26	573_cpu_act	8192	22	180224
27	579_fri_c0_250_5	250	6	1500
28	581_fri_c3_500_25	500	26	13000
29	582_fri_c1_500_25	500	26	13000
30	583_fri_c1_1000_50	1000	51	51000
31	584_fri_c4_500_25	500	26	13000
32	586_fri_c3_1000_25	1000	26	26000
33	588_fri_c4_1000_100	1000	101	101000
34	589_fri_c2_1000_25	1000	26	26000
35	590_fri_c0_1000_50	1000	51	51000
36	591_fri_c1_100_10	100	11	1100
37	592_fri_c4_1000_25	1000	26	26000
38	593_fri_c1_1000_10	1000	11	11000
39	594_fri_c2_100_5	100	6	600
40	595_fri_c0_1000_10	1000	11	11000
41	596_fri_c2_250_5	250	6	1500
42	597_fri_c2_500_5	500	6	3000
43	598_fri_c0_1000_25	1000	26	26000
44	599_fri_c2_1000_5	1000	6	6000
45	601_fri_c1_250_5	250	6	1500
46	602_fri_c3_250_10	250	11	2750
47	603_fri_c0_250_50	250	51	12750
48	604_fri_c4_500_10	500	11	5500
49	605_fri_c2_250_25	250	26	6500
50	606_fri_c2_1000_10	1000	11	11000
51	607_fri_c4_1000_50	1000	51	51000
52	608_fri_c3_1000_10	1000	11	11000
53	609_fri_c0_1000_5	1000	6	6000
54	611_fri_c3_100_5	100	6	600

	Dataset Name	Rows	Columns	Rows × Columns
55	612_fri_c1_1000_5	1000	6	6000
56	613_fri_c3_250_5	250	6	1500
57	615_fri_c4_250_10	250	11	2750
58	616_fri_c4_500_50	500	51	25500
59	617_fri_c3_500_5	500	6	3000
60	618_fri_c3_1000_50	1000	51	51000
61	620_fri_c1_1000_25	1000	26	26000
62	621_fri_c0_100_10	100	11	1100
63	622_fri_c2_1000_50	1000	51	51000
64	623_fri_c4_1000_10	1000	11	11000
65	624_fri_c0_100_5	100	6	600
66	626_fri_c2_500_50	500	51	25500
67	627_fri_c2_500_10	500	11	5500
68	628_fri_c3_1000_5	1000	6	6000
69	631_fri_c1_500_5	500	6	3000
70	633_fri_c0_500_25	500	26	13000
71	634_fri_c2_100_10	100	11	1100
72	635_fri_c0_250_10	250	11	2750
73	637_fri_c1_500_50	500	51	25500
74	641_fri_c1_500_10	500	11	5500
75	643_fri_c2_500_25	500	26	13000
76	644_fri_c4_250_25	250	26	6500
77	645_fri_c3_500_50	500	51	25500
78	646_fri_c3_500_10	500	11	5500
79	647_fri_c1_250_10	250	11	2750
80	648_fri_c1_250_50	250	51	12750
81	649_fri_c0_500_5	500	6	3000
82	650_fri_c0_500_50	500	51	25500
83	651_fri_c0_100_25	100	26	2600
84	653_fri_c0_250_25	250	26	6500
85	654_fri_c0_500_10	500	11	5500
86	656_fri_c1_100_5	100	6	600
87	657_fri_c2_250_10	250	11	2750
88	658_fri_c3_250_25	250	26	6500
89	663_rabe_266	120	3	360
90	665_sleuth_case2002	147	7	1029
91	666_rmtsa_ladata	508	11	5588
92	678_visualizing_environmental	111	4	444
93	687_sleuth_ex1605	62	6	372
94	690_visualizing_galaxy	323	5	1615
95	695_chafield_4	235	13	3055
96	712_chscase_geyser1	222	3	666
97	feynman_III_12_43	100000	3	300000
98	feynman_III_15_12	100000	4	400000
99	feynman_III_15_14	100000	4	400000
100	feynman_III_15_27	100000	4	400000
101	feynman_III_17_37	100000	4	400000
102	feynman_III_7_38	100000	4	400000
103	feynman_III_8_54	100000	4	400000
104	feynman_II_10_9	100000	4	400000
105	feynman_II_11_28	100000	3	300000
106	feynman_II_13_23	100000	4	400000
107	feynman_II_13_34	100000	4	400000
108	feynman_II_15_4	100000	4	400000

	Dataset Name	Rows	Columns	Rows × Columns
109	feynman.II_15_5	100000	4	400000
110	feynman.II_24_17	100000	4	400000
111	feynman.II_27_16	100000	4	400000
112	feynman.II_27_18	100000	3	300000
113	feynman.II_34_2	100000	4	400000
114	feynman.II_34_29a	100000	4	400000
115	feynman.II_34_2a	100000	4	400000
116	feynman.II_37_1	100000	4	400000
117	feynman.II_38_14	100000	3	300000
118	feynman.II_3_24	100000	3	300000
119	feynman.II_4_23	100000	4	400000
120	feynman.II_8_31	100000	3	300000
121	feynman.II_8_7	100000	4	400000
122	feynman.II_10_7	100000	4	400000
123	feynman.II_12_1	100000	3	300000
124	feynman.II_12_4	100000	4	400000
125	feynman.II_12_5	100000	3	300000
126	feynman.II_14_3	100000	4	400000
127	feynman.II_14_4	100000	3	300000
128	feynman.II_15_10	100000	4	400000
129	feynman.II_16_6	100000	4	400000
130	feynman.II_18_12	100000	4	400000
131	feynman.II_25_13	100000	3	300000
132	feynman.II_26_2	100000	3	300000
133	feynman.II_27_6	100000	4	400000
134	feynman.II_29_4	100000	3	300000
135	feynman.II_30_3	100000	4	400000
136	feynman.II_30_5	100000	4	400000
137	feynman.II_34_1	100000	4	400000
138	feynman.II_34_14	100000	4	400000
139	feynman.II_34_27	100000	3	300000
140	feynman.II_37_4	100000	4	400000
141	feynman.II_39_1	100000	3	300000
142	feynman.II_39_11	100000	4	400000
143	feynman.II_43_31	100000	4	400000
144	feynman.II_47_23	100000	4	400000
145	feynman.II_48_2	100000	4	400000
146	feynman.II_6_2	100000	3	300000
147	feynman.II_6_2b	100000	4	400000
148	nikuradse_1	362	3	1086
149	strogatz_bacres1	400	3	1200
150	strogatz_bacres2	400	3	1200
151	strogatz_barmag1	400	3	1200
152	strogatz_barmag2	400	3	1200
153	strogatz_glider1	400	3	1200
154	strogatz_glider2	400	3	1200
155	strogatz_lv1	400	3	1200
156	strogatz_lv2	400	3	1200
157	strogatz_predprey1	400	3	1200
158	strogatz_predprey2	400	3	1200
159	strogatz_shearflow1	400	3	1200
160	strogatz_shearflow2	400	3	1200
161	strogatz_vdp1	400	3	1200
162	strogatz_vdp2	400	3	1200

E. Detailed Results: Classification

	Dataset Name	Algorithm	Mean Accuracy [0-1] \uparrow	Mean Precision \uparrow	Mean Recall \uparrow	Mean MCC \uparrow
1	GAMETES_Epistasis_2.Way_20atts_0.1H_EDM_1.1	Ours	0.653854	0.669697	0.655529	0.32489
2	GAMETES_Epistasis_2.Way_20atts_0.4H_EDM_1.1	Ours	0.759479	0.777411	0.761283	0.538387
3	GAMETES_Epistasis_3.Way_20atts_0.2H_EDM_1.1	Ours	0.659583	0.662087	0.660329	0.322405
4	GAMETES_Heterogeneity_20atts_1600.Het_0.4_0.2_...	Ours	0.691042	0.692929	0.691785	0.384708
5	GAMETES_Heterogeneity_20atts_1600.Het_0.4_0.2_...	Ours	0.671354	0.674906	0.672593	0.347478
6	Hill_Valley_with_noise	Ours	0.555693	0.56096	0.555904	0.116711
7	Hill_Valley_without_noise	Ours	0.634979	0.63918	0.635376	0.274511
8	agaricus_lepiota	Ours	0.999959	0.999961	0.999957	0.999918
9	allbp	Ours	0.96287	0.607804	0.511241	0.486371
10	allhyper	Ours	0.98	0.514222	0.470816	0.562103
11	allhypoth	Ours	0.956366	0.787001	0.737647	0.698695
12	allrep	Ours	0.967285	0.573905	0.476258	0.385945
13	analcatdata_aids	Ours	0.496667	0.575589	0.528433	0.127752
14	analcatdata_asbestos	Ours	0.747059	0.756768	0.759368	0.514386
15	analcatdata_authorship	Ours	0.998817	0.9992	0.99921	0.998268
16	analcatdata_bankruptcy	Ours	0.83	0.829187	0.813175	0.641827
17	analcatdata_boxing1	Ours	0.834722	0.826879	0.801451	0.625709
18	analcatdata_boxing2	Ours	0.771605	0.778168	0.769354	0.547147
19	analcatdata_creditscore	Ours	0.971667	0.947156	0.981818	0.925927
20	analcatdata_cyyoung8092	Ours	0.741667	0.642799	0.584171	0.224909
21	analcatdata_cyyoung9302	Ours	0.864912	0.755211	0.758342	0.505288
22	analcatdata_dmft	Ours	0.206875	0.209936	0.210983	0.053707
23	analcatdata_fraud	Ours	0.677778	0.631362	0.640972	0.246998
24	analcatdata_germangss	Ours	0.321667	0.389592	0.339092	0.129106
25	analcatdata_happiness	Ours	0.491667	0.493704	0.51127	0.30306
26	analcatdata_japansolvent	Ours	0.706061	0.72914	0.702196	0.4281
27	analcatdata_lawsuit	Ours	0.978616	0.913018	0.915771	0.82225
28	ann_thyroid	Ours	0.949676	0.872635	0.755052	0.664545
29	appendicitis	Ours	0.862121	0.749118	0.752361	0.492146
30	australian	Ours	0.853623	0.852566	0.852809	0.705318
31	auto	Ours	0.847967	0.857068	0.8448	0.802945
32	backache	Ours	0.819444	0.615342	0.562372	0.165026
33	balance_scale	Ours	0.890667	0.593734	0.642615	0.806576
34	banana	Ours	0.89978	0.902141	0.895135	0.79724
35	biomed	Ours	0.965079	0.968146	0.955684	0.923524
36	breast	Ours	0.959286	0.956566	0.953688	0.910165
37	breast_cancer	Ours	0.698851	0.622068	0.579049	0.194912
38	breast_cancer_wisconsin	Ours	0.961696	0.966384	0.952519	0.918735
39	breast_w	Ours	0.959286	0.955439	0.955047	0.910433
40	buggyCrx	Ours	0.849275	0.848633	0.850343	0.698912
41	bupa	Ours	0.589372	0.623767	0.597582	0.219039
42	calendarDOW	Ours	0.594583	0.575761	0.563412	0.489319
43	car	Ours	0.941522	0.863757	0.874365	0.874208
44	car_evaluation	Ours	0.950193	0.872229	0.916856	0.895672
45	cars	Ours	0.995359	0.995025	0.99148	0.991464
46	chess	Ours	0.985729	0.985873	0.985597	0.971471
47	churn	Ours	0.884433	0.780368	0.654586	0.414033
48	clean1	Ours	0.881944	0.883391	0.891644	0.774906
49	cleve	Ours	0.808197	0.808921	0.805756	0.614373
50	cleveland	Ours	0.535519	0.289752	0.288754	0.246545
51	cleveland_nominal	Ours	0.531694	0.281539	0.282674	0.23382
52	cloud	Ours	0.837879	0.845554	0.845053	0.788497
53	cmc	Ours	0.537401	0.520275	0.505161	0.276955
54	colic	Ours	0.820721	0.814725	0.801837	0.616045
55	collins	Ours	1	1	1	1
56	confidence	Ours	0.793333	0.796278	0.802759	0.760388
57	contraceptive	Ours	0.456384	0.438475	0.436322	0.156417
58	corral	Ours	1	1	1	1
59	credit_a	Ours	0.851449	0.851033	0.853532	0.704528
60	credit_g	Ours	0.727333	0.666042	0.640079	0.304229
61	crx	Ours	0.846377	0.846859	0.847505	0.694431
62	dermatology	Ours	0.954505	0.952888	0.954587	0.944266
63	diabetes	Ours	0.750866	0.732876	0.692291	0.422677
64	dis	Ours	0.984592	0.761389	0.645043	0.37364
65	ecoli	Ours	0.867677	0.852846	0.818471	0.814701
66	flags	Ours	0.425	0.413098	0.392699	0.254926
67	flare	Ours	0.806231	0.594014	0.542021	0.122528
68	german	Ours	0.723	0.667077	0.634947	0.299559
69	glass	Ours	0.69187	0.663835	0.65902	0.575001
70	glass2	Ours	0.80303	0.813394	0.80243	0.615146
71	haberman	Ours	0.734946	0.656579	0.588955	0.228624
72	hayes_roth	Ours	0.741667	0.807642	0.723313	0.593912
73	heart_c	Ours	0.808197	0.808419	0.801124	0.609371

	Dataset Name	Algorithm	Mean Accuracy [0-1] \uparrow	Mean Precision \uparrow	Mean Recall \uparrow	Mean MCC \uparrow
74	heart.h	Ours	0.79661	0.791894	0.765024	0.555181
75	heart.statlog	Ours	0.828395	0.832279	0.818623	0.650413
76	hepatitis	Ours	0.815054	0.716643	0.635302	0.335239
77	horse_colic	Ours	0.82027	0.814153	0.801003	0.614658
78	house_votes_84	Ours	0.95249	0.948284	0.952441	0.900652
79	hungarian	Ours	0.812429	0.803013	0.781021	0.582977
80	hypothyroid	Ours	0.972617	0.889952	0.795092	0.675621
81	ionosphere	Ours	0.901878	0.895478	0.892366	0.787616
82	iris	Ours	0.946667	0.948496	0.946156	0.921595
83	iris	Ours	1	1	1	1
84	kr_vs_kp	Ours	0.985573	0.985682	0.985419	0.971101
85	krkopt	Ours	0.695747	0.729317	0.62841	0.659415
86	labor	Ours	0.913889	0.906515	0.916243	0.818887
87	led24	Ours	0.723698	0.722053	0.723278	0.693398
88	led7	Ours	0.733542	0.733753	0.731413	0.704506
89	lupus	Ours	0.731481	0.719018	0.713359	0.427516
90	lymphography	Ours	0.801111	0.696942	0.711982	0.620561
91	magic	Ours	0.835156	0.849248	0.787159	0.633245
92	mfeat_fourier	Ours	0.843417	0.84611	0.844234	0.8265
93	mfeat_karhunen	Ours	0.973667	0.974178	0.973739	0.970786
94	mfeat_morphological	Ours	0.730333	0.731324	0.72966	0.701354
95	mfeat_zernike	Ours	0.825667	0.823871	0.826379	0.806484
96	mofn_3_7_10	Ours	1	1	1	1
97	molecular_biology_promoters	Ours	0.833333	0.85465	0.83638	0.689479
98	monk1	Ours	0.999107	0.999	0.999231	0.99823
99	monk2	Ours	0.81157	0.867278	0.736535	0.587969
100	monk3	Ours	0.980781	0.980822	0.980718	0.961539
101	movement_libras	Ours	0.814815	0.830163	0.823724	0.803783
102	mushroom	Ours	1	1	1	1
103	mux6	Ours	0.974359	0.975281	0.976794	0.951989
104	new_thyroid	Ours	0.94186	0.944832	0.905906	0.874122
105	nursery	Ours	0.965509	0.961679	0.882496	0.949436
106	page_blocks	Ours	0.963866	0.852621	0.794459	0.79896
107	parity5	Ours	0.952381	0.956111	0.97	0.924597
108	parity5-5	Ours	1	1	1	1
109	pendigits	Ours	0.993285	0.993397	0.993287	0.99254
110	phoneme	Ours	0.892969	0.877483	0.860792	0.738053
111	pima	Ours	0.745887	0.726364	0.688215	0.412293
112	postoperative_patient_data	Ours	0.75	0.37791	0.495556	-0.007968
113	prnn_crabs	Ours	0.9675	0.967838	0.96769	0.935501
114	prnn_fglass	Ours	0.687805	0.653144	0.655095	0.569007
115	prnn_synth	Ours	0.876667	0.879281	0.876959	0.756139
116	prof	Ours	0.640741	0.558732	0.535917	0.091385
117	ring	Ours	0.711644	0.817582	0.709742	0.515948
118	saheart	Ours	0.716846	0.692179	0.635139	0.321519
119	satimage	Ours	0.910282	0.897146	0.890226	0.889301
120	schizo	Ours	0.556373	0.426085	0.380525	0.077767
121	segmentation	Ours	0.970491	0.970609	0.970437	0.965598
122	solar_flare_1	Ours	0.695767	0.673568	0.650753	0.607893
123	solar_flare_2	Ours	0.716511	0.609754	0.585798	0.637871
124	sonar	Ours	0.810317	0.817667	0.810397	0.627877
125	soybean	Ours	0.908642	0.951553	0.940519	0.90012
126	spambase	Ours	0.916793	0.919352	0.90635	0.825531
127	spect	Ours	0.769753	0.677874	0.740606	0.412112
128	spectf	Ours	0.865238	0.83142	0.861399	0.690856
129	splice	Ours	0.913584	0.896234	0.932801	0.868379
130	tae	Ours	0.603226	0.619652	0.608631	0.418806
131	texture	Ours	0.987909	0.988061	0.987948	0.986709
132	threeOf9	Ours	0.984142	0.984099	0.984287	0.968383
133	tic_tac_toe	Ours	0.989062	0.990975	0.985149	0.976097
134	tokyo1	Ours	0.925	0.920875	0.915029	0.83581
135	twonorm	Ours	0.975518	0.975525	0.97553	0.951054
136	vehicle	Ours	0.714706	0.704578	0.724239	0.623572
137	vote	Ours	0.959004	0.956313	0.959582	0.915865
138	vowel	Ours	0.969529	0.97055	0.971676	0.966636
139	waveform_21	Ours	0.853967	0.860253	0.853314	0.785179
140	waveform_40	Ours	0.8584	0.86213	0.85963	0.790698
141	wdbc	Ours	0.960819	0.964085	0.952579	0.916542
142	wine_quality_red	Ours	0.66625	0.378358	0.337689	0.458883
143	wine_quality_white	Ours	0.625544	0.463491	0.361405	0.429912
144	wine_recognition	Ours	0.984259	0.982731	0.986844	0.97621
145	xd6	Ours	0.999829	0.999863	0.999775	0.999638
146	yeast	Ours	0.590991	0.5583	0.536017	0.467647

	Dataset Name	Algorithm	Mean Accuracy [0-1] \uparrow	Mean Precision \uparrow	Mean Recall \uparrow	Mean MCC \uparrow
1	GAMETES_Epistasis_2.Way_20atts_0.1H_EDM_1..1	GB	0.623229	0.624565	0.623842	0.248402
2	GAMETES_Epistasis_2.Way_20atts_0.4H_EDM_1..1	GB	0.726458	0.728732	0.726848	0.455558
3	GAMETES_Epistasis_3.Way_20atts_0.2H_EDM_1..1	GB	0.538438	0.538718	0.538705	0.077424
4	GAMETES_Heterogeneity_20atts_1600.Het_0.4_0.2....	GB	0.681458	0.682047	0.6818	0.363846
5	GAMETES_Heterogeneity_20atts_1600.Het_0.4_0.2....	GB	0.699792	0.700784	0.700226	0.401008
6	Hill_Valley_with_noise	GB	0.554321	0.555855	0.555435	0.111285
7	Hill_Valley_without_noise	GB	0.592044	0.592688	0.592331	0.185017
8	agaricus_lepiota	GB	0.999939	0.999944	0.999932	0.999876
9	allbp	GB	0.95766	0.590159	0.443807	0.342181
10	allhyper	GB	0.970508	0.423912	0.353124	0.206518
11	allhypoth	GB	0.953714	0.811196	0.641956	0.644284
12	allrep	GB	0.969581	0.609249	0.364862	0.302243
13	analcatdata_aids	GB	0.583333	0.589636	0.580516	0.182331
14	analcatdata_asbestos	GB	0.747059	0.747547	0.751964	0.49769
15	analcatdata_authorship	GB	0.984615	0.985233	0.969084	0.977613
16	analcatdata_bankruptcy	GB	0.83	0.824993	0.822897	0.649452
17	analcatdata_boxing1	GB	0.813889	0.812901	0.779798	0.588689
18	analcatdata_boxing2	GB	0.777778	0.78448	0.777737	0.561874
19	analcatdata_creditscore	GB	0.968333	0.961483	0.960753	0.91991
20	analcatdata_cyyoung8092	GB	0.775	0.717926	0.682384	0.398269
21	analcatdata_cyyoung9302	GB	0.822807	0.675207	0.653659	0.328368
22	analcatdata_dmft	GB	0.178542	0.183872	0.180861	0.015109
23	analcatdata_fraud	GB	0.648148	0.500728	0.543459	0.10025
24	analcatdata_germangss	GB	0.379583	0.389557	0.387283	0.183886
25	analcatdata_happiness	GB	0.416667	0.416698	0.421005	0.175526
26	analcatdata_japansolvent	GB	0.784848	0.792169	0.779848	0.568687
27	analcatdata_lawsuit	GB	0.97673	0.90845	0.913457	0.80917
28	ann_thyroid	GB	0.996366	0.975408	0.988119	0.974825
29	appendicitis	GB	0.859091	0.77631	0.739596	0.499832
30	australian	GB	0.849034	0.847615	0.84868	0.696252
31	auto	GB	0.769919	0.773981	0.757548	0.701018
32	backache	GB	0.841667	0.460661	0.509057	0.029151
33	balance_scale	GB	0.865333	0.606516	0.631755	0.758318
34	banana	GB	0.900314	0.90167	0.89636	0.798009
35	biomed	GB	0.894444	0.892326	0.87181	0.762962
36	breast	GB	0.960476	0.955636	0.957545	0.913107
37	breast_cancer	GB	0.705172	0.6248	0.560431	0.175343
38	breast_cancer_wisconsin	GB	0.963158	0.964401	0.957024	0.921303
39	breast_w	GB	0.961429	0.957154	0.958785	0.915855
40	buggyCrx	GB	0.858696	0.859042	0.86369	0.722678
41	bupa	GB	0.583575	0.591633	0.589798	0.181393
42	calendarDOW	GB	0.61625	0.62223	0.584366	0.517025
43	car	GB	0.994509	0.978554	0.981028	0.988196
44	car_evaluation	GB	0.993064	0.979688	0.974963	0.985009
45	cars	GB	0.994515	0.997182	0.989806	0.989731
46	chess	GB	0.995104	0.995157	0.995047	0.990204
47	churn	GB	0.9474	0.938357	0.832441	0.763161
48	clean1	GB	0.987153	0.985786	0.988452	0.974225
49	cleve	GB	0.791803	0.793232	0.793268	0.586226
50	cleveland	GB	0.546448	0.270395	0.275676	0.22961
51	cleveland_nominal	GB	0.537705	0.238366	0.26069	0.193917
52	cloud	GB	0.818182	0.828609	0.829335	0.762896
53	cmc	GB	0.557966	0.54335	0.527052	0.31305
54	colic	GB	0.826126	0.824393	0.806089	0.629612
55	collins	GB	0.998282	0.998984	0.99794	0.998115
56	confidence	GB	0.737778	0.750556	0.75937	0.699787
57	contraceptive	GB	0.521921	0.499421	0.489867	0.253712
58	corral	GB	0.997917	0.998039	0.998039	0.996078
59	credit_a	GB	0.851208	0.851167	0.854755	0.705898
60	credit_g	GB	0.751833	0.701701	0.66482	0.363336
61	crx	GB	0.848792	0.849765	0.851219	0.700959
62	dermatology	GB	0.972072	0.967065	0.970117	0.965051
63	diabetes	GB	0.762987	0.744642	0.716934	0.460197
64	dis	GB	0.981987	0.65732	0.579602	0.214954
65	ecoli	GB	0.870707	0.849951	0.806586	0.819111
66	flags	GB	0.450926	0.394487	0.385558	0.280164
67	flare	GB	0.826791	0.473673	0.515531	0.047305
68	german	GB	0.751833	0.710151	0.664039	0.370144
69	glass	GB	0.760163	0.70551	0.667744	0.662973
70	glass2	GB	0.853535	0.851578	0.853562	0.704992
71	haberman	GB	0.72043	0.466626	0.525402	0.059925
72	hayes_roth	GB	0.814583	0.851083	0.849469	0.715987
73	heart_c	GB	0.803825	0.801057	0.7984	0.599376

	Dataset Name	Algorithm	Mean Accuracy [0-1] \uparrow	Mean Precision \uparrow	Mean Recall \uparrow	Mean MCC \uparrow
74	heart.h	GB	0.810734	0.802262	0.788048	0.589686
75	heart.statlog	GB	0.809259	0.810886	0.801569	0.611764
76	hepatitis	GB	0.809677	0.679517	0.615463	0.297586
77	horse_colic	GB	0.825676	0.824893	0.803777	0.627761
78	house_votes_84	GB	0.956322	0.952215	0.956129	0.908305
79	hungarian	GB	0.822599	0.812434	0.796415	0.608083
80	hypothyroid	GB	0.960295	0.821943	0.690758	0.492934
81	ionosphere	GB	0.930047	0.934373	0.912484	0.846345
82	iris	GB	0.941111	0.942046	0.940897	0.912551
83	irish	GB	1	1	1	1
84	kr_vs_kp	GB	0.995833	0.995906	0.995753	0.991659
85	krkopt	GB	0.741625	0.760553	0.740988	0.711356
86	labor	GB	0.858333	0.853776	0.853226	0.698621
87	led24	GB	0.72375	0.72816	0.723058	0.693332
88	led7	GB	0.735573	0.743535	0.73404	0.707107
89	lupus	GB	0.711111	0.709199	0.67349	0.377305
90	lymphography	GB	0.841111	0.807208	0.820962	0.698158
91	magic	GB	0.882404	0.881367	0.858048	0.739042
92	mfeat_fourier	GB	0.8295	0.834299	0.829938	0.810929
93	mfeat_karhunen	GB	0.9455	0.945762	0.946128	0.939481
94	mfeat_morphological	GB	0.725333	0.723968	0.726472	0.698335
95	mfeat_zernike	GB	0.78575	0.793694	0.786749	0.762353
96	mofn_3_7_10	GB	1	1	1	1
97	molecular_biology_promoters	GB	0.868182	0.868368	0.876079	0.743991
98	monk1	GB	1	1	1	1
99	monk2	GB	0.990909	0.989906	0.991143	0.981029
100	monk3	GB	0.989189	0.989524	0.988837	0.97836
101	movement_libras	GB	0.694444	0.708348	0.704736	0.674975
102	mushroom	GB	0.999795	0.999802	0.999787	0.99959
103	mux6	GB	0.997436	0.997778	0.997436	0.995212
104	new_thyroid	GB	0.945736	0.941511	0.924322	0.886921
105	nursery	GB	0.999961	0.999969	0.99997	0.999943
106	page_blocks	GB	0.972664	0.868281	0.827087	0.850277
107	parity5	GB	0.090476	0.067937	0.117778	-0.796165
108	parity5-5	GB	0.418667	0.365513	0.436051	-0.148251
109	pendigits	GB	0.992345	0.992358	0.992296	0.991493
110	phoneme	GB	0.875948	0.851969	0.848601	0.700499
111	pima	GB	0.761255	0.74057	0.714152	0.453575
112	postoperative_patient_data	GB	0.753704	0.378159	0.497421	-0.010038
113	prnn_crabs	GB	0.900833	0.899298	0.902222	0.801455
114	prnn_fglass	GB	0.752846	0.707223	0.675052	0.652292
115	prnn_synth	GB	0.850667	0.853065	0.852173	0.705186
116	profB	GB	0.681975	0.63178	0.597035	0.220191
117	ring	GB	0.969257	0.969738	0.96917	0.938908
118	saheart	GB	0.70681	0.67291	0.639235	0.309307
119	satimage	GB	0.914193	0.901445	0.893554	0.894136
120	schizo	GB	0.593137	0.201384	0.331625	-0.011261
121	segmentation	GB	0.981097	0.981188	0.980893	0.977969
122	solarflare_1	GB	0.726455	0.683291	0.670855	0.647261
123	solarflare_2	GB	0.750623	0.645701	0.601199	0.682929
124	sonar	GB	0.842063	0.852871	0.841717	0.694243
125	soybean	GB	0.926914	0.961583	0.947355	0.920555
126	spambase	GB	0.952805	0.951705	0.949151	0.900847
127	spect	GB	0.825309	0.723452	0.687107	0.404084
128	spectf	GB	0.885238	0.85755	0.861073	0.717264
129	splice	GB	0.966092	0.959544	0.965494	0.945171
130	tae	GB	0.570968	0.576691	0.571238	0.362031
131	texture	GB	0.987394	0.987468	0.987381	0.98614
132	threeOf9	GB	0.999029	0.998991	0.999088	0.998079
133	tic_tac_toe	GB	1	1	1	1
134	tokyo1	GB	0.924132	0.919607	0.914589	0.834114
135	twonorm	GB	0.9725	0.972497	0.97251	0.945006
136	vehicle	GB	0.757843	0.760925	0.766135	0.677476
137	vote	GB	0.955556	0.95252	0.956258	0.908732
138	vowel	GB	0.904209	0.907806	0.907502	0.894871
139	waveform_21	GB	0.849167	0.849025	0.848961	0.773966
140	waveform_40	GB	0.856067	0.856348	0.856601	0.784493
141	wdbc	GB	0.963743	0.965021	0.957761	0.922668
142	wine_quality_red	GB	0.669896	0.37233	0.355688	0.474829
143	wine_quality_white	GB	0.655816	0.467276	0.390307	0.47736
144	wine_recognition	GB	0.941667	0.944792	0.945446	0.912963
145	xd6	GB	1	1	1	1
146	yeast	GB	0.597973	0.558935	0.518458	0.47637

	Dataset Name	Algorithm	Mean Accuracy [0-1] \uparrow	Mean Precision \uparrow	Mean Recall \uparrow	Mean MCC \uparrow
1	GAMETES_Epistasis_2.Way_20atts_0.1H_EDM_1..1	KNN	0.575208	0.580815	0.576832	0.157566
2	GAMETES_Epistasis_2.Way_20atts_0.4H_EDM_1..1	KNN	0.700521	0.707414	0.702078	0.409406
3	GAMETES_Epistasis_3.Way_20atts_0.2H_EDM_1..1	KNN	0.54875	0.550881	0.549925	0.100793
4	GAMETES_Heterogeneity_20atts_1600.Het_0.4_0.2....	KNN	0.635208	0.637862	0.636591	0.274444
5	GAMETES_Heterogeneity_20atts_1600.Het_0.4_0.2....	KNN	0.641563	0.644375	0.642843	0.287202
6	Hill_Valley_with_noise	KNN	0.58011	0.58036	0.580044	0.160401
7	Hill_Valley_without_noise	KNN	0.625652	0.626107	0.625637	0.251741
8	agaricus_lepiota	KNN	1	1	1	1
9	allbp	KNN	0.960839	0.594804	0.410202	0.357546
10	allhyper	KNN	0.973201	0.356974	0.296536	0.074057
11	allhypoth	KNN	0.922016	0.381923	0.335883	0.030621
12	allrep	KNN	0.967329	0.291937	0.260474	0.052416
13	analcatdata_aids	KNN	0.296667	0.310278	0.291746	-0.38327
14	analcatdata_asbestos	KNN	0.764706	0.761949	0.763459	0.524178
15	analcatdata_authorship	KNN	0.99645	0.996997	0.995303	0.994826
16	analcatdata_bankruptcy	KNN	0.84	0.830575	0.839841	0.670505
17	analcatdata_boxing1	KNN	0.715278	0.706486	0.667477	0.364821
18	analcatdata_boxing2	KNN	0.681481	0.697911	0.688397	0.385563
19	analcatdata_creditscore	KNN	0.975	0.959535	0.976108	0.933492
20	analcatdata_cyyoung8092	KNN	0.738333	0.677489	0.598784	0.265392
21	analcatdata_cyyoung9302	KNN	0.859649	0.75266	0.739636	0.488029
22	analcatdata_dmft	KNN	0.182292	0.197581	0.185948	0.019608
23	analcatdata_fraud	KNN	0.688889	0.576025	0.591276	0.199142
24	analcatdata_germangss	KNN	0.30125	0.308871	0.310429	0.079609
25	analcatdata_happiness	KNN	0.458333	0.469555	0.460833	0.22387
26	analcatdata_japansolvent	KNN	0.712121	0.744517	0.701263	0.438671
27	analcatdata_lawsuit	KNN	0.977358	0.906733	0.913347	0.810517
28	ann_thyroid	KNN	0.940208	0.832906	0.571052	0.463327
29	appendicitis	KNN	0.860606	0.741393	0.755686	0.486307
30	australian	KNN	0.72343	0.728803	0.709709	0.4379
31	auto	KNN	0.579675	0.594855	0.540941	0.449717
32	backache	KNN	0.848148	0.615213	0.553968	0.167803
33	balance_scale	KNN	0.8944	0.596403	0.645229	0.813959
34	banana	KNN	0.901006	0.902585	0.896997	0.799558
35	biomed	KNN	0.957143	0.961794	0.944795	0.906047
36	breast	KNN	0.661905	0.613687	0.586445	0.197624
37	breast_cancer	KNN	0.721264	0.666939	0.592926	0.247492
38	breast_cancer_wisconsin	KNN	0.929825	0.934065	0.916267	0.849919
39	breast_w	KNN	0.965476	0.961363	0.9628	0.924101
40	buggyCrx	KNN	0.757729	0.760932	0.748297	0.50896
41	bupa	KNN	0.572464	0.59432	0.581677	0.175034
42	calendarDOW	KNN	0.610833	0.592366	0.584055	0.510121
43	car	KNN	0.927168	0.895108	0.703662	0.838492
44	car_evaluation	KNN	0.922158	0.919812	0.711223	0.825496
45	cars	KNN	0.722363	0.640956	0.617134	0.483621
46	chess	KNN	0.964323	0.964682	0.963998	0.928678
47	churn	KNN	0.8914	0.868898	0.628793	0.434725
48	clean1	KNN	0.857292	0.858204	0.865504	0.723617
49	cleve	KNN	0.683607	0.684074	0.682067	0.365891
50	cleveland	KNN	0.527869	0.161106	0.21256	0.070687
51	cleveland_nominal	KNN	0.545902	0.290312	0.289269	0.248132
52	cloud	KNN	0.771212	0.781427	0.776051	0.699808
53	cmc	KNN	0.52226	0.505838	0.494587	0.260738
54	colic	KNN	0.806306	0.80382	0.782485	0.585441
55	collins	KNN	0.991409	0.989001	0.990664	0.990539
56	confidence	KNN	0.788889	0.804741	0.799648	0.753815
57	contraceptive	KNN	0.479322	0.457819	0.448306	0.183288
58	corral	KNN	0.9375	0.939173	0.936509	0.875434
59	credit_a	KNN	0.755072	0.759579	0.743276	0.502428
60	credit_g	KNN	0.7035	0.59722	0.518064	0.082173
61	crx	KNN	0.764493	0.769839	0.754682	0.524168
62	dermatology	KNN	0.966216	0.962508	0.961136	0.958376
63	diabetes	KNN	0.741558	0.724068	0.685483	0.406733
64	dis	KNN	0.984459	0.492425	0.499798	-0.001237
65	ecoli	KNN	0.874747	0.855106	0.83126	0.824807
66	flags	KNN	0.437037	0.400088	0.381754	0.268685
67	flare	KNN	0.815576	0.620187	0.550175	0.153951
68	german	KNN	0.694167	0.605427	0.51138	0.066478
69	glass	KNN	0.708943	0.660893	0.665182	0.598934
70	glass2	KNN	0.836364	0.838123	0.832347	0.669981
71	haberman	KNN	0.74086	0.658995	0.592716	0.237863
72	hayes_roth	KNN	0.703125	0.744172	0.672182	0.532058
73	heart_c	KNN	0.693443	0.693642	0.682456	0.375656

	Dataset Name	Algorithm	Mean Accuracy [0-1] \uparrow	Mean Precision \uparrow	Mean Recall \uparrow	Mean MCC \uparrow
74	heart.h	KNN	0.79096	0.785242	0.758757	0.542648
75	heart.statlog	KNN	0.701235	0.699152	0.692409	0.391261
76	hepatitis	KNN	0.823656	0.777807	0.633933	0.371221
77	horse_colic	KNN	0.8	0.796235	0.773937	0.569391
78	house_votes_84	KNN	0.918774	0.912232	0.919218	0.831325
79	hungarian	KNN	0.811299	0.802042	0.776375	0.577313
80	hypothyroid	KNN	0.957609	0.890294	0.604244	0.38972
81	ionosphere	KNN	0.899531	0.918884	0.866985	0.783441
82	iris	KNN	0.96	0.959955	0.961187	0.940858
83	irish	KNN	0.895333	0.893324	0.899321	0.792576
84	kr_vs_kw	KNN	0.962708	0.963357	0.962118	0.925472
85	krkopt	KNN	0.694393	0.723243	0.616437	0.657941
86	labor	KNN	0.902778	0.88994	0.904609	0.790458
87	led24	KNN	0.719375	0.71828	0.719201	0.688519
88	led7	KNN	0.734844	0.735903	0.732953	0.706234
89	lupus	KNN	0.707407	0.697309	0.678856	0.370492
90	lymphography	KNN	0.828889	0.665212	0.669381	0.663572
91	magic	KNN	0.820128	0.836148	0.766126	0.598151
92	mfeat_fourier	KNN	0.843167	0.845374	0.844022	0.826185
93	mfeat_karhunen	KNN	0.974167	0.974626	0.974237	0.971342
94	mfeat_morphological	KNN	0.49625	0.503202	0.499322	0.442156
95	mfeat_zernike	KNN	0.80375	0.803931	0.804011	0.782129
96	mofn_3_7_10	KNN	0.94956	0.942055	0.905287	0.845842
97	molecular_biology_promoters	KNN	0.787879	0.807907	0.796693	0.603439
98	monk1	KNN	0.977976	0.978604	0.978628	0.957228
99	monk2	KNN	0.819284	0.888553	0.741561	0.611311
100	monk3	KNN	0.967568	0.967501	0.967727	0.935225
101	movement_libras	KNN	0.834722	0.846461	0.846434	0.824496
102	mushroom	KNN	1	1	1	1
103	mx6	KNN	0.964103	0.965422	0.967609	0.93287
104	new_thyroid	KNN	0.952713	0.950851	0.926477	0.899944
105	nursery	KNN	0.971052	0.97872	0.831748	0.957694
106	page_blocks	KNN	0.960974	0.854309	0.745411	0.778077
107	parity5	KNN	0.295238	0.302262	0.331111	-0.353682
108	parity5-5	KNN	0.564148	0.568952	0.564415	0.133119
109	pendigits	KNN	0.993406	0.993464	0.993404	0.992673
110	phoneme	KNN	0.899414	0.884585	0.870135	0.754534
111	pima	KNN	0.749351	0.73247	0.688519	0.41817
112	postoperative_patient_data	KNN	0.694444	0.371555	0.459955	-0.107881
113	prnn_crabs	KNN	0.9575	0.956101	0.959952	0.916017
114	prnn_fglass	KNN	0.708943	0.661658	0.675863	0.600603
115	prnn_synth	KNN	0.880667	0.883485	0.88098	0.764359
116	prof	KNN	0.665679	0.609744	0.527343	0.107218
117	ring	KNN	0.74464	0.827009	0.743116	0.563877
118	saheart	KNN	0.666667	0.579849	0.550582	0.141674
119	satimage	KNN	0.910256	0.896759	0.892094	0.889304
120	schizo	KNN	0.594118	0.199057	0.331733	-0.00342
121	segmentation	KNN	0.970635	0.970616	0.970609	0.965743
122	solar_flare_1	KNN	0.710582	0.662313	0.649605	0.626002
123	solar_flare_2	KNN	0.735981	0.609737	0.583493	0.66378
124	sonar	KNN	0.834127	0.83663	0.832012	0.668502
125	soybean	KNN	0.912346	0.945973	0.934624	0.90453
126	spambase	KNN	0.929099	0.929205	0.921804	0.850957
127	spect	KNN	0.803704	0.682675	0.67267	0.3521
128	spectf	KNN	0.902857	0.909448	0.858244	0.761771
129	splice	KNN	0.915569	0.898316	0.932485	0.870437
130	tae	KNN	0.595699	0.607383	0.598616	0.401498
131	texture	KNN	0.990879	0.990947	0.990867	0.989972
132	threeOf9	KNN	0.973463	0.974155	0.97316	0.947306
133	tic_tac_toe	KNN	0.973785	0.974429	0.968572	0.942939
134	tokyo1	KNN	0.914062	0.905875	0.90773	0.813534
135	twonorm	KNN	0.976171	0.976173	0.976199	0.952372
136	vehicle	KNN	0.683529	0.678035	0.694529	0.579958
137	vote	KNN	0.924521	0.919829	0.926626	0.846383
138	vowel	KNN	0.988215	0.988325	0.988808	0.987057
139	waveform_21	KNN	0.855633	0.862016	0.85494	0.787715
140	waveform_40	KNN	0.858433	0.861729	0.859645	0.790496
141	wdbc	KNN	0.930117	0.932585	0.917786	0.850077
142	wine_quality_red	KNN	0.645208	0.400918	0.317696	0.418081
143	wine_quality_white	KNN	0.629558	0.617262	0.340278	0.424703
144	wine_recognition	KNN	0.962037	0.965207	0.966592	0.943086
145	xd6	KNN	0.999316	0.999478	0.999029	0.998505
146	yeast	KNN	0.607545	0.565962	0.516628	0.488806

	Dataset Name	Algorithm	Mean Accuracy [0-1] \uparrow	Mean Precision \uparrow	Mean Recall \uparrow	Mean MCC \uparrow
1	GAMETES_Epistasis_2.Way_20atts_0.1H_EDM_1.1	Linear	0.480938	0.458951	0.48729	-0.028143
2	GAMETES_Epistasis_2.Way_20atts_0.4H_EDM_1.1	Linear	0.473333	0.496988	0.479564	-0.039612
3	GAMETES_Epistasis_3.Way_20atts_0.2H_EDM_1.1	Linear	0.505729	0.507804	0.507221	0.014985
4	GAMETES_Heterogeneity_20atts_1600.Het_0.4_0.2....	Linear	0.478437	0.48032	0.485211	-0.030165
5	GAMETES_Heterogeneity_20atts_1600.Het_0.4_0.2....	Linear	0.484792	0.479447	0.490373	-0.01969
6	Hill_Valley_with_noise	Linear	0.750754	0.822602	0.752891	0.570721
7	Hill_Valley_without_noise	Linear	0.707133	0.810475	0.709951	0.510171
8	agaricus_lepiota	Linear	0.999795	0.999807	0.999782	0.999589
9	allbp	Linear	0.961943	0.583252	0.435259	0.409765
10	allhyper	Linear	0.974923	0.487764	0.368148	0.297414
11	allhypoth	Linear	0.96702	0.83573	0.798871	0.772537
12	allrep	Linear	0.970508	0.683944	0.352076	0.311429
13	analcatdata_aids	Linear	0.496667	0.512831	0.534504	0.114762
14	analcatdata_asbestos	Linear	0.752941	0.764759	0.771761	0.53506
15	analcatdata_authorship	Linear	0.997041	0.997884	0.997759	0.995666
16	analcatdata_bankruptcy	Linear	0.89	0.900066	0.871944	0.772301
17	analcatdata_boxing1	Linear	0.838889	0.831318	0.809579	0.638054
18	analcatdata_boxing2	Linear	0.77284	0.77663	0.775514	0.551979
19	analcatdata_creditscore	Linear	0.915	0.888418	0.923768	0.806581
20	analcatdata_cyyoung8092	Linear	0.748333	0.71625	0.618471	0.310801
21	analcatdata_cyyoung9302	Linear	0.859649	0.760837	0.770128	0.520873
22	analcatdata_dmft	Linear	0.19	0.164537	0.194179	0.033217
23	analcatdata_fraud	Linear	0.67037	0.481918	0.551085	0.111244
24	analcatdata_germangss	Linear	0.372917	0.374384	0.377683	0.17133
25	analcatdata_happiness	Linear	0.469444	0.499339	0.480794	0.265205
26	analcatdata_japansolvent	Linear	0.787879	0.795813	0.777249	0.569436
27	analcatdata_lawsuit	Linear	0.978616	0.916424	0.921551	0.828755
28	ann_thyroid	Linear	0.955069	0.868876	0.70503	0.635564
29	appendicitis	Linear	0.872727	0.788722	0.761552	0.537643
30	australian	Linear	0.849758	0.848129	0.849725	0.697812
31	auto	Linear	0.752033	0.758928	0.751128	0.678864
32	backache	Linear	0.839815	0.438873	0.500904	0.005885
33	balance_scale	Linear	0.985067	0.944644	0.989285	0.974323
34	banana	Linear	0.574811	0.642197	0.526298	0.113951
35	biomed	Linear	0.736508	0.71901	0.706934	0.423777
36	breast	Linear	0.96119	0.958669	0.955371	0.913977
37	breast_cancer	Linear	0.69023	0.535635	0.53289	0.101867
38	breast_cancer_wisconsin	Linear	0.974269	0.97617	0.969331	0.945425
39	breast_w	Linear	0.964048	0.96164	0.959009	0.920576
40	buggyCrx	Linear	0.849517	0.84847	0.84804	0.696465
41	bupa	Linear	0.613043	0.620401	0.618705	0.239021
42	calendarDOW	Linear	0.624583	0.61399	0.605714	0.530132
43	car	Linear	0.917341	0.872273	0.863776	0.820822
44	car_evaluation	Linear	0.921291	0.855849	0.854512	0.827701
45	cars	Linear	0.992405	0.991843	0.9892	0.986014
46	chess	Linear	0.972656	0.972628	0.972708	0.945335
47	churn	Linear	0.864333	0.809637	0.513192	0.125185
48	clean1	Linear	0.971181	0.969412	0.972937	0.942318
49	cleve	Linear	0.851366	0.849208	0.851395	0.700411
50	cleveland	Linear	0.572678	0.282709	0.299559	0.293684
51	cleveland_nominal	Linear	0.563388	0.279341	0.293658	0.255622
52	cloud	Linear	0.342424	0.353508	0.358721	0.142428
53	cmc	Linear	0.501356	0.485464	0.472785	0.218378
54	colic	Linear	0.812162	0.808513	0.788018	0.595843
55	collins	Linear	1	1	1	1
56	confidence	Linear	0.791111	0.773889	0.793056	0.759626
57	contraceptive	Linear	0.540565	0.518234	0.509752	0.28441
58	corral	Linear	0.882292	0.880782	0.883999	0.764551
59	credit_a	Linear	0.852415	0.851813	0.850519	0.702298
60	credit_g	Linear	0.757333	0.710864	0.665865	0.372272
61	crx	Linear	0.85	0.850795	0.846674	0.697414
62	dermatology	Linear	0.969369	0.966814	0.96621	0.961977
63	diabetes	Linear	0.768831	0.753791	0.717294	0.469189
64	dis	Linear	0.984857	0.492428	0.5	0
65	ecoli	Linear	0.885859	0.87216	0.85102	0.841187
66	flags	Linear	0.462037	0.348462	0.377677	0.287972
67	flare	Linear	0.829283	0.595478	0.535652	0.12783
68	german	Linear	0.753167	0.708126	0.670058	0.375508
69	glass	Linear	0.621138	0.535314	0.528464	0.461073
70	glass2	Linear	0.684848	0.693779	0.689655	0.383066
71	haberman	Linear	0.731183	0.603774	0.540267	0.131531
72	hayes_roth	Linear	0.521875	0.555751	0.568605	0.265495
73	heart_c	Linear	0.847541	0.846791	0.841921	0.688653

	Dataset Name	Algorithm	Mean Accuracy [0-1] \uparrow	Mean Precision \uparrow	Mean Recall \uparrow	Mean MCC \uparrow
74	heart.h	Linear	0.819774	0.81881	0.789051	0.606259
75	heart.statlog	Linear	0.842593	0.84248	0.835538	0.677814
76	hepatitis	Linear	0.825806	0.718776	0.661382	0.373473
77	horse_colic	Linear	0.813964	0.8109	0.789035	0.599212
78	house_votes_84	Linear	0.952107	0.948088	0.951188	0.899222
79	hungarian	Linear	0.837853	0.835924	0.803843	0.638102
80	hypothyroid	Linear	0.972828	0.879405	0.809378	0.683784
81	ionosphere	Linear	0.881221	0.897518	0.84736	0.742733
82	iris	Linear	0.961111	0.96375	0.963009	0.943526
83	iris	Linear	1	1	1	1
84	kr_vs_kw	Linear	0.97151	0.971492	0.971469	0.94296
85	krkopt	Linear	0.404936	0.417892	0.412894	0.332323
86	labor	Linear	0.925	0.91797	0.926321	0.84014
87	led24	Linear	0.725365	0.724639	0.725013	0.695144
88	led7	Linear	0.739688	0.741364	0.736986	0.711586
89	lupus	Linear	0.764815	0.755433	0.746526	0.499081
90	lymphography	Linear	0.835556	0.723817	0.725014	0.684257
91	magic	Linear	0.790124	0.781407	0.745224	0.525377
92	mfeat_fourier	Linear	0.8195	0.820409	0.820496	0.799844
93	mfeat_karhunen	Linear	0.948167	0.948802	0.948749	0.942459
94	mfeat_morphological	Linear	0.74125	0.747294	0.743323	0.71533
95	mfeat_zernike	Linear	0.821	0.817336	0.821383	0.801516
96	mofn_3_7_10	Linear	1	1	1	1
97	molecular_biology_promoters	Linear	0.919697	0.924414	0.921116	0.845227
98	monk1	Linear	0.738393	0.826608	0.741431	0.561117
99	monk2	Linear	0.65427	0.327135	0.5	0
100	monk3	Linear	0.97958	0.979676	0.979446	0.959118
101	movement_libras	Linear	0.741204	0.756347	0.754199	0.724956
102	mushroom	Linear	0.999754	0.999763	0.999745	0.999508
103	mx6	Linear	0.619231	0.62953	0.630525	0.25987
104	new_thyroid	Linear	0.95814	0.952671	0.940826	0.912416
105	nursery	Linear	0.924884	0.903061	0.874039	0.889699
106	page_blocks	Linear	0.962861	0.869096	0.741621	0.790378
107	parity5	Linear	0.295238	0.161111	0.411111	-0.177778
108	parity5-5	Linear	0.465037	0.260692	0.491501	-0.017747
109	pendigits	Linear	0.955556	0.954989	0.955076	0.950612
110	phoneme	Linear	0.746068	0.690885	0.660528	0.350007
111	pima	Linear	0.774026	0.761064	0.721232	0.480235
112	postoperative_patient_data	Linear	0.751852	0.377968	0.496337	-0.011313
113	prnn_crabs	Linear	0.991667	0.990527	0.992572	0.983082
114	prnn_fglass	Linear	0.625203	0.53561	0.532143	0.46585
115	prnn_synth	Linear	0.872	0.872465	0.873961	0.74639
116	prof	Linear	0.742963	0.713757	0.694255	0.406987
117	ring	Linear	0.76268	0.775659	0.762389	0.537863
118	saheart	Linear	0.704659	0.695624	0.601297	0.278692
119	satimage	Linear	0.86001	0.827536	0.814275	0.827081
120	schizo	Linear	0.594118	0.198789	0.33184	-0.00623
121	segmentation	Linear	0.950866	0.95124	0.950425	0.942725
122	solar_flare_1	Linear	0.742857	0.68659	0.672345	0.669937
123	solar_flare_2	Linear	0.761215	0.640604	0.604137	0.695362
124	sonar	Linear	0.777778	0.781779	0.779092	0.560707
125	soybean	Linear	0.92642	0.957506	0.948757	0.919781
126	spambase	Linear	0.903294	0.901447	0.894805	0.796205
127	spect	Linear	0.843827	0.766715	0.710397	0.468957
128	spectf	Linear	0.803333	0.758452	0.74046	0.496567
129	splice	Linear	0.960293	0.953551	0.957961	0.935626
130	tae	Linear	0.52043	0.536375	0.530949	0.299079
131	texture	Linear	0.997697	0.997742	0.997653	0.997468
132	threeOf9	Linear	0.804207	0.804279	0.803193	0.607446
133	tic_tac_toe	Linear	0.984201	0.988054	0.977674	0.965661
134	tokyo1	Linear	0.919792	0.917604	0.906875	0.824321
135	twonorm	Linear	0.97795	0.977926	0.977993	0.955919
136	vehicle	Linear	0.797843	0.802044	0.804879	0.730841
137	vote	Linear	0.954789	0.952864	0.953859	0.906684
138	vowel	Linear	0.845118	0.847877	0.848793	0.830133
139	waveform_21	Linear	0.8675	0.868035	0.867198	0.801874
140	waveform_40	Linear	0.868067	0.868539	0.868586	0.802597
141	wdbc	Linear	0.973977	0.976152	0.968829	0.9449
142	wine_quality_red	Linear	0.596458	0.317116	0.279905	0.339421
143	wine_quality_white	Linear	0.538095	0.338107	0.238882	0.264965
144	wine_recognition	Linear	0.936111	0.943046	0.93633	0.904157
145	xd6	Linear	0.82188	0.816704	0.767	0.581403
146	yeast	Linear	0.594482	0.554987	0.513609	0.475075

	Dataset Name	Algorithm	Mean Accuracy [0-1] \uparrow	Mean Precision \uparrow	Mean Recall \uparrow	Mean MCC \uparrow
1	GAMETES_Epistasis_2.Way_20atts_0.1H_EDM_1.1	NeuralNet	0.585729	0.585261	0.585838	0.171095
2	GAMETES_Epistasis_2.Way_20atts_0.4H_EDM_1.1	NeuralNet	0.708542	0.709424	0.417870	
3	GAMETES_Epistasis_3.Way_20atts_0.2H_EDM_1.1	NeuralNet	0.517500	0.517558	0.517636	0.035193
4	GAMETES_Heterogeneity_20atts_1600.Het_0.4_0.2_...	NeuralNet	0.644687	0.645142	0.646459	0.291590
5	GAMETES_Heterogeneity_20atts_1600.Het_0.4_0.2_...	NeuralNet	0.650833	0.651469	0.652644	0.304104
6	Hill_Valley_with_noise	NeuralNet	0.545405	0.550122	0.610026	0.146337
7	Hill_Valley_without_noise	NeuralNet	0.554458	0.560038	0.622925	0.168091
8	agaricus_lepiota	NeuralNet	0.985820	0.985703	0.985919	0.971621
9	allbp	NeuralNet	0.956777	0.359956	0.360469	0.074941
10	allhyper	NeuralNet	0.973466	0.275000	0.267759	0.000000
11	allhypoth	NeuralNet	0.922060	0.333333	0.307353	0.000000
12	allrep	NeuralNet	0.967241	0.250000	0.241810	0.000000
13	analcatdata_aids	NeuralNet	0.470000	0.502937	0.524160	0.040197
14	analcatdata_asbestos	NeuralNet	0.766667	0.785112	0.779735	0.563728
15	analcatdata_authorship	NeuralNet	0.995266	0.996488	0.994588	0.993077
16	analcatdata_bankruptcy	NeuralNet	0.813333	0.829782	0.822063	0.659108
17	analcatdata_boxing1	NeuralNet	0.688889	0.598661	0.652703	0.243174
18	analcatdata_boxing2	NeuralNet	0.669136	0.668420	0.694571	0.361372
19	analcatdata_creditscore	NeuralNet	0.805000	0.793736	0.774231	0.556686
20	analcatdata_cyyoung8092	NeuralNet	0.776667	0.710353	0.738116	0.439706
21	analcatdata_cyyoung9302	NeuralNet	0.873684	0.815863	0.795422	0.597854
22	analcatdata_dmft	NeuralNet	0.205208	0.211099	0.221483	0.052217
23	analcatdata_fraud	NeuralNet	0.648148	0.584841	0.613591	0.207258
24	analcatdata_germangss	NeuralNet	0.311250	0.316450	0.324626	0.090982
25	analcatdata_happiness	NeuralNet	0.491667	0.486905	0.473810	0.259076
26	analcatdata_japansolvent	NeuralNet	0.781818	0.809458	0.805020	0.614055
27	analcatdata_lawsuit	NeuralNet	0.961006	0.897202	0.824873	0.707293
28	ann_thyroid	NeuralNet	0.967685	0.809154	0.826367	0.743097
29	appendicitis	NeuralNet	0.851515	0.767637	0.752789	0.501828
30	australian	NeuralNet	0.843720	0.842648	0.841904	0.684523
31	auto	NeuralNet	0.688618	0.667752	0.695618	0.595821
32	backache	NeuralNet	0.821296	0.536126	0.545019	0.091842
33	balance_scale	NeuralNet	0.928000	0.795545	0.799846	0.875203
34	banana	NeuralNet	0.864403	0.854274	0.876375	0.730268
35	biomed	NeuralNet	0.891270	0.879832	0.882356	0.761581
36	breast	NeuralNet	0.961190	0.964554	0.952326	0.916753
37	breast_cancer	NeuralNet	0.722414	0.615661	0.678091	0.284733
38	breast_cancer_wisconsin	NeuralNet	0.960234	0.959006	0.957697	0.916536
39	breast_w	NeuralNet	0.964762	0.967518	0.956630	0.924005
40	buggyCrx	NeuralNet	0.853382	0.852646	0.852663	0.705261
41	bupa	NeuralNet	0.582609	0.587326	0.590296	0.177548
42	calendarDOW	NeuralNet	0.591250	0.564882	0.572987	0.485498
43	car	NeuralNet	0.886705	0.645797	0.678965	0.743524
44	car_evaluation	NeuralNet	0.957707	0.760487	0.730270	0.909268
45	cars	NeuralNet	0.764557	0.656525	0.689043	0.562526
46	chess	NeuralNet	0.990937	0.990997	0.990887	0.981884
47	churn	NeuralNet	0.905467	0.705715	0.855562	0.539217
48	clean1	NeuralNet	0.965625	0.966918	0.964145	0.931036
49	cleve	NeuralNet	0.781421	0.789767	0.785457	0.575013
50	cleveland	NeuralNet	0.556284	0.292572	0.284658	0.274622
51	cleveland_nominal	NeuralNet	0.546995	0.277967	0.268059	0.259451
52	cloud	NeuralNet	0.251515	0.268453	0.263668	0.014947
53	cmc	NeuralNet	0.552768	0.526055	0.537211	0.305936
54	colic	NeuralNet	0.800901	0.784415	0.794422	0.578367
55	collins	NeuralNet	0.631959	0.603885	0.575876	0.596168
56	confidence	NeuralNet	0.748889	0.775926	0.774537	0.723127
57	contraceptive	NeuralNet	0.549605	0.521371	0.531815	0.300551
58	corral	NeuralNet	0.990625	0.993262	0.989018	0.982066
59	credit_a	NeuralNet	0.855314	0.853688	0.854426	0.708084
60	credit_g	NeuralNet	0.718500	0.633586	0.655008	0.286997
61	crx	NeuralNet	0.847585	0.846356	0.846279	0.692615
62	dermatology	NeuralNet	0.958559	0.957059	0.952279	0.948802
63	diabetes	NeuralNet	0.745238	0.704854	0.721165	0.425190
64	dis	NeuralNet	0.984857	0.500000	0.492428	0.000000
65	ecoli	NeuralNet	0.866162	0.822123	0.835700	0.814340
66	flags	NeuralNet	0.454630	0.410999	0.418892	0.292760
67	flare	NeuralNet	0.820093	0.568488	0.642486	0.193622
68	german	NeuralNet	0.721833	0.644865	0.664890	0.308723
69	glass	NeuralNet	0.634959	0.556708	0.535536	0.490254
70	glass2	NeuralNet	0.754545	0.764611	0.763772	0.528184
71	haberman	NeuralNet	0.721505	0.581981	0.616532	0.193974
72	hayes_roth	NeuralNet	0.725000	0.773298	0.741867	0.597668
73	heart_c	NeuralNet	0.812022	0.815221	0.812394	0.627410

	Dataset Name	Algorithm	Mean Accuracy [0-1] \uparrow	Mean Precision \uparrow	Mean Recall \uparrow	Mean MCC \uparrow
74	heart.h	NeuralNet	0.774576	0.745714	0.767058	0.511602
75	heart.statlog	NeuralNet	0.801235	0.799560	0.798810	0.598298
76	hepatitis	NeuralNet	0.816129	0.691785	0.717233	0.404004
77	horse_colic	NeuralNet	0.791441	0.767537	0.787856	0.554577
78	house_votes_84	NeuralNet	0.949425	0.948397	0.945097	0.893421
79	hungarian	NeuralNet	0.793785	0.770260	0.781005	0.550523
80	hypothyroid	NeuralNet	0.950395	0.500000	0.475197	0.000000
81	ionosphere	NeuralNet	0.927230	0.916240	0.927374	0.843267
82	iris	NeuralNet	0.916667	0.918241	0.924952	0.884396
83	irish	NeuralNet	0.976667	0.977974	0.975260	0.953207
84	kr_vs_kw	NeuralNet	0.990000	0.989985	0.990051	0.980036
85	krkopt	NeuralNet	0.745432	0.478336	0.429315	0.717063
86	labor	NeuralNet	0.883333	0.892945	0.868836	0.755731
87	led24	NeuralNet	0.705365	0.705415	0.703774	0.672870
88	led7	NeuralNet	0.735469	0.733776	0.739016	0.706936
89	lupus	NeuralNet	0.712963	0.710248	0.705527	0.413480
90	lymphography	NeuralNet	0.836667	0.742958	0.734830	0.693317
91	magic	NeuralNet	0.874658	0.847898	0.874354	0.721732
92	mfeat_fourier	NeuralNet	0.818500	0.819016	0.815613	0.798834
93	mfeat_karhunen	NeuralNet	0.961833	0.962581	0.962295	0.957653
94	mfeat_morphological	NeuralNet	0.737667	0.738714	0.730848	0.712418
95	mfeat_zernike	NeuralNet	0.827750	0.828335	0.823932	0.809025
96	mofn_3_7_10	NeuralNet	0.999874	0.999921	0.999691	0.999612
97	molecular_biology_promoters	NeuralNet	0.745455	0.769183	0.767587	0.536550
98	monk1	NeuralNet	0.900893	0.903577	0.911824	0.815310
99	monk2	NeuralNet	0.915152	0.903421	0.910310	0.818805
100	monk3	NeuralNet	0.976276	0.976377	0.976514	0.952887
101	movement_libras	NeuralNet	0.778704	0.795320	0.795058	0.766881
102	mushroom	NeuralNet	0.993415	0.993650	0.993265	0.986915
103	mx6	NeuralNet	0.943590	0.949145	0.945417	0.894395
104	new_thyroid	NeuralNet	0.916279	0.914935	0.890192	0.838054
105	nursery	NeuralNet	0.970473	0.746161	0.728799	0.957097
106	page_blocks	NeuralNet	0.956195	0.599961	0.622472	0.754415
107	parity5	NeuralNet	0.128571	0.125833	0.120278	-0.749556
108	parity5-5	NeuralNet	0.901481	0.901240	0.905031	0.806210
109	pendigits	NeuralNet	0.992102	0.992029	0.992150	0.991228
110	phoneme	NeuralNet	0.858125	0.819394	0.834342	0.653326
111	pima	NeuralNet	0.757576	0.722562	0.737934	0.459277
112	postoperative_patient_data	NeuralNet	0.616667	0.430137	0.422865	-0.134581
113	prnn_crabs	NeuralNet	0.970833	0.974441	0.969353	0.943719
114	prnn_fglass	NeuralNet	0.642276	0.573701	0.555254	0.503537
115	prnn_synth	NeuralNet	0.863333	0.869550	0.867224	0.736697
116	prof	NeuralNet	0.660000	0.569709	0.599023	0.165549
117	ring	NeuralNet	0.967320	0.967348	0.967515	0.934863
118	saheart	NeuralNet	0.698208	0.654281	0.661048	0.314901
119	satimage	NeuralNet	0.894380	0.865557	0.882729	0.869960
120	schizo	NeuralNet	0.560784	0.416122	0.438102	0.134946
121	segmentation	NeuralNet	0.955772	0.955819	0.956235	0.948619
122	solar_flare_1	NeuralNet	0.711111	0.641237	0.634488	0.630834
123	solar_flare_2	NeuralNet	0.743458	0.595600	0.617318	0.672688
124	sonar	NeuralNet	0.844444	0.847896	0.848892	0.696714
125	soybean	NeuralNet	0.885679	0.908994	0.903971	0.875395
126	spambase	NeuralNet	0.933623	0.929705	0.931154	0.860840
127	spect	NeuralNet	0.822840	0.717052	0.719485	0.433855
128	spectf	NeuralNet	0.855714	0.818914	0.829624	0.645212
129	splice	NeuralNet	0.868025	0.859335	0.855673	0.786508
130	tae	NeuralNet	0.535484	0.543220	0.545302	0.311698
131	texture	NeuralNet	0.997182	0.997211	0.997186	0.996905
132	threeOf9	NeuralNet	0.988673	0.988757	0.988827	0.977576
133	tic_tac_toe	NeuralNet	0.910417	0.886942	0.916250	0.802401
134	tokyo1	NeuralNet	0.919965	0.910703	0.914601	0.825215
135	twonorm	NeuralNet	0.973649	0.973740	0.973626	0.947366
136	vehicle	NeuralNet	0.795098	0.804081	0.800503	0.729591
137	vote	NeuralNet	0.948276	0.947088	0.947381	0.894389
138	vowel	NeuralNet	0.963300	0.964049	0.962838	0.959821
139	waveform_21	NeuralNet	0.855033	0.855107	0.856384	0.783666
140	waveform_40	NeuralNet	0.846667	0.847626	0.848218	0.771493
141	wdbc	NeuralNet	0.961404	0.958843	0.959549	0.918218
142	wine_quality_red	NeuralNet	0.599792	0.286262	0.284769	0.351061
143	wine_quality_white	NeuralNet	0.562789	0.251547	0.252105	0.313237
144	wine_recognition	NeuralNet	0.969444	0.973278	0.966759	0.954492
145	xd6	NeuralNet	1.000000	1.000000	1.000000	1.000000
146	yeast	NeuralNet	0.588401	0.512226	0.507737	0.467686

	Dataset Name	Algorithm	Mean Accuracy [0-1] \uparrow	Mean Precision \uparrow	Mean Recall \uparrow	Mean MCC \uparrow
1	GAMETES_Epistasis_2.Way_20atts_0.1H_EDM_1..1	RF	0.592813	0.593805	0.593487	0.18729
2	GAMETES_Epistasis_2.Way_20atts_0.4H_EDM_1..1	RF	0.716042	0.717502	0.716862	0.434362
3	GAMETES_Epistasis_3.Way_20atts_0.2H_EDM_1..1	RF	0.569167	0.570024	0.569777	0.1398
4	GAMETES_Heterogeneity_20atts_1600.Het_0.4_0.2....	RF	0.65	0.650981	0.650655	0.301635
5	GAMETES_Heterogeneity_20atts_1600.Het_0.4_0.2....	RF	0.676042	0.676914	0.676607	0.35352
6	Hill_Valley_with_noise	RF	0.566667	0.567162	0.566994	0.134155
7	Hill_Valley_without_noise	RF	0.591358	0.592646	0.592079	0.18472
8	agaricus_lepiota	RF	1	1	1	1
9	allbp	RF	0.961192	0.602601	0.412937	0.363661
10	allhyper	RF	0.973289	0.348426	0.280262	0.059236
11	allhypoth	RF	0.942175	0.803611	0.509489	0.499523
12	allrep	RF	0.966976	0.344607	0.268917	0.076523
13	analcatdata_aids	RF	0.353333	0.387989	0.361032	-0.235453
14	analcatdata_asbestos	RF	0.747059	0.751587	0.757251	0.507501
15	analcatdata_authorship	RF	0.990533	0.99233	0.984122	0.986218
16	analcatdata_bankruptcy	RF	0.84	0.830198	0.836468	0.666737
17	analcatdata_boxing1	RF	0.804167	0.789302	0.774962	0.562319
18	analcatdata_boxing2	RF	0.746914	0.753484	0.750487	0.503755
19	analcatdata_creditscore	RF	0.968333	0.949908	0.973839	0.921332
20	analcatdata_cyyoung8092	RF	0.808333	0.817405	0.70781	0.502572
21	analcatdata_cyyoung9302	RF	0.857895	0.764068	0.721255	0.46788
22	analcatdata_dmft	RF	0.184792	0.19342	0.18849	0.022857
23	analcatdata_fraud	RF	0.7	0.609319	0.612659	0.209653
24	analcatdata_germangss	RF	0.161667	0.158693	0.161677	-0.116714
25	analcatdata_happiness	RF	0.216667	0.247496	0.232063	-0.121818
26	analcatdata_japansolvent	RF	0.842424	0.859372	0.841978	0.699035
27	analcatdata_lawsuit	RF	0.978616	0.937273	0.906068	0.828542
28	ann_thyroid	RF	0.996111	0.974214	0.985039	0.97328
29	appendicitis	RF	0.862121	0.77616	0.761159	0.516606
30	australian	RF	0.858696	0.856531	0.857277	0.713777
31	auto	RF	0.8	0.82009	0.792282	0.741249
32	backache	RF	0.837963	0.487991	0.519393	0.054565
33	balance_scale	RF	0.841333	0.564501	0.606117	0.712345
34	banana	RF	0.89522	0.895011	0.892572	0.787576
35	biomed	RF	0.903968	0.913905	0.873959	0.785684
36	breast	RF	0.96881	0.963213	0.969114	0.932255
37	breast_cancer	RF	0.722989	0.663864	0.616834	0.275302
38	breast_cancer_wisconsin	RF	0.955848	0.95673	0.949492	0.906034
39	breast_w	RF	0.970714	0.965086	0.971185	0.9362
40	buggyCrx	RF	0.87029	0.868878	0.87036	0.739192
41	bupa	RF	0.555072	0.55896	0.55824	0.117196
42	calendarDOW	RF	0.6225	0.601339	0.598965	0.523132
43	car	RF	0.962813	0.90768	0.891529	0.920316
44	car_evaluation	RF	0.964162	0.90028	0.9145	0.923467
45	cars	RF	0.95443	0.945243	0.934689	0.916105
46	chess	RF	0.990938	0.991027	0.990844	0.981871
47	churn	RF	0.917	0.938249	0.707636	0.602217
48	clean1	RF	0.904861	0.905297	0.900208	0.80544
49	cleve	RF	0.821858	0.820319	0.823499	0.643642
50	cleveland	RF	0.554098	0.284665	0.287316	0.257013
51	cleveland_nominal	RF	0.538251	0.29455	0.298114	0.255859
52	cloud	RF	0.348485	0.35541	0.37207	0.149374
53	cmc	RF	0.506667	0.482102	0.477236	0.228526
54	colic	RF	0.840991	0.844669	0.815516	0.658974
55	collins	RF	0.999313	0.999313	0.999038	0.999242
56	confidence	RF	0.782222	0.815463	0.797389	0.743977
57	contraceptive	RF	0.510847	0.484453	0.477114	0.233082
58	corral	RF	0.99375	0.993687	0.993942	0.987625
59	credit_a	RF	0.861836	0.86093	0.861414	0.722311
60	credit_g	RF	0.762667	0.727824	0.65338	0.372782
61	crx	RF	0.862319	0.861499	0.860795	0.722277
62	dermatology	RF	0.972973	0.971601	0.968303	0.966415
63	diabetes	RF	0.758442	0.736482	0.716768	0.452329
64	dis	RF	0.985033	0.573135	0.508874	0.050971
65	ecoli	RF	0.879293	0.859011	0.833699	0.832325
66	flags	RF	0.469444	0.446879	0.428278	0.306985
67	flare	RF	0.804206	0.606957	0.562855	0.162851
68	german	RF	0.7615	0.735306	0.656369	0.382524
69	glass	RF	0.793496	0.768921	0.737416	0.709925
70	glass2	RF	0.866667	0.868614	0.86623	0.734613
71	haberman	RF	0.706452	0.597622	0.57313	0.167371
72	hayes_roth	RF	0.81875	0.849932	0.854616	0.718032
73	heart_c	RF	0.823497	0.821805	0.821258	0.642999

	Dataset Name	Algorithm	Mean Accuracy [0-1] \uparrow	Mean Precision \uparrow	Mean Recall \uparrow	Mean MCC \uparrow
74	heart.h	RF	0.812429	0.803651	0.791494	0.594451
75	heart.statlog	RF	0.824074	0.822665	0.816857	0.639373
76	hepatitis	RF	0.8	0.729485	0.625241	0.325763
77	horse_colic	RF	0.843243	0.847947	0.817756	0.664626
78	house_votes_84	RF	0.954023	0.951141	0.952488	0.903554
79	hungarian	RF	0.833333	0.823948	0.807803	0.631089
80	hypothyroid	RF	0.961664	0.871592	0.661778	0.486384
81	ionosphere	RF	0.934272	0.933031	0.923157	0.855937
82	iris	RF	0.948889	0.950367	0.949603	0.924185
83	irish	RF	0.999	0.999006	0.998942	0.997946
84	kr_vs_kw	RF	0.990938	0.991119	0.990747	0.981865
85	krkopt	RF	0.750249	0.760036	0.747196	0.721422
86	labor	RF	0.925	0.919127	0.920991	0.836918
87	led24	RF	0.71724	0.716457	0.716799	0.685937
88	led7	RF	0.732656	0.737603	0.730783	0.703823
89	lupus	RF	0.677778	0.662729	0.668674	0.328853
90	lymphography	RF	0.861111	0.727772	0.73409	0.729926
91	magic	RF	0.880967	0.879621	0.856553	0.735806
92	mfeat_fourier	RF	0.832417	0.83273	0.8336	0.814312
93	mfeat_karhunen	RF	0.962333	0.962286	0.962723	0.958194
94	mfeat_morphological	RF	0.7005	0.699192	0.700314	0.667651
95	mfeat_zernike	RF	0.781583	0.777452	0.782013	0.757641
96	mofn_3_7_10	RF	0.997484	0.998403	0.994355	0.992711
97	molecular_biology_promoters	RF	0.907576	0.907391	0.912776	0.819971
98	monk1	RF	1	1	1	1
99	monk2	RF	0.832782	0.82718	0.79573	0.621766
100	monk3	RF	0.98048	0.980418	0.980483	0.960899
101	movement_libras	RF	0.790278	0.797014	0.798489	0.777306
102	mushroom	RF	1	1	1	1
103	mx6	RF	0.939744	0.944234	0.9448	0.888858
104	new_thyroid	RF	0.949612	0.949849	0.923227	0.895017
105	nursery	RF	0.990856	0.992722	0.969001	0.98661
106	page_blocks	RF	0.974795	0.885377	0.856833	0.862329
107	parity5	RF	0.061905	0.054444	0.067778	-0.87586
108	parity5-5	RF	0.596889	0.598563	0.598106	0.196663
109	pendigits	RF	0.991617	0.991755	0.991702	0.990689
110	phoneme	RF	0.907524	0.891557	0.884286	0.775755
111	pima	RF	0.759957	0.73681	0.715334	0.451304
112	postoperative_patient_data	RF	0.640741	0.389869	0.431934	-0.154795
113	prnn_crabs	RF	0.92	0.919792	0.921353	0.841109
114	prnn_fglass	RF	0.788618	0.760492	0.731584	0.703691
115	prnn_synth	RF	0.846	0.851007	0.845242	0.696126
116	prof	RF	0.668395	0.607657	0.559177	0.158267
117	ring	RF	0.95205	0.952935	0.952216	0.905151
118	saheart	RF	0.70681	0.674563	0.62945	0.29905
119	satimage	RF	0.916887	0.908773	0.890325	0.897563
120	schizo	RF	0.587745	0.199647	0.329257	-0.021156
121	segmentation	RF	0.979509	0.979535	0.979382	0.97612
122	solar_flare_1	RF	0.730688	0.714603	0.688479	0.654436
123	solar_flare_2	RF	0.740187	0.632358	0.610569	0.668219
124	sonar	RF	0.820635	0.832932	0.818413	0.650891
125	soybean	RF	0.931358	0.965342	0.959584	0.925446
126	spambase	RF	0.954542	0.956436	0.948223	0.904614
127	spect	RF	0.821605	0.714415	0.695816	0.407145
128	spectf	RF	0.90381	0.888917	0.867458	0.754996
129	splice	RF	0.969592	0.966513	0.965407	0.950437
130	tae	RF	0.621505	0.626625	0.623188	0.439679
131	texture	RF	0.979061	0.979271	0.979157	0.976976
132	threeOf9	RF	0.992233	0.99182	0.992679	0.984498
133	tic_tac_toe	RF	0.988194	0.990204	0.983946	0.974115
134	tokyo1	RF	0.927778	0.922725	0.919434	0.842092
135	twonorm	RF	0.974077	0.974071	0.974099	0.94817
136	vehicle	RF	0.747059	0.743724	0.755626	0.664236
137	vote	RF	0.957854	0.956191	0.956952	0.913103
138	vowel	RF	0.970707	0.971521	0.972488	0.967922
139	waveform_21	RF	0.854867	0.855389	0.854524	0.783095
140	waveform_40	RF	0.856033	0.857514	0.856918	0.785608
141	wdbc	RF	0.958187	0.959796	0.951737	0.911386
142	wine_quality_red	RF	0.699062	0.398787	0.358419	0.514626
143	wine_quality_white	RF	0.68932	0.571892	0.399087	0.522513
144	wine_recognition	RF	0.969444	0.969947	0.973605	0.953864
145	xd6	RF	0.999316	0.999479	0.999034	0.998511
146	yeast	RF	0.621396	0.565004	0.529681	0.506088

	Dataset Name	Algorithm	Mean Accuracy [0-1] \uparrow	Mean Precision \uparrow	Mean Recall \uparrow	Mean MCC \uparrow
1	GAMETES_Epistasis_2.Way_20atts_0.1H_EDM_1.1	LGBM	0.600625	0.601217	0.600913	0.20213
2	GAMETES_Epistasis_2.Way_20atts_0.4H_EDM_1.1	LGBM	0.725521	0.727364	0.72608	0.453438
3	GAMETES_Epistasis_3.Way_20atts_0.2H_EDM_1.1	LGBM	0.546354	0.54645	0.546371	0.092821
4	GAMETES_Heterogeneity_20atts_1600.Het_0.4_0.2....	LGBM	0.665	0.665684	0.665486	0.33117
5	GAMETES_Heterogeneity_20atts_1600.Het_0.4_0.2....	LGBM	0.682604	0.683213	0.682965	0.366177
6	Hill_Valley_with_noise	LGBM	0.580247	0.580742	0.580552	0.161293
7	Hill_Valley_without_noise	LGBM	0.594513	0.596329	0.59553	0.191853
8	agaricus_lepiota	LGBM	1	1	1	1
9	allbp	LGBM	0.974525	0.804793	0.678941	0.67448
10	allhyper	LGBM	0.988565	0.717225	0.650713	0.76277
11	allhypoth	LGBM	0.985853	0.923067	0.895773	0.902718
12	allrep	LGBM	0.984768	0.796444	0.735259	0.750835
13	analcatdata_aids	LGBM	0.35	0.175	0.483333	0
14	analcatdata_asbestos	LGBM	0.77451	0.782152	0.786	0.566685
15	analcatdata_authorship	LGBM	0.990335	0.991843	0.982204	0.985941
16	analcatdata_bankruptcy	LGBM	0.676667	0.613571	0.710516	0.421595
17	analcatdata_boxing1	LGBM	0.668056	0.645938	0.595761	0.233457
18	analcatdata_boxing2	LGBM	0.780247	0.794117	0.779873	0.573408
19	analcatdata_creditscore	LGBM	0.986667	0.973684	0.990276	0.962419
20	analcatdata_cyyoung8092	LGBM	0.798333	0.765406	0.732137	0.492857
21	analcatdata_cyyoung9302	LGBM	0.847368	0.735986	0.747946	0.47124
22	analcatdata_dmft	LGBM	0.200208	0.208616	0.203876	0.041659
23	analcatdata_fraud	LGBM	0.7	0.366667	0.516667	0
24	analcatdata_germangss	LGBM	0.373333	0.380059	0.376709	0.169657
25	analcatdata_happiness	LGBM	0.444444	0.426318	0.43869	0.237565
26	analcatdata_japansolvent	LGBM	0.815152	0.821257	0.809405	0.627538
27	analcatdata_lawsuit	LGBM	0.986792	0.955017	0.938743	0.8882
28	ann_thyroid	LGBM	0.996669	0.978271	0.986658	0.97706
29	appendicitis	LGBM	0.859091	0.753043	0.758115	0.496495
30	australian	LGBM	0.855314	0.853435	0.854054	0.707463
31	auto	LGBM	0.823577	0.843036	0.822394	0.771473
32	backache	LGBM	0.835185	0.586381	0.533229	0.112935
33	balance_scale	LGBM	0.861333	0.64243	0.646857	0.753419
34	banana	LGBM	0.896918	0.897183	0.893869	0.79104
35	biomed	LGBM	0.901587	0.895857	0.884865	0.779757
36	breast	LGBM	0.964524	0.958979	0.963574	0.922501
37	breast_cancer	LGBM	0.712644	0.660383	0.615009	0.266742
38	breast_cancer_wisconsin	LGBM	0.964912	0.966561	0.958654	0.925122
39	breast_w	LGBM	0.965476	0.959964	0.96463	0.924528
40	buggyCrx	LGBM	0.872947	0.871543	0.871865	0.743374
41	bupa	LGBM	0.559903	0.562541	0.561954	0.12449
42	calendarDOW	LGBM	0.600833	0.5825	0.574801	0.497894
43	car	LGBM	0.994316	0.98707	0.986767	0.987641
44	car_evaluation	LGBM	0.993738	0.985846	0.985837	0.98658
45	cars	LGBM	0.972152	0.965391	0.963578	0.948032
46	chess	LGBM	0.994062	0.994134	0.993976	0.98811
47	churn	LGBM	0.960233	0.952108	0.876124	0.824569
48	clean1	LGBM	0.997917	0.998125	0.997707	0.995829
49	cleve	LGBM	0.800546	0.799896	0.800955	0.600648
50	cleveland	LGBM	0.548087	0.314911	0.304379	0.277223
51	cleveland_nominal	LGBM	0.539891	0.30768	0.302665	0.263412
52	cloud	LGBM	0.465152	0.490845	0.477279	0.293241
53	cmc	LGBM	0.531751	0.510656	0.505896	0.272571
54	colic	LGBM	0.823874	0.818533	0.804626	0.622744
55	collins	LGBM	0.990378	0.988866	0.989741	0.989378
56	confidence	LGBM	0.777778	0.791537	0.79613	0.744283
57	contraceptive	LGBM	0.531751	0.510656	0.505896	0.272571
58	corral	LGBM	1	1	1	1
59	credit_a	LGBM	0.862319	0.8612	0.860714	0.721891
60	credit_g	LGBM	0.760667	0.712023	0.6798	0.389833
61	crx	LGBM	0.862319	0.861024	0.860974	0.721986
62	dermatology	LGBM	0.966667	0.957741	0.962793	0.958454
63	diabetes	LGBM	0.743506	0.7179	0.708364	0.425803
64	dis	LGBM	0.990552	0.902409	0.759103	0.637092
65	ecoli	LGBM	0.866162	0.825708	0.800146	0.81292
66	flags	LGBM	0.47963	0.451151	0.432137	0.324978
67	flare	LGBM	0.816822	0.64016	0.573647	0.202066
68	german	LGBM	0.757667	0.713125	0.680203	0.39152
69	glass	LGBM	0.762602	0.712419	0.68008	0.666747
70	glass2	LGBM	0.872727	0.870638	0.873207	0.743677
71	haberman	LGBM	0.70914	0.604596	0.576643	0.176236
72	hayes_roth	LGBM	0.80625	0.824961	0.826361	0.701695
73	heart_c	LGBM	0.811475	0.809545	0.807614	0.617022

	Dataset Name	Algorithm	Mean Accuracy [0-1] \uparrow	Mean Precision \uparrow	Mean Recall \uparrow	Mean MCC \uparrow
74	heart.h	LGBM	0.784746	0.770482	0.769739	0.539905
75	heart.statlog	LGBM	0.812346	0.811347	0.807426	0.618626
76	hepatitis	LGBM	0.811828	0.718382	0.685423	0.393035
77	horse_colic	LGBM	0.82027	0.816101	0.801575	0.617131
78	house_votes_84	LGBM	0.955172	0.951344	0.953965	0.905267
79	hungarian	LGBM	0.79548	0.779852	0.771316	0.550672
80	hypothyroid	LGBM	0.982096	0.919059	0.887098	0.803823
81	ionosphere	LGBM	0.941315	0.94698	0.926107	0.872606
82	iris	LGBM	0.945556	0.947153	0.946102	0.919454
83	iris	LGBM	1	1	1	1
84	kr_vs_kw	LGBM	0.994167	0.99427	0.994067	0.988337
85	krkopt	LGBM	0.669435	0.575325	0.617445	0.632213
86	labor	LGBM	0.830556	0.819286	0.827496	0.639012
87	led24	LGBM	0.689531	0.689134	0.689131	0.65508
88	led7	LGBM	0.733333	0.737842	0.731273	0.704584
89	lupus	LGBM	0.746296	0.740188	0.730262	0.465089
90	lymphography	LGBM	0.831111	0.74156	0.743542	0.669946
91	magic	LGBM	0.880827	0.880668	0.855238	0.73546
92	mfeat_fourier	LGBM	0.844167	0.844966	0.845643	0.827265
93	mfeat_karhunen	LGBM	0.957833	0.957751	0.958593	0.953202
94	mfeat_morphological	LGBM	0.681667	0.680566	0.681202	0.646662
95	mfeat_zernike	LGBM	0.789167	0.797656	0.789418	0.766043
96	mofn_3_7_10	LGBM	0.998742	0.999192	0.997327	0.99649
97	molecular_biology_promoters	LGBM	0.892424	0.891829	0.894953	0.786658
98	monk1	LGBM	1	1	1	1
99	monk2	LGBM	0.906887	0.906045	0.886986	0.792558
100	monk3	LGBM	0.98018	0.980204	0.980092	0.960293
101	movement_libras	LGBM	0.749537	0.770434	0.761865	0.733694
102	mushroom	LGBM	1	1	1	1
103	mxn6	LGBM	0.861538	0.867661	0.865525	0.732914
104	new_thyroid	LGBM	0.942636	0.937915	0.916178	0.87871
105	nursery	LGBM	0.999987	0.99999	0.99999	0.999981
106	page_blocks	LGBM	0.972785	0.867976	0.843822	0.85222
107	parity5	LGBM	0.366667	0.183333	0.5	0
108	parity5-5	LGBM	0.858815	0.859047	0.859071	0.718117
109	pendigits	LGBM	0.991572	0.991622	0.991519	0.990634
110	phoneme	LGBM	0.895035	0.874754	0.872023	0.746735
111	pima	LGBM	0.748052	0.721769	0.710611	0.431994
112	postoperative_patient_data	LGBM	0.740741	0.376373	0.488783	-0.032547
113	prnn_crabs	LGBM	0.948333	0.946881	0.950147	0.89697
114	prnn_fglass	LGBM	0.762602	0.712419	0.68008	0.666747
115	prnn_synth	LGBM	0.852	0.854008	0.851682	0.705631
116	prof	LGBM	0.64716	0.587869	0.573848	0.160865
117	ring	LGBM	0.970248	0.970265	0.970235	0.9405
118	saheart	LGBM	0.677419	0.635696	0.623404	0.258328
119	satimage	LGBM	0.922145	0.912742	0.901401	0.903979
120	schizo	LGBM	0.49902	0.38156	0.374371	0.048628
121	segmentation	LGBM	0.985786	0.985921	0.985762	0.983441
122	solarflare_1	LGBM	0.767196	0.746387	0.718967	0.701043
123	solarflare_2	LGBM	0.740343	0.640344	0.618496	0.668787
124	sonar	LGBM	0.852381	0.856818	0.853737	0.710409
125	soybean	LGBM	0.929877	0.958896	0.95042	0.923242
126	spambase	LGBM	0.957691	0.955772	0.955507	0.911273
127	spect	LGBM	0.827778	0.724311	0.699483	0.420503
128	spectf	LGBM	0.882857	0.850989	0.858873	0.708961
129	splice	LGBM	0.962644	0.954979	0.96381	0.93975
130	tae	LGBM	0.504301	0.517239	0.507952	0.264958
131	texture	LGBM	0.987879	0.987909	0.98791	0.986671
132	threeOf9	LGBM	1	1	1	1
133	tic_tac_toe	LGBM	0.999653	0.999733	0.999517	0.99925
134	tokyo1	LGBM	0.926736	0.920958	0.919076	0.839989
135	twonorm	LGBM	0.96982	0.96981	0.969834	0.939645
136	vehicle	LGBM	0.762941	0.76602	0.770803	0.684356
137	vote	LGBM	0.949425	0.946945	0.949192	0.896069
138	vowel	LGBM	0.938889	0.942074	0.941	0.933086
139	waveform_21	LGBM	0.850967	0.850802	0.850766	0.776635
140	waveform_40	LGBM	0.8539	0.85423	0.854521	0.781403
141	wdbc	LGBM	0.966959	0.968536	0.961098	0.929554
142	wine_quality_red	LGBM	0.684479	0.393475	0.360834	0.493296
143	wine_quality_white	LGBM	0.671395	0.521475	0.399357	0.497333
144	wine_recognition	LGBM	0.980556	0.977947	0.982913	0.970321
145	xd6	LGBM	0.999658	0.999479	0.999749	0.999227
146	yeast	LGBM	0.579167	0.479634	0.457764	0.44834

F. Detailed Results: Regression

	Dataset Name	Algorithm	R^2 Mean \uparrow	MAE \downarrow	MSE \downarrow	Spearman coeff. \uparrow
1	1027_ESL	Ours	0.814821	0.32415	0.364286	0.915777
2	1028_SWD	Ours	0.242729	0.453667	0.488667	0.547945
3	1029_LEV	Ours	0.441602	0.4215	0.503833	0.693376
4	1030_ERA	Ours	0.326374	1.253	2.581	0.533985
5	1089_USCrime	Ours	0.761386	13.656667	343.763333	0.85516
6	1096_FacultySalaries	Ours	0.554916	1.917929	6.254915	0.881548
7	1199_BNG_echoMonths	Ours	0.457349	8.99762	135.514966	0.642297
8	192_vineyard	Ours	0.48772	2.319091	9.080212	0.733184
9	197_cpu_act	Ours	0.954674	2.228371	15.159589	0.933337
10	210_cloud	Ours	0.724912	0.327201	0.320947	0.899352
11	225_puma8NH	Ours	0.655114	2.554851	10.963756	0.802862
12	227_cpu_small	Ours	0.962504	2.425178	12.472524	0.915629
13	228_elusage	Ours	0.668637	9.680586	168.506463	0.800816
14	229_pwLinear	Ours	0.778315	1.596004	4.202897	0.889358
15	294_satellite_image	Ours	0.903787	0.243849	0.469801	0.960742
16	4544_GeographicalOriginalofMusic	Ours	0.647891	0.42381	0.365307	0.804204
17	503_wind	Ours	0.764658	2.485348	10.531015	0.876728
18	505_tecator	Ours	0.990744	0.83921	1.839203	0.984015
19	519_vinnie	Ours	0.714124	1.248684	2.573246	0.8475
20	522_pm10	Ours	0.231741	0.590352	0.589455	0.521897
21	523_analcatdata_neavote	Ours	0.936044	0.508333	0.911667	0.867378
22	529_pollen	Ours	0.736858	1.254833	2.573448	0.852636
23	547_no2	Ours	0.451527	0.433395	0.306515	0.675206
24	560_bodyfat	Ours	0.967746	0.797175	2.210489	0.986474
25	562_cpu_small	Ours	0.96248	2.425747	12.479398	0.91551
26	573_cpu_act	Ours	0.954674	2.228371	15.159589	0.933337
27	579_fri_c0_250_5	Ours	0.747212	0.378935	0.234794	0.867755
28	581_fri_c3_500_25	Ours	0.880145	0.274256	0.119619	0.927998
29	582_fri_c1_500_25	Ours	0.862309	0.287687	0.138304	0.92724
30	583_fri_c1_1000_50	Ours	0.874207	0.275637	0.125888	0.933612
31	584_fri_c4_500_25	Ours	0.862294	0.278452	0.137559	0.922143
32	586_fri_c3_1000_25	Ours	0.922484	0.217843	0.07711	0.950582
33	588_fri_c4_1000_100	Ours	0.833808	0.317965	0.168277	0.916987
34	589_fri_c2_1000_25	Ours	0.864343	0.28611	0.133228	0.914812
35	590_fri_c0_1000_50	Ours	0.777288	0.367084	0.215868	0.886631
36	591_fri_c1_100_10	Ours	0.79392	0.355943	0.205423	0.891629
37	592_fri_c4_1000_25	Ours	0.910138	0.230571	0.088991	0.939652
38	593_fri_c1_1000_10	Ours	0.918017	0.223762	0.081748	0.95081
39	594_fri_c2_100_5	Ours	0.698965	0.404108	0.277513	0.822206
40	595_fri_c0_1000_10	Ours	0.836771	0.320007	0.163036	0.917968
41	596_fri_c2_250_5	Ours	0.855819	0.288189	0.137918	0.908562
42	597_fri_c2_500_5	Ours	0.902917	0.242846	0.096258	0.930817
43	598_fri_c0_1000_25	Ours	0.807318	0.348594	0.190418	0.904452
44	599_fri_c2_1000_5	Ours	0.928995	0.205654	0.070798	0.953063
45	601_fri_c1_250_5	Ours	0.874268	0.260361	0.117707	0.931272
46	602_fri_c3_250_10	Ours	0.852551	0.287054	0.139902	0.915365
47	603_fri_c0_250_50	Ours	0.550945	0.522681	0.427257	0.765852
48	604_fri_c4_500_10	Ours	0.903939	0.2345	0.095063	0.936377
49	605_fri_c2_250_25	Ours	0.776405	0.366254	0.219222	0.866843
50	606_fri_c2_1000_10	Ours	0.895583	0.251408	0.102217	0.92564
51	607_fri_c4_1000_50	Ours	0.904882	0.233976	0.093041	0.9444
52	608_fri_c3_1000_10	Ours	0.928383	0.201985	0.070179	0.955772
53	609_fri_c0_1000_5	Ours	0.883291	0.272286	0.119157	0.945173
54	611_fri_c3_100_5	Ours	0.843342	0.290307	0.13585	0.878346

	Dataset Name	Algorithm	R^2 Mean \uparrow	MAE \downarrow	MSE \downarrow	Spearman coeff. \uparrow
55	612_fri.c1_1000_5	Ours	0.929314	0.204331	0.067296	0.961312
56	613_fri.c3_250_5	Ours	0.879142	0.269598	0.123383	0.919196
57	615_fri.c4_250_10	Ours	0.821346	0.326316	0.17978	0.879216
58	616_fri.c4_500_50	Ours	0.860252	0.288322	0.138104	0.915084
59	617_fri.c3_500_5	Ours	0.902494	0.233656	0.095288	0.944492
60	618_fri.c3_1000_50	Ours	0.89088	0.254606	0.105341	0.924638
61	620_fri.c1_1000_25	Ours	0.896452	0.25679	0.103944	0.943626
62	621_fri.c0_100_10	Ours	0.514948	0.504627	0.420885	0.719398
63	622_fri.c2_1000_50	Ours	0.868326	0.285977	0.130393	0.908663
64	623_fri.c4_1000_10	Ours	0.910817	0.225429	0.085886	0.942258
65	624_fri.c0_100_5	Ours	0.680657	0.409647	0.264711	0.828772
66	626_fri.c2_500_50	Ours	0.81207	0.339832	0.185641	0.868545
67	627_fri.c2_500_10	Ours	0.870395	0.265378	0.120164	0.90524
68	628_fri.c3_1000_5	Ours	0.935337	0.19653	0.064458	0.959792
69	631_fri.c1_500_5	Ours	0.887184	0.251644	0.111008	0.937762
70	633_fri.c0_500_25	Ours	0.755927	0.38867	0.23952	0.870913
71	634_fri.c2_100_10	Ours	0.681313	0.430383	0.299145	0.775288
72	635_fri.c0_250_10	Ours	0.747336	0.383817	0.229537	0.858411
73	637_fri.c1_500_50	Ours	0.756928	0.384564	0.240337	0.873713
74	641_fri.c1_500_10	Ours	0.903447	0.248122	0.096938	0.947524
75	643_fri.c2_500_25	Ours	0.815767	0.340522	0.183284	0.861509
76	644_fri.c4_250_25	Ours	0.831484	0.298289	0.159565	0.899765
77	645_fri.c3_500_50	Ours	0.853164	0.292239	0.14205	0.911955
78	646_fri.c3_500_10	Ours	0.904141	0.237812	0.093509	0.941917
79	647_fri.c1_250_10	Ours	0.844011	0.300114	0.153291	0.902739
80	648_fri.c1_250_50	Ours	0.731215	0.40498	0.267496	0.853423
81	649_fri.c0_500_5	Ours	0.825379	0.322537	0.173292	0.912715
82	650_fri.c0_500_50	Ours	0.731406	0.409569	0.265992	0.86738
83	651_fri.c0_100_25	Ours	0.464538	0.616188	0.580735	0.723058
84	653_fri.c0_250_25	Ours	0.714149	0.420427	0.275512	0.840435
85	654_fri.c0_500_10	Ours	0.763131	0.375268	0.230507	0.875866
86	656_fri.c1_100_5	Ours	0.67904	0.380913	0.25083	0.859699
87	657_fri.c2_250_10	Ours	0.845575	0.294064	0.144781	0.850391
88	658_fri.c3_250_25	Ours	0.813686	0.323878	0.188254	0.904333
89	663_rabe_266	Ours	0.986557	3.859722	34.615278	0.990176
90	665_sleuth_case2002	Ours	0.30437	5.34	59.04	0.363676
91	666_rmtsa.ladata	Ours	0.571491	1.314268	3.314505	0.619187
92	678_visualizing_environmental	Ours	0.2157	2.418534	9.419031	0.525967
93	687_sleuth_ex1605	Ours	0.304948	8.969231	130.948718	0.584203
94	690_visualizing_galaxy	Ours	0.975347	10.611795	221.629231	0.982753
95	695_chatfield.4	Ours	0.827115	13.107853	363.147952	0.923092
96	712_chscase_geyser1	Ours	0.743774	5.067407	40.359259	0.726834
97	feynman_III_12_43	Ours	0.999991	0.001792	0.000006	0.999995
98	feynman_III_15_12	Ours	0.995147	0.243424	0.12736	0.996878
99	feynman_III_15_14	Ours	0.997892	0.000219	0.000001	0.999857
100	feynman_III_15_27	Ours	0.998984	0.036029	0.007256	0.999844
101	feynman_III_17_37	Ours	0.999504	0.072285	0.012494	0.999817
102	feynman_III_7_38	Ours	0.999296	0.44518	0.910481	0.999843
103	feynman_III_8_54	Ours	0.983559	0.028682	0.002052	0.989254
104	feynman_II_10_9	Ours	0.99925	0.003165	0.000046	0.999862
105	feynman_II_11_28	Ours	0.999989	0.000632	0.000001	0.999986
106	feynman_II_13_23	Ours	0.999854	0.007621	0.000216	0.999949
107	feynman_II_13_34	Ours	0.999318	0.031981	0.003025	0.999782
108	feynman_II_15_4	Ours	0.999476	0.0789	0.014319	0.999783

	Dataset Name	Algorithm	R^2 Mean \uparrow	MAE \downarrow	MSE \downarrow	Spearman coeff. \uparrow
109	feynman.II_15_5	Ours	0.999482	0.07829	0.014174	0.999788
110	feynman.II_24_17	Ours	0.999776	0.0083	0.000166	0.999914
111	feynman.II_27_16	Ours	0.999722	0.879617	2.226821	0.999874
112	feynman.II_27_18	Ours	0.999991	0.05168	0.006177	0.999996
113	feynman.II_34_2	Ours	0.999737	0.104771	0.024674	0.999839
114	feynman.II_34_29a	Ours	0.999321	0.002835	0.000036	0.999847
115	feynman.II_34_2a	Ours	0.999342	0.005635	0.000138	0.999846
116	feynman.II_37_1	Ours	0.999751	0.252268	0.137842	0.999861
117	feynman.II_38_14	Ours	0.999986	0.000496	0.000001	0.999995
118	feynman.II_3_24	Ours	0.999958	0.000135	0.0	0.999996
119	feynman.II_4_23	Ours	0.99888	0.000461	0.000001	0.999842
120	feynman.II_8_31	Ours	0.999991	0.025679	0.001567	0.999996
121	feynman.II_8_7	Ours	0.998964	0.001101	0.000008	0.999871
122	feynman.I_10_7	Ours	0.999848	0.007695	0.000223	0.999948
123	feynman.I_12_1	Ours	0.999991	0.011145	0.000234	0.999995
124	feynman.I_12_4	Ours	0.998486	0.000332	0.000001	0.99987
125	feynman.I_12_5	Ours	0.999991	0.011157	0.000232	0.999995
126	feynman.I_14_3	Ours	0.999736	0.209823	0.098519	0.99984
127	feynman.I_14_4	Ours	0.99999	0.025775	0.001563	0.999996
128	feynman.I_15_10	Ours	0.999485	0.031841	0.002294	0.999806
129	feynman.I_16_6	Ours	0.999825	0.009806	0.000227	0.999923
130	feynman.I_18_12	Ours	0.999752	0.079259	0.013642	0.999844
131	feynman.I_25_13	Ours	0.999975	0.001993	0.000015	0.999994
132	feynman.I_26_2	Ours	0.999975	0.001382	0.000006	0.999993
133	feynman.I_27_6	Ours	0.999587	0.0044	0.000053	0.999807
134	feynman.I_29_4	Ours	0.999931	0.003808	0.000121	0.999993
135	feynman.I_30_3	Ours	0.994476	0.105824	0.036724	0.996563
136	feynman.I_30_5	Ours	0.999392	0.001463	0.000009	0.999856
137	feynman.I_34_1	Ours	0.999445	0.018951	0.001767	0.999906
138	feynman.I_34_14	Ours	0.999759	0.014131	0.000633	0.999936
139	feynman.I_34_27	Ours	0.999991	0.001779	0.000006	0.999995
140	feynman.I_37_4	Ours	0.999656	0.035048	0.002833	0.999879
141	feynman.I_39_1	Ours	0.999991	0.016769	0.000526	0.999995
142	feynman.I_39_11	Ours	0.999296	0.039029	0.006582	0.999853
143	feynman.I_43_31	Ours	0.999746	0.209029	0.095828	0.99984
144	feynman.I_47_23	Ours	0.999546	0.008663	0.000206	0.999846
145	feynman.I_48_2	Ours	0.999926	0.0575089	0.766039	0.999952
146	feynman.I_6_2	Ours	0.999986	0.000099	0.0	0.999994
147	feynman.I_6_2b	Ours	0.999519	0.000746	0.000002	0.999776
148	nikuradse.1	Ours	0.997497	0.004895	0.000064	0.989449
149	strogatz_bacres1	Ours	0.997635	0.04384	0.016487	0.987143
150	strogatz_bacres2	Ours	0.995697	0.031386	0.018891	0.997317
151	strogatz_barmag1	Ours	0.988846	0.005775	0.000823	0.998904
152	strogatz_barmag2	Ours	0.997224	0.005008	0.000216	0.99758
153	strogatz_glider1	Ours	0.985167	0.061423	0.009102	0.991621
154	strogatz_glider2	Ours	0.977176	0.073873	0.019675	0.978445
155	strogatz_lv1	Ours	0.467779	0.227348	7.977268	0.994459
156	strogatz_lv2	Ours	0.627065	0.087129	0.584009	0.992025
157	strogatz_predprey1	Ours	0.931857	0.127998	0.776514	0.991957
158	strogatz_predprey2	Ours	0.990725	0.060801	0.022346	0.996018
159	strogatz_shearflow1	Ours	0.98088	0.019286	0.006435	0.996114
160	strogatz_shearflow2	Ours	0.990451	0.007028	0.000487	0.993458
161	strogatz_vdp1	Ours	0.956707	0.100081	0.144906	0.946581
162	strogatz_vdp2	Ours	0.999936	0.000357	0.000001	0.999972

	Dataset Name	Algorithm	R^2 Mean \uparrow	MAE \downarrow	MSE \downarrow	Spearman coeff. \uparrow
1	1027_ESL	GB	0.843825	0.411648	0.306425	0.933898
2	1028_SWD	GB	0.40216	0.500758	0.386582	0.629681
3	1029_LEV	GB	0.544847	0.487292	0.41125	0.741157
4	1030_ERA	GB	0.354067	1.265373	2.476943	0.561748
5	1089_USCrime	GB	0.735817	15.812908	388.658039	0.829873
6	1096_FacultySalaries	GB	0.655666	1.692329	5.266757	0.867306
7	1199_BNG_echoMonths	GB	0.459803	9.042931	134.895122	0.647074
8	192_vineyard	GB	0.414016	2.540394	10.447293	0.70301
9	197_cpu_act	GB	0.985098	1.577219	4.927499	0.966054
10	210_cloud	GB	0.744946	0.315625	0.247581	0.911323
11	225_puma8NH	GB	0.666022	2.541262	10.616178	0.810667
12	227_cpu_small	GB	0.977728	1.927811	7.364241	0.95139
13	228_elusage	GB	0.662711	9.845451	185.548119	0.769757
14	229_pwLinear	GB	0.866772	1.230784	2.497797	0.929715
15	294_satellite_image	GB	0.891701	0.427456	0.528769	0.944031
16	4544_GeographicalOriginalofMusic	GB	0.735437	0.370617	0.272636	0.8508
17	503_wind	GB	0.792332	2.344334	9.286841	0.890397
18	505_tecator	GB	0.994561	0.720312	1.089333	0.990542
19	519_vinnie	GB	0.677588	1.331072	2.918281	0.835808
20	522_pm10	GB	0.40249	0.52595	0.458839	0.643265
21	523_analcatdata_neavote	GB	0.946617	0.587192	0.766019	0.86266
22	529_pollen	GB	0.766195	1.194947	2.284538	0.866195
23	547_no2	GB	0.579428	0.376816	0.23371	0.744537
24	560_bodyfat	GB	0.96948	0.447498	2.047946	0.989411
25	562_cpu_small	GB	0.977697	1.928112	7.378158	0.951374
26	573_cpu_act	GB	0.985101	1.574965	4.926176	0.966219
27	579_fri_c0_250_5	GB	0.826108	0.310522	0.159872	0.905514
28	581_fri_c3_500_25	GB	0.901667	0.241635	0.097505	0.942909
29	582_fri_c1_500_25	GB	0.896002	0.247032	0.104206	0.945404
30	583_fri_c1_1000_50	GB	0.92859	0.206142	0.070994	0.959217
31	584_fri_c4_500_25	GB	0.892647	0.248087	0.105783	0.93504
32	586_fri_c3_1000_25	GB	0.934247	0.197888	0.06533	0.958883
33	588_fri_c4_1000_100	GB	0.91912	0.221115	0.081493	0.94965
34	589_fri_c2_1000_25	GB	0.932203	0.201979	0.066672	0.962761
35	590_fri_c0_1000_50	GB	0.887233	0.261766	0.109249	0.940085
36	591_fri_c1_100_10	GB	0.764455	0.35971	0.233366	0.858847
37	592_fri_c4_1000_25	GB	0.917861	0.217352	0.080926	0.95125
38	593_fri_c1_1000_10	GB	0.950663	0.172583	0.049184	0.970845
39	594_fri_c2_100_5	GB	0.680408	0.406565	0.294247	0.809223
40	595_fri_c0_1000_10	GB	0.905908	0.240498	0.093701	0.950441
41	596_fri_c2_250_5	GB	0.885681	0.255633	0.108273	0.927558
42	597_fri_c2_500_5	GB	0.932894	0.199733	0.066737	0.953171
43	598_fri_c0_1000_25	GB	0.906981	0.241539	0.091942	0.952676
44	599_fri_c2_1000_5	GB	0.956357	0.162371	0.043482	0.971351
45	601_fri_c1_250_5	GB	0.903114	0.23158	0.090293	0.941958
46	602_fri_c3_250_10	GB	0.819989	0.302515	0.170535	0.912131
47	603_fri_c0_250_50	GB	0.779161	0.359235	0.209984	0.892731
48	604_fri_c4_500_10	GB	0.911427	0.228038	0.087185	0.938375
49	605_fri_c2_250_25	GB	0.841342	0.308476	0.154068	0.903712
50	606_fri_c2_1000_10	GB	0.942107	0.186805	0.056795	0.962095
51	607_fri_c4_1000_50	GB	0.920848	0.214492	0.076891	0.953161
52	608_fri_c3_1000_10	GB	0.933739	0.191745	0.064433	0.960649
53	609_fri_c0_1000_5	GB	0.925105	0.218052	0.07637	0.960385
54	611_fri_c3_100_5	GB	0.787867	0.332415	0.184403	0.874185

	Dataset Name	Algorithm	R^2 Mean \uparrow	MAE \downarrow	MSE \downarrow	Spearman coeff. \uparrow
55	612_fri.c1_1000_5	GB	0.950666	0.167881	0.0469	0.971885
56	613_fri.c3_250_5	GB	0.888793	0.255482	0.112866	0.930164
57	615_fri.c4_250_10	GB	0.825742	0.309544	0.175729	0.899653
58	616_fri.c4_500_50	GB	0.870546	0.266212	0.126715	0.918094
59	617_fri.c3_500_5	GB	0.91477	0.212436	0.083035	0.952741
60	618_fri.c3_1000_50	GB	0.917416	0.217763	0.079267	0.941898
61	620_fri.c1_1000_25	GB	0.930267	0.20674	0.070272	0.959332
62	621_fri.c0_100_10	GB	0.673515	0.409779	0.282499	0.833133
63	622_fri.c2_1000_50	GB	0.928422	0.208101	0.070624	0.951736
64	623_fri.c4_1000_10	GB	0.9289	0.198136	0.068375	0.952496
65	624_fri.c0_100_5	GB	0.775367	0.344426	0.185308	0.86807
66	626_fri.c2_500_50	GB	0.89591	0.252418	0.103325	0.934982
67	627_fri.c2_500_10	GB	0.913013	0.21429	0.080541	0.946179
68	628_fri.c3_1000_5	GB	0.945819	0.180783	0.053809	0.967147
69	631_fri.c1_500_5	GB	0.914616	0.224312	0.083882	0.951624
70	633_fri.c0_500_25	GB	0.866778	0.28306	0.130135	0.927416
71	634_fri.c2_100_10	GB	0.707546	0.403375	0.27576	0.802657
72	635_fri.c0_250_10	GB	0.795412	0.341222	0.183931	0.883243
73	637_fri.c1_500_50	GB	0.891905	0.25252	0.106855	0.944885
74	641_fri.c1_500_10	GB	0.92871	0.207534	0.071374	0.961263
75	643_fri.c2_500_25	GB	0.900465	0.247269	0.098138	0.933107
76	644_fri.c4_250_25	GB	0.784022	0.333082	0.209017	0.878636
77	645_fri.c3_500_50	GB	0.861811	0.277696	0.133277	0.907534
78	646_fri.c3_500_10	GB	0.911923	0.220252	0.085503	0.945606
79	647_fri.c1_250_10	GB	0.887172	0.252802	0.109562	0.928647
80	648_fri.c1_250_50	GB	0.837642	0.303371	0.159559	0.905972
81	649_fri.c0_500_5	GB	0.903218	0.241655	0.096167	0.949057
82	650_fri.c0_500_50	GB	0.862419	0.289007	0.135707	0.930885
83	651_fri.c0_100_25	GB	0.567311	0.556682	0.462681	0.804561
84	653_fri.c0_250_25	GB	0.775675	0.36665	0.215326	0.87306
85	654_fri.c0_500_10	GB	0.868828	0.277005	0.127472	0.931783
86	656_fri.c1_100_5	GB	0.693063	0.372854	0.241055	0.859148
87	657_fri.c2_250_10	GB	0.883046	0.255819	0.110549	0.905226
88	658_fri.c3_250_25	GB	0.809951	0.331847	0.192954	0.88508
89	663_rabe_266	GB	0.99757	1.6694	6.247533	0.997376
90	665_sleuth_case2002	GB	0.301035	5.605296	59.782738	0.463527
91	666_rmftsa.ladata	GB	0.531554	1.35438	3.540895	0.612809
92	678_visualizing_environmental	GB	0.182869	2.393865	9.85989	0.524717
93	687_sleuth_ex1605	GB	0.424127	8.230798	109.769692	0.664333
94	690_visualizing_galaxy	GB	0.972577	11.648016	246.035465	0.980595
95	695_chatfield.4	GB	0.811831	13.754273	394.666729	0.928151
96	712_chscase_geyser1	GB	0.708235	5.390796	46.218939	0.72483
97	feynman_III_12_43	GB	0.999777	0.009144	0.000146	0.999862
98	feynman_III_15_12	GB	0.891242	1.271665	2.854668	0.952377
99	feynman_III_15_14	GB	0.99803	0.000417	0.000001	0.997153
100	feynman_III_15_27	GB	0.998772	0.061388	0.00875	0.999203
101	feynman_III_17_37	GB	0.998614	0.146078	0.03494	0.999072
102	feynman_III_7_38	GB	0.998941	0.823206	1.369195	0.999285
103	feynman_III_8_54	GB	0.303233	0.250471	0.086956	0.53352
104	feynman_II_10_9	GB	0.998956	0.005424	0.000064	0.999375
105	feynman_II_11_28	GB	0.999746	0.00345	0.000022	0.999751
106	feynman_II_13_23	GB	0.999942	0.006635	0.000085	0.999973
107	feynman_II_13_34	GB	0.999747	0.025141	0.001124	0.999878
108	feynman_II_15_4	GB	0.998739	0.145999	0.034424	0.999112

	Dataset Name	Algorithm	R^2 Mean \uparrow	MAE \downarrow	MSE \downarrow	Spearman coeff. \uparrow
109	feynman.II_15_5	GB	0.998703	0.148046	0.035469	0.999086
110	feynman.II_24_17	GB	0.999786	0.009717	0.000159	0.999882
111	feynman.II_27_16	GB	0.999038	2.006489	7.70378	0.999233
112	feynman.II_27_18	GB	0.99981	0.258533	0.124766	0.999873
113	feynman.II_34_2	GB	0.999065	0.224284	0.087908	0.999368
114	feynman.II_34_29a	GB	0.998903	0.005328	0.000058	0.999263
115	feynman.II_34_2a	GB	0.99894	0.010497	0.000223	0.999292
116	feynman.II_37_1	GB	0.999126	0.526923	0.483049	0.999449
117	feynman.II_38_14	GB	0.99978	0.002308	0.00001	0.999871
118	feynman.II_3_24	GB	0.999799	0.0005	0.000001	0.999807
119	feynman.II_4_23	GB	0.998778	0.000766	0.000001	0.999227
120	feynman.II_8_31	GB	0.999808	0.130123	0.031723	0.999874
121	feynman.II_8_7	GB	0.998564	0.002103	0.000012	0.999034
122	feynman.I_10_7	GB	0.999942	0.006637	0.000085	0.999973
123	feynman.I_12_1	GB	0.999779	0.057045	0.005667	0.999862
124	feynman.I_12_4	GB	0.998729	0.000545	0.000001	0.99867
125	feynman.I_12_5	GB	0.999781	0.056772	0.005631	0.999864
126	feynman.I_14_3	GB	0.999038	0.452357	0.35937	0.999355
127	feynman.I_14_4	GB	0.999809	0.128623	0.031144	0.999872
128	feynman.I_15_10	GB	0.999736	0.025599	0.001176	0.999875
129	feynman.I_16_6	GB	0.999426	0.021044	0.000744	0.999705
130	feynman.I_18_12	GB	0.999048	0.177748	0.052272	0.999372
131	feynman.I_25_13	GB	0.999765	0.008456	0.000144	0.999842
132	feynman.I_26_2	GB	0.999807	0.005237	0.000048	0.999892
133	feynman.I_27_6	GB	0.999183	0.007485	0.000104	0.999555
134	feynman.I_29_4	GB	0.999734	0.01411	0.000467	0.999786
135	feynman.I_30_3	GB	0.944169	0.456395	0.371263	0.949052
136	feynman.I_30_5	GB	0.999247	0.002193	0.000011	0.999604
137	feynman.I_34_1	GB	0.999499	0.027293	0.001592	0.999795
138	feynman.I_34_14	GB	0.999718	0.019595	0.00074	0.999877
139	feynman.I_34_27	GB	0.999779	0.009122	0.000145	0.999862
140	feynman.I_37_4	GB	0.999358	0.055282	0.005287	0.999542
141	feynman.I_39_1	GB	0.999782	0.085379	0.01271	0.999865
142	feynman.I_39_11	GB	0.998941	0.071568	0.009894	0.999318
143	feynman.I_43_31	GB	0.999045	0.452485	0.359654	0.999359
144	feynman.I_47_23	GB	0.999262	0.013819	0.000336	0.99958
145	feynman.I_48_2	GB	0.999781	1.116941	2.259847	0.999851
146	feynman.I_6_2	GB	0.999765	0.000483	0.0	0.999888
147	feynman.I_6_2b	GB	0.996133	0.002474	0.000014	0.99801
148	nikuradse.1	GB	0.996922	0.006384	0.000078	0.989391
149	strogatz_bacres1	GB	0.998239	0.045395	0.01087	0.972479
150	strogatz_bacres2	GB	0.993985	0.047292	0.026821	0.9961
151	strogatz_barmag1	GB	0.981286	0.009798	0.001255	0.992695
152	strogatz_barmag2	GB	0.991133	0.011211	0.000591	0.984098
153	strogatz_glider1	GB	0.979589	0.079676	0.012392	0.988568
154	strogatz_glider2	GB	0.96412	0.092327	0.031138	0.976937
155	strogatz_lv1	GB	0.340567	0.223821	6.248533	0.938462
156	strogatz_lv2	GB	-0.898451	0.150845	0.729317	0.759218
157	strogatz_predprey1	GB	0.940588	0.146252	0.646596	0.988357
158	strogatz_predprey2	GB	0.989898	0.077975	0.024433	0.994818
159	strogatz_shearflow1	GB	0.940203	0.030389	0.013452	0.987928
160	strogatz_shearflow2	GB	0.978294	0.012743	0.001115	0.994161
161	strogatz_vdp1	GB	0.966731	0.115695	0.090597	0.953146
162	strogatz_vdp2	GB	0.999862	0.000618	0.000001	0.999838

	Dataset Name	Algorithm	R^2 Mean \uparrow	MAE \downarrow	MSE \downarrow	Spearman coeff. \uparrow
1	1027_ESL	KNN	0.807879	0.41613	0.37531	0.913604
2	1028_SWD	KNN	0.343418	0.510123	0.424094	0.600515
3	1029_LEV	KNN	0.513662	0.493256	0.439421	0.722121
4	1030_ERA	KNN	0.345674	1.26361	2.507198	0.552753
5	1089_USCrime	KNN	0.703708	14.772808	412.108062	0.826278
6	1096_FacultySalaries	KNN	0.53663	1.953896	6.991502	0.868185
7	1199_LNG_echoMonths	KNN	0.334282	10.376265	166.239817	0.569137
8	192_vineyard	KNN	0.373565	2.628693	10.633359	0.689823
9	197_cpu_act	KNN	0.888774	4.247011	36.847611	0.795425
10	210_cloud	KNN	0.658076	0.36535	0.381462	0.854528
11	225_puma8NH	KNN	0.616011	2.766587	12.207019	0.78323
12	227_cpu_small	KNN	0.886621	4.300175	37.553102	0.791214
13	228_elusage	KNN	0.67304	9.506251	174.1098	0.784325
14	229_pwLinear	KNN	0.70406	1.855126	5.603834	0.857754
15	294_satellite_image	KNN	0.908938	0.257462	0.444755	0.957693
16	4544_GeographicalOriginalofMusic	KNN	0.388877	0.554609	0.637352	0.600053
17	503_wind	KNN	0.745951	2.583735	11.36322	0.866253
18	505_tecator	KNN	0.987731	1.073242	2.476996	0.981551
19	519_vinnie	KNN	0.569558	1.526279	3.896591	0.775169
20	522_pm10	KNN	0.180996	0.626031	0.634458	0.442965
21	523_analcatdata_neavote	KNN	0.924445	0.611024	1.116954	0.845462
22	529_pollen	KNN	0.695374	1.337789	2.97923	0.832418
23	547_no2	KNN	0.16756	0.528659	0.466909	0.431959
24	560_bodyfat	KNN	0.594354	4.289598	27.442293	0.768671
25	562_cpu_small	KNN	0.88669	4.299562	37.534212	0.791279
26	573_cpu_act	KNN	0.888807	4.246408	36.835197	0.795559
27	579_fri_c0_250_5	KNN	0.757979	0.370055	0.226623	0.88502
28	581_fri_c3_500_25	KNN	0.406513	0.614419	0.594702	0.641756
29	582_fri_c1_500_25	KNN	0.299068	0.671775	0.702257	0.590878
30	583_fri_c1_1000_50	KNN	0.273415	0.695145	0.725051	0.52937
31	584_fri_c4_500_25	KNN	0.398744	0.628441	0.600895	0.633638
32	586_fri_c3_1000_25	KNN	0.424535	0.602009	0.574932	0.671286
33	588_fri_c4_1000_100	KNN	0.16538	0.731393	0.843612	0.446299
34	589_fri_c2_1000_25	KNN	0.430646	0.60814	0.561002	0.663878
35	590_fri_c0_1000_50	KNN	0.361098	0.639875	0.622629	0.655584
36	591_fri_c1_100_10	KNN	0.389413	0.631294	0.603467	0.625965
37	592_fri_c4_1000_25	KNN	0.406186	0.615368	0.590089	0.604161
38	593_fri_c1_1000_10	KNN	0.661404	0.458173	0.338014	0.817027
39	594_fri_c2_100_5	KNN	0.502196	0.518513	0.462946	0.755388
40	595_fri_c0_1000_10	KNN	0.698886	0.441745	0.301583	0.863617
41	596_fri_c2_250_5	KNN	0.719608	0.395027	0.26364	0.853442
42	597_fri_c2_500_5	KNN	0.850351	0.289368	0.147574	0.906158
43	598_fri_c0_1000_25	KNN	0.463055	0.593894	0.531968	0.742612
44	599_fri_c2_1000_5	KNN	0.890694	0.248991	0.108977	0.934203
45	601_fri_c1_250_5	KNN	0.793778	0.324212	0.193876	0.884709
46	602_fri_c3_250_10	KNN	0.455146	0.563242	0.516874	0.658824
47	603_fri_c0_250_50	KNN	0.235183	0.68487	0.728843	0.557173
48	604_fri_c4_500_10	KNN	0.609512	0.480458	0.38484	0.777255
49	605_fri_c2_250_25	KNN	0.271431	0.696507	0.713535	0.526729
50	606_fri_c2_1000_10	KNN	0.650717	0.45814	0.343237	0.809788
51	607_fri_c4_1000_50	KNN	0.281967	0.663103	0.700438	0.538739
52	608_fri_c3_1000_10	KNN	0.696365	0.420994	0.296792	0.824605
53	609_fri_c0_1000_5	KNN	0.884304	0.270184	0.118083	0.945111
54	611_fri_c3_100_5	KNN	0.771813	0.358065	0.198926	0.83584

	Dataset Name	Algorithm	R^2 Mean \uparrow	MAE \downarrow	MSE \downarrow	Spearman coeff. \uparrow
55	612_fri.c1_1000_5	KNN	0.889513	0.246193	0.105308	0.942656
56	613_fri.c3_250_5	KNN	0.826467	0.322477	0.175191	0.893465
57	615_fri.c4_250_10	KNN	0.530654	0.543859	0.468519	0.708213
58	616_fri.c4_500_50	KNN	0.210018	0.706435	0.783715	0.476024
59	617_fri.c3_500_5	KNN	0.859534	0.273003	0.137508	0.922143
60	618_fri.c3_1000_50	KNN	0.311386	0.653644	0.664081	0.557806
61	620_fri.c1_1000_25	KNN	0.375528	0.65647	0.631844	0.608514
62	621_fri.c0_100_10	KNN	0.340703	0.582888	0.578592	0.623509
63	622_fri.c2_1000_50	KNN	0.30276	0.681954	0.691447	0.546624
64	623_fri.c4_1000_10	KNN	0.639109	0.454332	0.34839	0.782942
65	624_fri.c0_100_5	KNN	0.673186	0.407632	0.274295	0.828027
66	626_fri.c2_500_50	KNN	0.271654	0.69571	0.725827	0.533412
67	627_fri.c2_500_10	KNN	0.512372	0.521552	0.452715	0.723344
68	628_fri.c3_1000_5	KNN	0.91219	0.222372	0.08751	0.949091
69	631_fri.c1_500_5	KNN	0.79166	0.328605	0.205153	0.885727
70	633_fri.c0_500_25	KNN	0.429249	0.614029	0.565441	0.726973
71	634_fri.c2_100_10	KNN	0.387796	0.588892	0.585368	0.667469
72	635_fri.c0_250_10	KNN	0.567253	0.509036	0.396825	0.780319
73	637_fri.c1_500_50	KNN	0.190612	0.726046	0.802992	0.454106
74	641_fri.c1_500_10	KNN	0.587863	0.509599	0.414111	0.768669
75	643_fri.c2_500_25	KNN	0.274152	0.678898	0.723671	0.520608
76	644_fri.c4_250_25	KNN	0.258696	0.673705	0.715887	0.551216
77	645_fri.c3_500_50	KNN	0.256191	0.680995	0.726216	0.473903
78	646_fri.c3_500_10	KNN	0.583347	0.496202	0.410688	0.736341
79	647_fri.c1_250_10	KNN	0.509284	0.555339	0.478257	0.700949
80	648_fri.c1_250_50	KNN	0.239375	0.73117	0.763044	0.527385
81	649_fri.c0_500_5	KNN	0.825017	0.323343	0.173445	0.91166
82	650_fri.c0_500_50	KNN	0.329263	0.653483	0.668729	0.665897
83	651_fri.c0_100_25	KNN	0.273143	0.722003	0.791156	0.576842
84	653_fri.c0_250_25	KNN	0.362009	0.629356	0.618463	0.648122
85	654_fri.c0_500_10	KNN	0.624287	0.478936	0.368239	0.821772
86	656_fri.c1_100_5	KNN	0.615747	0.408661	0.303597	0.832531
87	657_fri.c2_250_10	KNN	0.52039	0.524871	0.457067	0.705652
88	658_fri.c3_250_25	KNN	0.244797	0.690289	0.760943	0.501852
89	663_rabe_266	KNN	0.986017	3.951143	36.343619	0.990686
90	665_sleuth_case2002	KNN	0.319907	5.308863	57.668582	0.364329
91	666_rmftsa.ladata	KNN	0.543656	1.347936	3.553963	0.594365
92	678_visualizing_environmental	KNN	0.216664	2.405815	9.418845	0.509588
93	687_sleuth_ex1605	KNN	0.362567	8.921237	126.531474	0.616783
94	690_visualizing_galaxy	KNN	0.974681	10.682558	227.37364	0.98197
95	695_chatfield.4	KNN	0.790414	14.388273	433.325924	0.907828
96	712_chscase_geyser1	KNN	0.680253	5.669016	50.502146	0.714195
97	feynman_III_12_43	KNN	0.999991	0.001777	0.000006	0.999995
98	feynman_III_15_12	KNN	0.994051	0.270764	0.156133	0.996194
99	feynman_III_15_14	KNN	0.997769	0.000253	0.000001	0.999808
100	feynman_III_15_27	KNN	0.999043	0.038169	0.006827	0.999828
101	feynman_III_17_37	KNN	0.99911	0.096243	0.022444	0.999635
102	feynman_III_7_38	KNN	0.999347	0.477064	0.844295	0.999832
103	feynman_III_8_54	KNN	0.983681	0.02859	0.002037	0.989199
104	feynman_II_10_9	KNN	0.99927	0.003401	0.000045	0.999839
105	feynman_II_11_28	KNN	0.99999	0.000628	0.000001	0.999989
106	feynman_II_13_23	KNN	0.999866	0.010269	0.000198	0.999946
107	feynman_II_13_34	KNN	0.999176	0.043096	0.003654	0.999666
108	feynman_II_15_4	KNN	0.999175	0.098492	0.022525	0.999618

	Dataset Name	Algorithm	R^2 Mean \uparrow	MAE \downarrow	MSE \downarrow	Spearman coeff. \uparrow
109	feynman.II_15_5	KNN	0.999182	0.097892	0.02238	0.999623
110	feynman.II_24_17	KNN	0.999337	0.015251	0.000493	0.99979
111	feynman.II_27_16	KNN	0.999712	0.943228	2.311306	0.999871
112	feynman.II_27_18	KNN	0.99999	0.05433	0.006645	0.999995
113	feynman.II_34_2	KNN	0.999754	0.104578	0.023089	0.999851
114	feynman.II_34_29a	KNN	0.999327	0.003067	0.000035	0.999831
115	feynman.II_34_2a	KNN	0.999376	0.00603	0.000131	0.999834
116	feynman.II_37_1	KNN	0.999759	0.25402	0.133153	0.999863
117	feynman.II_38_14	KNN	0.999988	0.000494	0.000001	0.999995
118	feynman.II_3_24	KNN	0.999937	0.000166	0.0	0.999995
119	feynman.II_4_23	KNN	0.999001	0.000481	0.000001	0.999828
120	feynman.II_8_31	KNN	0.99999	0.027024	0.001644	0.999996
121	feynman.II_8_7	KNN	0.999104	0.001143	0.000007	0.999852
122	feynman.I_10_7	KNN	0.999864	0.010321	0.000201	0.999946
123	feynman.I_12_1	KNN	0.999991	0.011106	0.000228	0.999995
124	feynman.I_12_4	KNN	0.997699	0.000432	0.000002	0.99983
125	feynman.I_12_5	KNN	0.999991	0.011098	0.000227	0.999995
126	feynman.I_14_3	KNN	0.999752	0.209515	0.092489	0.99985
127	feynman.I_14_4	KNN	0.99999	0.02702	0.001652	0.999995
128	feynman.I_15_10	KNN	0.999192	0.043141	0.0036	0.999669
129	feynman.I_16_6	KNN	0.999751	0.012993	0.000322	0.999905
130	feynman.I_18_12	KNN	0.999626	0.093342	0.020564	0.99971
131	feynman.I_25_13	KNN	0.999976	0.002032	0.000015	0.999994
132	feynman.I_26_2	KNN	0.999978	0.001406	0.000005	0.999994
133	feynman.I_27_6	KNN	0.999582	0.004684	0.000053	0.999834
134	feynman.I_29_4	KNN	0.999932	0.004091	0.00012	0.999992
135	feynman.I_30_3	KNN	0.99288	0.119795	0.047354	0.995613
136	feynman.I_30_5	KNN	0.999445	0.00152	0.000008	0.99985
137	feynman.I_34_1	KNN	0.999636	0.021039	0.001158	0.999894
138	feynman.I_34_14	KNN	0.999778	0.016803	0.000582	0.999919
139	feynman.I_34_27	KNN	0.999991	0.001764	0.000006	0.999995
140	feynman.I_37_4	KNN	0.999138	0.05649	0.007095	0.999686
141	feynman.I_39_1	KNN	0.999991	0.01667	0.000513	0.999995
142	feynman.I_39_11	KNN	0.999384	0.04124	0.005749	0.999838
143	feynman.I_43_31	KNN	0.999757	0.209387	0.091568	0.99985
144	feynman.I_47_23	KNN	0.999595	0.008944	0.000184	0.999845
145	feynman.I_48_2	KNN	0.999928	0.589222	0.745672	0.999961
146	feynman.I_6_2	KNN	0.999987	0.000101	0.0	0.999994
147	feynman.I_6_2b	KNN	0.999483	0.000834	0.000002	0.999805
148	nikuradse.1	KNN	0.997674	0.004855	0.000059	0.989526
149	strogatz_bacres1	KNN	0.997879	0.053442	0.013004	0.972305
150	strogatz_bacres2	KNN	0.996195	0.03314	0.016602	0.99762
151	strogatz_barmag1	KNN	0.992561	0.004546	0.000537	0.998896
152	strogatz_barmag2	KNN	0.997663	0.003313	0.000188	0.995749
153	strogatz_glider1	KNN	0.985515	0.056925	0.008836	0.992129
154	strogatz_glider2	KNN	0.966362	0.074246	0.030366	0.976969
155	strogatz_lv1	KNN	0.50793	0.217824	7.069078	0.990073
156	strogatz_lv2	KNN	0.717427	0.073722	0.390647	0.986078
157	strogatz_predprey1	KNN	0.928159	0.129424	0.802643	0.991541
158	strogatz_predprey2	KNN	0.989005	0.071363	0.027123	0.996229
159	strogatz_shearflow1	KNN	0.982855	0.013993	0.006231	0.998894
160	strogatz_shearflow2	KNN	0.99096	0.005983	0.000436	0.997075
161	strogatz_vdp1	KNN	0.954852	0.101241	0.147223	0.942659
162	strogatz_vdp2	KNN	0.999066	0.000899	0.000007	0.998801

	Dataset Name	Algorithm	R^2 Mean \uparrow	MAE \downarrow	MSE \downarrow	Spearman coeff. \uparrow
1	1027_ESL	Linear	0.850755	0.40513	0.292207	0.935449
2	1028_SWD	Linear	0.378101	0.511349	0.401739	0.620222
3	1029_LEV	Linear	0.557796	0.488484	0.399588	0.749403
4	1030_ERA	Linear	0.369205	1.243903	2.418982	0.579253
5	1089_USCrime	Linear	0.812045	13.428465	265.112604	0.843669
6	1096_FacultySalaries	Linear	0.001744	1.531526	10.476934	0.902399
7	1199_LNG_echoMonths	Linear	0.439689	9.255462	139.918052	0.614086
8	192_vineyard	Linear	0.454057	2.328044	9.162236	0.735941
9	197_cpu_act	Linear	0.723461	6.035876	92.707762	0.775688
10	210_cloud	Linear	0.822553	0.268041	0.16666	0.917689
11	225_puma8NH	Linear	0.372844	3.661451	19.939988	0.657494
12	227_cpu_small	Linear	0.711964	6.121275	96.531839	0.766317
13	228_elusage	Linear	0.713334	9.274947	152.617535	0.847493
14	229_pwLinear	Linear	0.740945	1.75077	4.883573	0.865478
15	294_satellite_image	Linear	0.698746	1.017789	1.47091	0.881093
16	4544_GeographicalOriginalofMusic	Linear	0.798082	0.33812	0.206275	0.874131
17	503_wind	Linear	0.758431	2.523946	10.804286	0.87057
18	505_tecator	Linear	0.995984	0.601854	0.810324	0.993431
19	519_vinnie	Linear	0.690202	1.309108	2.799677	0.842285
20	522_pm10	Linear	0.141843	0.63939	0.665433	0.391699
21	523_analcatdata_neavote	Linear	0.936059	0.646718	0.917932	0.858835
22	529_pollen	Linear	0.790313	1.133391	2.047134	0.875056
23	547_no2	Linear	0.490508	0.410635	0.283465	0.719061
24	560_bodyfat	Linear	0.976067	0.491859	1.56724	0.990758
25	562_cpu_small	Linear	0.711911	6.116167	96.550215	0.766791
26	573_cpu_act	Linear	0.723469	6.036166	92.704662	0.775619
27	579_fri_c0_250_5	Linear	0.660825	0.434944	0.311665	0.816355
28	581_fri_c3_500_25	Linear	0.264277	0.720032	0.733977	0.498327
29	582_fri_c1_500_25	Linear	0.257659	0.713191	0.743551	0.50301
30	583_fri_c1_1000_50	Linear	0.281638	0.718036	0.716633	0.519465
31	584_fri_c4_500_25	Linear	0.281899	0.714623	0.713502	0.513447
32	586_fri_c3_1000_25	Linear	0.279202	0.705495	0.718378	0.509394
33	588_fri_c4_1000_100	Linear	0.267338	0.708425	0.738718	0.46675
34	589_fri_c2_1000_25	Linear	0.276266	0.707726	0.712125	0.528804
35	590_fri_c0_1000_50	Linear	0.699727	0.413517	0.290709	0.83999
36	591_fri_c1_100_10	Linear	0.178503	0.785305	0.799211	0.465915
37	592_fri_c4_1000_25	Linear	0.246001	0.727384	0.748549	0.445209
38	593_fri_c1_1000_10	Linear	0.287045	0.712731	0.712397	0.541301
39	594_fri_c2_100_5	Linear	0.041581	0.76735	0.901306	0.366065
40	595_fri_c0_1000_10	Linear	0.704631	0.420814	0.294328	0.837616
41	596_fri_c2_250_5	Linear	0.277518	0.688422	0.685956	0.540818
42	597_fri_c2_500_5	Linear	0.276542	0.70663	0.720696	0.528983
43	598_fri_c0_1000_25	Linear	0.703118	0.4217	0.293105	0.834738
44	599_fri_c2_1000_5	Linear	0.28865	0.712516	0.710183	0.545248
45	601_fri_c1_250_5	Linear	0.289959	0.682671	0.662813	0.530686
46	602_fri_c3_250_10	Linear	0.180244	0.742043	0.779903	0.40493
47	603_fri_c0_250_50	Linear	0.712692	0.407259	0.274058	0.841514
48	604_fri_c4_500_10	Linear	0.248273	0.728724	0.744357	0.480085
49	605_fri_c2_250_25	Linear	0.24698	0.717057	0.736453	0.513876
50	606_fri_c2_1000_10	Linear	0.308385	0.690089	0.680073	0.557761
51	607_fri_c4_1000_50	Linear	0.220702	0.714655	0.758194	0.458222
52	608_fri_c3_1000_10	Linear	0.278023	0.707177	0.706622	0.475936
53	609_fri_c0_1000_5	Linear	0.728649	0.408021	0.276379	0.853735
54	611_fri_c3_100_5	Linear	0.194105	0.703612	0.689233	0.559348

	Dataset Name	Algorithm	R^2 Mean \uparrow	MAE \downarrow	MSE \downarrow	Spearman coeff. \uparrow
55	612_fri.c1_1000_5	Linear	0.229149	0.728327	0.735948	0.470516
56	613_fri.c3_250_5	Linear	0.263946	0.724662	0.746828	0.505514
57	615_fri.c4_250_10	Linear	0.276361	0.708448	0.71733	0.471958
58	616_fri.c4_500_50	Linear	0.205509	0.728739	0.788715	0.453025
59	617_fri.c3_500_5	Linear	0.216635	0.735879	0.76765	0.449461
60	618_fri.c3_1000_50	Linear	0.265698	0.69623	0.7071	0.472572
61	620_fri.c1_1000_25	Linear	0.250131	0.738213	0.757734	0.478474
62	621_fri.c0_100_10	Linear	0.602227	0.44443	0.341376	0.774586
63	622_fri.c2_1000_50	Linear	0.263696	0.715922	0.729433	0.507265
64	623_fri.c4_1000_10	Linear	0.267106	0.710196	0.709202	0.452199
65	624_fri.c0_100_5	Linear	0.603562	0.462771	0.321688	0.771278
66	626_fri.c2_500_50	Linear	0.217673	0.728059	0.777863	0.472951
67	627_fri.c2_500_10	Linear	0.243343	0.694881	0.702719	0.532132
68	628_fri.c3_1000_5	Linear	0.266377	0.7262	0.731738	0.472058
69	631_fri.c1_500_5	Linear	0.241078	0.733383	0.74539	0.469951
70	633_fri.c0_500_25	Linear	0.690121	0.432924	0.302853	0.828156
71	634_fri.c2_100_10	Linear	0.299368	0.636631	0.675419	0.605714
72	635_fri.c0_250_10	Linear	0.603044	0.476327	0.356965	0.774646
73	637_fri.c1_500_50	Linear	0.217729	0.739307	0.775907	0.463339
74	641_fri.c1_500_10	Linear	0.258236	0.729422	0.743619	0.532342
75	643_fri.c2_500_25	Linear	0.147409	0.755978	0.850757	0.386658
76	644_fri.c4_250_25	Linear	0.184237	0.725411	0.784909	0.448349
77	645_fri.c3_500_50	Linear	0.235281	0.69956	0.744604	0.461882
78	646_fri.c3_500_10	Linear	0.311535	0.690855	0.674736	0.474915
79	647_fri.c1_250_10	Linear	0.258723	0.7324	0.721684	0.523531
80	648_fri.c1_250_50	Linear	0.309327	0.717734	0.685753	0.570247
81	649_fri.c0_500_5	Linear	0.722406	0.390243	0.275346	0.846715
82	650_fri.c0_500_50	Linear	0.745277	0.389934	0.252129	0.862324
83	651_fri.c0_100_25	Linear	0.565772	0.554044	0.460616	0.784511
84	653_fri.c0_250_25	Linear	0.700389	0.41904	0.287578	0.822729
85	654_fri.c0_500_10	Linear	0.676016	0.43907	0.31314	0.829225
86	656_fri.c1_100_5	Linear	0.144937	0.704332	0.691867	0.486115
87	657_fri.c2_250_10	Linear	0.19816	0.719233	0.771387	0.515301
88	658_fri.c3_250_25	Linear	0.1306	0.755051	0.86765	0.41002
89	663_rabe_266	Linear	0.968315	6.917994	81.304113	0.98143
90	665_sleuth_case2002	Linear	0.292627	5.592663	59.912708	0.426888
91	666_rmftsa.ladata	Linear	0.526431	1.38051	3.611345	0.633792
92	678_visualizing_environmental	Linear	0.309626	2.215614	8.264205	0.596919
93	687_sleuth_ex1605	Linear	0.445392	8.476614	106.578743	0.691451
94	690_visualizing_galaxy	Linear	0.897886	25.120121	922.100554	0.96885
95	695_chatfield.4	Linear	0.858441	12.031508	291.075407	0.935352
96	712_chscase_geyser1	Linear	0.758773	4.990649	38.312636	0.759
97	feynman_III_12_43	Linear	0.93145	0.159014	0.044833	0.983169
98	feynman_III_15_12	Linear	0.233931	3.736997	20.107373	0.423118
99	feynman_III_15_14	Linear	0.508537	0.007291	0.000148	0.975434
100	feynman_III_15_27	Linear	0.724087	0.910702	1.967749	0.979986
101	feynman_III_17_37	Linear	0.139988	3.57535	21.677414	0.376456
102	feynman_III_7_38	Linear	0.786887	11.464593	275.623411	0.979451
103	feynman_III_8_54	Linear	0.014734	0.314506	0.12296	0.111697
104	feynman_II_10_9	Linear	0.781668	0.07861	0.013397	0.982423
105	feynman_II_11_28	Linear	0.818812	0.093008	0.015337	0.95077
106	feynman_II_13_23	Linear	0.994665	0.057811	0.007887	0.998096
107	feynman_II_13_34	Linear	0.962289	0.299731	0.167243	0.991382
108	feynman_II_15_4	Linear	0.212968	3.567289	21.483525	0.428445

	Dataset Name	Algorithm	R^2	Mean \uparrow	MAE \downarrow	MSE \downarrow	Spearman coeff. \uparrow
109	feynman.II_15_5	Linear	0.210697	3.561805	21.58674	0.430193	
110	feynman.II_24_17	Linear	0.970472	0.118832	0.021962	0.997035	
111	feynman.II_27_16	Linear	0.802556	29.222483	1581.939504	0.983116	
112	feynman.II_27_18	Linear	0.878876	6.927826	79.418532	0.988165	
113	feynman.II_34_2	Linear	0.866166	2.617153	12.578403	0.981266	
114	feynman.II_34_29a	Linear	0.786954	0.072809	0.011172	0.979481	
115	feynman.II_34_2a	Linear	0.784677	0.146543	0.045263	0.979331	
116	feynman.II_37_1	Linear	0.886671	5.839289	62.60404	0.983136	
117	feynman.II_38_14	Linear	0.912099	0.048427	0.003988	0.989152	
118	feynman.II_3_24	Linear	0.637401	0.02403	0.001155	0.988254	
119	feynman.II_4_23	Linear	0.725582	0.01138	0.000309	0.979904	
120	feynman.II_8_31	Linear	0.879779	3.471949	19.902419	0.9882	
121	feynman.II_8_7	Linear	0.685304	0.032074	0.002524	0.97742	
122	feynman.I_10_7	Linear	0.994747	0.057704	0.007724	0.998101	
123	feynman.I_12_1	Linear	0.93089	0.999035	1.7756	0.983305	
124	feynman.I_12_4	Linear	0.556217	0.011239	0.000322	0.984439	
125	feynman.I_12_5	Linear	0.930938	0.998005	1.776479	0.983035	
126	feynman.I_14_3	Linear	0.865788	5.214275	50.142761	0.98086	
127	feynman.I_14_4	Linear	0.8794	3.437868	19.629161	0.987973	
128	feynman.I_15_10	Linear	0.961738	0.301978	0.170416	0.991385	
129	feynman.I_16_6	Linear	0.889599	0.286332	0.143153	0.944657	
130	feynman.I_18_12	Linear	0.505163	4.022895	27.178362	0.74989	
131	feynman.I_25_13	Linear	0.827937	0.242161	0.105885	0.983643	
132	feynman.I_26_2	Linear	0.68287	0.215662	0.079607	0.881601	
133	feynman.I_27_6	Linear	0.879933	0.089215	0.015361	0.971672	
134	feynman.I_29_4	Linear	0.688935	0.514013	0.545926	0.967886	
135	feynman.I_30_3	Linear	0.207866	1.646033	5.267315	0.398884	
136	feynman.I_30_5	Linear	0.788509	0.03806	0.003043	0.989051	
137	feynman.I_34_1	Linear	0.931204	0.309854	0.218704	0.986952	
138	feynman.I_34_14	Linear	0.966801	0.202536	0.08714	0.992547	
139	feynman.I_34_27	Linear	0.931503	0.158808	0.044902	0.983234	
140	feynman.I_37_4	Linear	0.13927	2.24074	7.086374	0.283763	
141	feynman.I_39_1	Linear	0.931472	1.499868	3.9914	0.983478	
142	feynman.I_39_11	Linear	0.822776	0.899057	1.655431	0.98159	
143	feynman.I_43_31	Linear	0.866215	5.246956	50.412573	0.981239	
144	feynman.I_47_23	Linear	0.916652	0.14283	0.037889	0.981369	
145	feynman.I_48_2	Linear	0.897016	25.196579	1063.490439	0.989542	
146	feynman.I_6_2	Linear	0.758179	0.016475	0.00044	0.918804	
147	feynman.I_6_2b	Linear	0.658535	0.022427	0.001232	0.846275	
148	nikuradse.1	Linear	0.638503	0.083324	0.009218	0.910944	
149	strogatz.bacres1	Linear	0.988248	0.216058	0.06944	0.856053	
150	strogatz.bacres2	Linear	0.984511	0.216704	0.06989	0.993564	
151	strogatz.barmag1	Linear	0.834231	0.034753	0.009313	0.944294	
152	strogatz.barmag2	Linear	0.04003	0.150235	0.067818	0.335486	
153	strogatz.glider1	Linear	0.108586	0.669491	0.542974	0.32942	
154	strogatz.glider2	Linear	0.687994	0.359401	0.264734	0.747661	
155	strogatz.lv1	Linear	-5.097275	0.700792	5.861402	-0.445025	
156	strogatz.lv2	Linear	0.11747	0.186607	0.1198	0.602734	
157	strogatz.predprey1	Linear	0.329958	1.0811	4.190106	0.719844	
158	strogatz.predprey2	Linear	0.898527	0.290779	0.234859	0.968529	
159	strogatz.shearflow1	Linear	0.071259	0.251107	0.256582	0.231905	
160	strogatz.shearflow2	Linear	0.220299	0.125655	0.041106	0.615767	
161	strogatz.vdp1	Linear	0.039449	0.775422	2.897968	0.654878	
162	strogatz.vdp2	Linear	0.999999	0.000078	0.0	1	

	Dataset Name	Algorithm	R^2 Mean \uparrow	MAE \downarrow	MSE \downarrow	Spearman coeff. \uparrow
1	1027_ESL	NeuralNet	0.852823	0.410395	2.893702e-01	0.937654
2	1028_SWD	NeuralNet	0.366961	0.506931	4.093295e-01	0.617072
3	1029_LEV	NeuralNet	0.545263	0.484831	4.109138e-01	0.742203
4	1030_ERA	NeuralNet	0.365520	1.244535	2.433973e+00	0.568572
5	1089_USCrime	NeuralNet	0.740107	15.647898	3.739526e+02	0.804915
6	1096_FacultySalaries	NeuralNet	0.784680	1.450788	3.476780e+00	0.883562
7	1199_BNG_echoMonths	NeuralNet	0.442570	9.068394	1.392056e+02	0.631720
8	192_vineyard	NeuralNet	0.600099	1.991144	6.537614e+00	0.726718
9	197_cpu_act	NeuralNet	0.975503	2.025710	8.246882e+00	0.954770
10	210_cloud	NeuralNet	0.747172	0.329699	2.759520e-01	0.888264
11	225_puma8NH	NeuralNet	0.662979	2.507061	1.071329e+01	0.810947
12	227_cpu_small	NeuralNet	0.968858	2.311537	1.036657e+01	0.938835
13	228_elusage	NeuralNet	0.784584	8.330419	1.142678e+02	0.810997
14	229_pwLinear	NeuralNet	0.798872	1.529199	3.789153e+00	0.898095
15	294_satellite_image	NeuralNet	0.902530	0.374750	4.760028e-01	0.951210
16	4544_GeographicalOriginalofMusic	NeuralNet	0.690027	0.408876	3.214000e-01	0.827174
17	503_wind	NeuralNet	0.795892	2.320634	9.126839e+00	0.892835
18	505_tecator	NeuralNet	0.918205	2.942551	1.807219e+01	0.945851
19	519_vinnie	NeuralNet	0.734397	1.232201	2.396868e+00	0.854593
20	522_pm10	NeuralNet	0.235241	0.599024	5.889134e-01	0.514193
21	523_analcatdata.neavote	NeuralNet	0.914215	0.796473	1.220032e+00	0.850378
22	529_pollen	NeuralNet	0.783172	1.153324	2.117322e+00	0.874001
23	547_no2	NeuralNet	0.542080	0.399243	2.557379e-01	0.730360
24	560_bodyfat	NeuralNet	0.961306	1.117585	2.658125e+00	0.981898
25	562_cpu_small	NeuralNet	0.969328	2.303671	1.022009e+01	0.938424
26	573_cpu_act	NeuralNet	0.976396	1.977254	7.861949e+00	0.954865
27	579_fri_c0_250_5	NeuralNet	0.858902	0.284880	1.311714e-01	0.925673
28	581_fri_c3_500_25	NeuralNet	0.215711	0.702565	7.842227e-01	0.490247
29	582_fri_c1_500_25	NeuralNet	0.140094	0.735744	8.611706e-01	0.469505
30	583_fri_c1_1000_50	NeuralNet	0.129949	0.748683	8.678001e-01	0.435474
31	584_fri_c4_500_25	NeuralNet	0.260464	0.672682	7.394183e-01	0.519414
32	586_fri_c3_1000_25	NeuralNet	0.594551	0.468461	4.028868e-01	0.764326
33	588_fri_c4_1000_100	NeuralNet	0.151236	0.740214	8.556538e-01	0.374383
34	589_fri_c2_1000_25	NeuralNet	0.492925	0.539173	4.984187e-01	0.707398
35	590_fri_c0_1000_50	NeuralNet	0.649386	0.456280	3.401131e-01	0.805546
36	591_fri_c1_100_10	NeuralNet	-0.020986	0.782549	1.005607e+00	0.401704
37	592_fri_c4_1000_25	NeuralNet	0.562524	0.494321	4.340235e-01	0.742200
38	593_fri_c1_1000_10	NeuralNet	0.873999	0.257171	1.261005e-01	0.930841
39	594_fri_c2_100_5	NeuralNet	0.383327	0.569770	6.085111e-01	0.667519
40	595_fri_c0_1000_10	NeuralNet	0.906380	0.243312	9.331033e-02	0.953951
41	596_fri_c2_250_5	NeuralNet	0.646729	0.427951	3.347499e-01	0.817476
42	597_fri_c2_500_5	NeuralNet	0.863733	0.274547	1.379375e-01	0.928026
43	598_fri_c0_1000_25	NeuralNet	0.819596	0.335204	1.778779e-01	0.904785
44	599_fri_c2_1000_5	NeuralNet	0.921722	0.205985	7.961486e-02	0.956788
45	601_fri_c1_250_5	NeuralNet	0.697394	0.390633	2.808596e-01	0.854169
46	602_fri_c3_250_10	NeuralNet	0.471516	0.542086	5.032179e-01	0.667044
47	603_fri_c0_250_50	NeuralNet	0.548627	0.519214	4.271940e-01	0.751120
48	604_fri_c4_500_10	NeuralNet	0.774700	0.342309	2.168632e-01	0.871671
49	605_fri_c2_250_25	NeuralNet	0.243484	0.693581	7.410648e-01	0.488701
50	606_fri_c2_1000_10	NeuralNet	0.875064	0.259213	1.219226e-01	0.934479
51	607_fri_c4_1000_50	NeuralNet	0.103459	0.743767	8.717138e-01	0.393737
52	608_fri_c3_1000_10	NeuralNet	0.892355	0.234260	1.056955e-01	0.941152
53	609_fri_c0_1000_5	NeuralNet	0.936046	0.201667	6.523782e-02	0.968197
54	611_fri_c3_100_5	NeuralNet	0.578785	0.474465	3.541383e-01	0.744211

	Dataset Name	Algorithm	R^2	Mean \uparrow	MAE \downarrow	MSE \downarrow	Spearman coeff. \uparrow
55	612_fri_c1_1000_5	NeuralNet	0.901813	0.232382	9.276487e-02	0.951857	
56	613_fri_c3_250_5	NeuralNet	0.687361	0.412556	3.149878e-01	0.831824	
57	615_fri_c4_250_10	NeuralNet	0.497194	0.537168	4.991084e-01	0.693061	
58	616_fri_c4_500_50	NeuralNet	0.091603	0.764015	9.019947e-01	0.375784	
59	617_fri_c3_500_5	NeuralNet	0.769612	0.338511	2.308483e-01	0.885101	
60	618_fri_c3_1000_50	NeuralNet	0.198645	0.696363	7.710063e-01	0.445806	
61	620_fri_c1_1000_25	NeuralNet	0.242152	0.686101	7.655733e-01	0.523801	
62	621_fri_c0_100_10	NeuralNet	0.564102	0.461186	3.743486e-01	0.780952	
63	622_fri_c2_1000_50	NeuralNet	0.152152	0.733028	8.396476e-01	0.436914	
64	623_fri_c4_1000_10	NeuralNet	0.840967	0.283853	1.582716e-01	0.912371	
65	624_fri_c0_100_5	NeuralNet	0.786115	0.338335	1.760822e-01	0.881955	
66	626_fri_c2_500_50	NeuralNet	0.071821	0.768397	9.230840e-01	0.395946	
67	627_fri_c2_500_10	NeuralNet	0.638732	0.419177	3.381697e-01	0.810315	
68	628_fri_c3_1000_5	NeuralNet	0.905089	0.227557	9.340655e-02	0.949961	
69	631_fri_c1_500_5	NeuralNet	0.7711559	0.351438	2.325012e-01	0.886770	
70	633_fri_c0_500_25	NeuralNet	0.690277	0.429273	3.037191e-01	0.832301	
71	634_fri_c2_100_10	NeuralNet	0.329548	0.613479	6.359580e-01	0.580100	
72	635_fri_c0_250_10	NeuralNet	0.781054	0.349538	1.974406e-01	0.881223	
73	637_fri_c1_500_50	NeuralNet	0.050588	0.788616	9.418987e-01	0.358172	
74	641_fri_c1_500_10	NeuralNet	0.734171	0.380561	2.662472e-01	0.863063	
75	643_fri_c2_500_25	NeuralNet	-0.047030	0.803269	1.042054e+00	0.334503	
76	644_fri_c4_250_25	NeuralNet	-0.098817	0.811740	1.055398e+00	0.307765	
77	645_fri_c3_500_50	NeuralNet	0.119247	0.736821	8.586971e-01	0.380650	
78	646_fri_c3_500_10	NeuralNet	0.750305	0.363450	2.430099e-01	0.846999	
79	647_fri_c1_250_10	NeuralNet	0.306954	0.633942	6.688702e-01	0.557775	
80	648_fri_c1_250_50	NeuralNet	0.211333	0.728166	7.866983e-01	0.493093	
81	649_fri_c0_500_5	NeuralNet	0.911711	0.232881	8.730737e-02	0.956813	
82	650_fri_c0_500_50	NeuralNet	0.664720	0.451717	3.326932e-01	0.818101	
83	651_fri_c0_100_25	NeuralNet	0.547258	0.555754	4.817018e-01	0.733383	
84	653_fri_c0_250_25	NeuralNet	0.620513	0.473479	3.620537e-01	0.789404	
85	654_fri_c0_500_10	NeuralNet	0.858299	0.296183	1.380846e-01	0.931270	
86	656_fri_c1_100_5	NeuralNet	0.426208	0.526906	4.847716e-01	0.728221	
87	657_fri_c2_250_10	NeuralNet	0.379947	0.587696	5.957274e-01	0.641508	
88	658_fri_c3_250_25	NeuralNet	0.039462	0.762112	9.574166e-01	0.388744	
89	663_rabe_266	NeuralNet	0.975598	5.949144	6.214602e+01	0.991636	
90	665_sleuth_case2002	NeuralNet	0.137285	6.182009	7.395436e+01	0.352857	
91	666_rmftsa_ladata	NeuralNet	0.600076	1.276154	2.988638e+00	0.613317	
92	678_visualizing_environmental	NeuralNet	0.300701	2.304259	8.481555e+00	0.545703	
93	687_sleuth_ex1605	NeuralNet	0.499403	7.711171	9.685532e+01	0.719613	
94	690_visualizing_galaxy	NeuralNet	0.949464	16.315438	4.578051e+02	0.976084	
95	695_chatfield_4	NeuralNet	0.823126	13.605473	3.618121e+02	0.924415	
96	712_chscase_geyser1	NeuralNet	0.758728	4.979575	3.836666e+01	0.746288	
97	feynman_III_12_43	NeuralNet	0.999754	0.009627	1.609622e-04	0.999973	
98	feynman_III_15_12	NeuralNet	0.994964	0.257667	1.323041e-01	0.996570	
99	feynman_III_15_14	NeuralNet	0.997831	0.000405	6.528335e-07	0.999321	
100	feynman_III_15_27	NeuralNet	0.998860	0.058674	8.163461e-03	0.999868	
101	feynman_III_17_37	NeuralNet	0.998990	0.113484	2.548044e-02	0.999682	
102	feynman_III_7_38	NeuralNet	0.999198	0.659432	1.038934e+00	0.999906	
103	feynman_III_8_54	NeuralNet	0.973600	0.027549	3.294157e-03	0.985185	
104	feynman_II_10_9	NeuralNet	0.999302	0.004321	4.284257e-05	0.999918	
105	feynman_II_11_28	NeuralNet	0.999608	0.004045	3.319564e-05	0.999887	
106	feynman_II_13_23	NeuralNet	0.999734	0.015028	3.925164e-04	0.999982	
107	feynman_II_13_34	NeuralNet	0.999698	0.026780	1.341865e-03	0.999974	
108	feynman_II_15_4	NeuralNet	0.999088	0.115679	2.489679e-02	0.999704	

	Dataset Name	Algorithm	R^2	Mean \uparrow	MAE \downarrow	MSE \downarrow	Spearman coeff. \uparrow
109	feynman.II_15_5	NeuralNet	0.999063	0.117654	2.562177e-02	0.999707	
110	feynman.II_24_17	NeuralNet	0.999730	0.010473	2.008074e-04	0.999984	
111	feynman.II_27_16	NeuralNet	0.999488	1.392176	4.111538e+00	0.999896	
112	feynman.II_27_18	NeuralNet	0.999613	0.360378	2.543454e-01	0.999967	
113	feynman.II_34_2	NeuralNet	0.999546	0.147771	4.276658e-02	0.999939	
114	feynman.II_34_29a	NeuralNet	0.999319	0.003836	3.560954e-05	0.999918	
115	feynman.II_34_2a	NeuralNet	0.999368	0.008007	1.326014e-04	0.999930	
116	feynman.II_37_1	NeuralNet	0.999598	0.338736	2.221163e-01	0.999941	
117	feynman.II_38_14	NeuralNet	0.999705	0.002604	1.338456e-05	0.999974	
118	feynman.II_3_24	NeuralNet	0.999165	0.000894	2.658922e-06	0.999905	
119	feynman.II_4_23	NeuralNet	0.998947	0.000658	1.181480e-06	0.999882	
120	feynman.II_8_31	NeuralNet	0.999722	0.165760	4.603600e-02	0.999971	
121	feynman.II_8_7	NeuralNet	0.998873	0.001809	9.074480e-06	0.999819	
122	feynman.I_10_7	NeuralNet	0.999815	0.012788	2.725433e-04	0.999984	
123	feynman.I_12_1	NeuralNet	0.999730	0.060529	6.957336e-03	0.999961	
124	feynman.I_12_4	NeuralNet	0.998552	0.000566	1.052145e-06	0.999400	
125	feynman.I_12_5	NeuralNet	0.999754	0.059734	6.328985e-03	0.999961	
126	feynman.I_14_3	NeuralNet	0.999627	0.270023	1.399226e-01	0.999927	
127	feynman.I_14_4	NeuralNet	0.999756	0.148655	3.972920e-02	0.999971	
128	feynman.I_15_10	NeuralNet	0.999703	0.027272	1.321566e-03	0.999974	
129	feynman.I_16_6	NeuralNet	0.999708	0.015255	3.794285e-04	0.999960	
130	feynman.I_18_12	NeuralNet	0.999239	0.151583	4.176557e-02	0.999755	
131	feynman.I_25_13	NeuralNet	0.999491	0.011609	3.132732e-04	0.999956	
132	feynman.I_26_2	NeuralNet	0.999546	0.007840	1.140345e-04	0.999932	
133	feynman.I_27_6	NeuralNet	0.999589	0.005413	5.256776e-05	0.999935	
134	feynman.I_29_4	NeuralNet	0.999101	0.024454	1.573681e-03	0.999931	
135	feynman.I_30_3	NeuralNet	0.995185	0.119984	3.204372e-02	0.995882	
136	feynman.I_30_5	NeuralNet	0.999058	0.002344	1.356262e-05	0.999919	
137	feynman.I_34_1	NeuralNet	0.999599	0.025631	1.276745e-03	0.999964	
138	feynman.I_34_14	NeuralNet	0.999574	0.025699	1.120748e-03	0.999979	
139	feynman.I_34_27	NeuralNet	0.999768	0.009631	1.522168e-04	0.999972	
140	feynman.I_37_4	NeuralNet	0.999066	0.065067	7.688136e-03	0.999745	
141	feynman.I_39_1	NeuralNet	0.999704	0.099840	1.730699e-02	0.999972	
142	feynman.I_39_11	NeuralNet	0.999561	0.045397	4.087927e-03	0.999941	
143	feynman.I_43_31	NeuralNet	0.999625	0.277835	1.415122e-01	0.999930	
144	feynman.I_47_23	NeuralNet	0.999516	0.010906	2.208181e-04	0.999953	
145	feynman.I_48_2	NeuralNet	0.999736	1.187750	2.731035e+00	0.999964	
146	feynman.I_6_2	NeuralNet	0.999627	0.000603	6.789286e-07	0.999945	
147	feynman.I_6_2b	NeuralNet	0.999403	0.001030	2.152602e-06	0.999781	
148	nikuradse.1	NeuralNet	0.917551	0.035698	2.117774e-03	0.975503	
149	strogatz.bacres1	NeuralNet	0.969642	0.252176	1.666494e-01	0.913027	
150	strogatz.bacres2	NeuralNet	0.974906	0.241574	1.112301e-01	0.993503	
151	strogatz.barmag1	NeuralNet	0.902097	0.036250	5.435290e-03	0.940557	
152	strogatz.barmag2	NeuralNet	0.680461	0.084798	1.988241e-02	0.643502	
153	strogatz.glider1	NeuralNet	0.118384	0.662337	5.375853e-01	0.306711	
154	strogatz.glider2	NeuralNet	0.797370	0.283208	1.690502e-01	0.765416	
155	strogatz.lv1	NeuralNet	0.439642	0.570618	5.150794e+00	0.163208	
156	strogatz.lv2	NeuralNet	0.607377	0.160983	2.700868e-01	0.694346	
157	strogatz.predprey1	NeuralNet	0.804045	0.589049	1.026594e+00	0.908491	
158	strogatz.predprey2	NeuralNet	0.948876	0.243723	1.185541e-01	0.983712	
159	strogatz.shearflow1	NeuralNet	0.467181	0.211420	1.315940e-01	0.444693	
160	strogatz.shearflow2	NeuralNet	0.462558	0.111373	2.764929e-02	0.729255	
161	strogatz.vdp1	NeuralNet	0.752528	0.523250	7.033177e-01	0.675935	
162	strogatz.vdp2	NeuralNet	0.980716	0.008563	1.598424e-04	0.992766	

	Dataset Name	Algorithm	R^2 Mean \uparrow	MAE \downarrow	MSE \downarrow	Spearman coeff. \uparrow
1	1027_ESL	RF	0.828191	0.401064	0.337169	0.926962
2	1028_SWD	RF	0.351163	0.509689	0.419149	0.603557
3	1029_LEV	RF	0.513733	0.494058	0.439321	0.721755
4	1030_ERA	RF	0.344498	1.263994	2.511468	0.551032
5	1089_USCrime	RF	0.787284	14.124231	307.610681	0.825673
6	1096_FacultySalaries	RF	0.646406	1.674051	5.056379	0.86207
7	1199_LNG_echoMonths	RF	0.466759	8.845958	133.148714	0.658935
8	192_vineyard	RF	0.436878	2.431581	9.063079	0.677302
9	197_cpu_act	RF	0.98191	1.698497	5.986437	0.960177
10	210_cloud	RF	0.749484	0.309371	0.26005	0.909837
11	225_puma8NH	RF	0.665886	2.50206	10.62004	0.810112
12	227_cpu_small	RF	0.975433	1.976695	8.121429	0.947948
13	228_elusage	RF	0.738112	8.737147	144.746379	0.792774
14	229_pwLinear	RF	0.836583	1.346275	3.055031	0.913973
15	294_satellite_image	RF	0.901088	0.356574	0.482946	0.948016
16	4544_GeographicalOriginalofMusic	RF	0.709701	0.391354	0.299695	0.832358
17	503_wind	RF	0.782594	2.380768	9.724192	0.886184
18	505_tecator	RF	0.988714	1.058452	2.278102	0.985042
19	519_vinnie	RF	0.65268	1.386581	3.146539	0.819722
20	522_pm10	RF	0.38052	0.536843	0.476258	0.635714
21	523_analcatdata_neavote	RF	0.946035	0.584734	0.773968	0.859502
22	529_pollen	RF	0.753629	1.222244	2.407963	0.859562
23	547_no2	RF	0.590758	0.372885	0.227522	0.737098
24	560_bodyfat	RF	0.967986	0.437872	2.131262	0.989025
25	562_cpu_small	RF	0.975361	1.978607	8.143903	0.947786
26	573_cpu_act	RF	0.98196	1.698095	5.969805	0.960181
27	579_fri_c0_250_5	RF	0.747678	0.384239	0.233941	0.870979
28	581_fri_c3_500_25	RF	0.864109	0.289336	0.135995	0.926033
29	582_fri_c1_500_25	RF	0.825411	0.323105	0.174802	0.910122
30	583_fri_c1_1000_50	RF	0.862768	0.284879	0.136845	0.926156
31	584_fri_c4_500_25	RF	0.846209	0.302163	0.152214	0.909411
32	586_fri_c3_1000_25	RF	0.892224	0.251459	0.107145	0.940938
33	588_fri_c4_1000_100	RF	0.876883	0.274382	0.124012	0.923148
34	589_fri_c2_1000_25	RF	0.875381	0.274231	0.122588	0.932206
35	590_fri_c0_1000_50	RF	0.770152	0.376476	0.22257	0.879496
36	591_fri_c1_100_10	RF	0.688072	0.424705	0.307654	0.831629
37	592_fri_c4_1000_25	RF	0.886852	0.258927	0.111977	0.934837
38	593_fri_c1_1000_10	RF	0.904628	0.242149	0.095112	0.944207
39	594_fri_c2_100_5	RF	0.653107	0.431547	0.323924	0.785614
40	595_fri_c0_1000_10	RF	0.825544	0.328153	0.173882	0.910602
41	596_fri_c2_250_5	RF	0.835352	0.310415	0.156812	0.902047
42	597_fri_c2_500_5	RF	0.894523	0.249443	0.104584	0.93249
43	598_fri_c0_1000_25	RF	0.810615	0.343871	0.187126	0.90705
44	599_fri_c2_1000_5	RF	0.92493	0.208877	0.074809	0.951968
45	601_fri_c1_250_5	RF	0.855096	0.2867	0.135888	0.916325
46	602_fri_c3_250_10	RF	0.795581	0.329389	0.19609	0.901573
47	603_fri_c0_250_50	RF	0.659874	0.449403	0.323374	0.833863
48	604_fri_c4_500_10	RF	0.882066	0.260423	0.116341	0.930626
49	605_fri_c2_250_25	RF	0.725294	0.403836	0.266039	0.850122
50	606_fri_c2_1000_10	RF	0.900382	0.244165	0.097612	0.942411
51	607_fri_c4_1000_50	RF	0.880011	0.263028	0.116614	0.931114
52	608_fri_c3_1000_10	RF	0.903813	0.233693	0.093653	0.946613
53	609_fri_c0_1000_5	RF	0.868003	0.290612	0.134467	0.933037
54	611_fri_c3_100_5	RF	0.714641	0.402382	0.24842	0.841404

	Dataset Name	Algorithm	R^2 Mean \uparrow	MAE \downarrow	MSE \downarrow	Spearman coeff. \uparrow
55	612_fri.c1_1000_5	RF	0.922967	0.208122	0.073467	0.958037
56	613_fri.c3_250_5	RF	0.849498	0.301571	0.152947	0.906948
57	615_fri.c4_250_10	RF	0.76537	0.36884	0.235968	0.871497
58	616_fri.c4_500_50	RF	0.835236	0.309777	0.16219	0.90138
59	617_fri.c3_500_5	RF	0.879998	0.255318	0.117882	0.933057
60	618_fri.c3_1000_50	RF	0.883478	0.264537	0.112224	0.923763
61	620_fri.c1_1000_25	RF	0.874473	0.282563	0.126939	0.931109
62	621_fri.c0_100_10	RF	0.569101	0.473485	0.378732	0.776792
63	622_fri.c2_1000_50	RF	0.874072	0.278149	0.124303	0.922776
64	623_fri.c4_1000_10	RF	0.897811	0.237144	0.098251	0.936852
65	624_fri.c0_100_5	RF	0.704611	0.393722	0.245705	0.847368
66	626_fri.c2_500_50	RF	0.823008	0.321812	0.175854	0.903049
67	627_fri.c2_500_10	RF	0.872773	0.259418	0.117884	0.925824
68	628_fri.c3_1000_5	RF	0.923906	0.212655	0.075839	0.955071
69	631_fri.c1_500_5	RF	0.866227	0.275814	0.131199	0.92734
70	633_fri.c0_500_25	RF	0.765071	0.386825	0.229933	0.875553
71	634_fri.c2_100_10	RF	0.638825	0.458935	0.335267	0.770125
72	635_fri.c0_250_10	RF	0.703241	0.413184	0.266993	0.838454
73	637_fri.c1_500_50	RF	0.797855	0.345077	0.19983	0.890665
74	641_fri.c1_500_10	RF	0.885827	0.265389	0.114417	0.939647
75	643_fri.c2_500_25	RF	0.828081	0.3241	0.170461	0.895178
76	644_fri.c4_250_25	RF	0.729438	0.386083	0.26263	0.869125
77	645_fri.c3_500_50	RF	0.828978	0.314482	0.165812	0.892874
78	646_fri.c3_500_10	RF	0.880021	0.266839	0.116977	0.926986
79	647_fri.c1_250_10	RF	0.811044	0.331034	0.185019	0.881623
80	648_fri.c1_250_50	RF	0.751043	0.383354	0.247733	0.861605
81	649_fri.c0_500_5	RF	0.82724	0.317792	0.171945	0.911659
82	650_fri.c0_500_50	RF	0.739479	0.404096	0.257992	0.870969
83	651_fri.c0_100_25	RF	0.474601	0.620371	0.56962	0.741504
84	653_fri.c0_250_25	RF	0.691073	0.435891	0.297447	0.840384
85	654_fri.c0_500_10	RF	0.787069	0.355176	0.207396	0.892637
86	656_fri.c1_100_5	RF	0.622067	0.420105	0.29974	0.826065
87	657_fri.c2_250_10	RF	0.841526	0.296253	0.150434	0.88202
88	658_fri.c3_250_25	RF	0.716241	0.411146	0.28833	0.851425
89	663_rabe_266	RF	0.988249	3.699082	29.70961	0.990613
90	665_sleuth_case2002	RF	0.21152	5.729268	66.67892	0.393441
91	666_rmftsa.ladata	RF	0.534759	1.339757	3.505726	0.620323
92	678_visualizing_environmental	RF	0.167423	2.409752	9.850855	0.519201
93	687_sleuth_ex1605	RF	0.478443	7.47383	97.048396	0.713633
94	690_visualizing_galaxy	RF	0.972833	10.963723	244.234181	0.980709
95	695_chatfield.4	RF	0.822858	13.143151	367.921677	0.928416
96	712_chscase_geyser1	RF	0.681945	5.679489	50.057784	0.715691
97	feynman_III_12_43	RF	0.999994	0.001455	0.000004	0.999997
98	feynman_III_15_12	RF	0.996401	0.218054	0.094469	0.997972
99	feynman_III_15_14	RF	0.998693	0.000186	0.0	0.999891
100	feynman_III_15_27	RF	0.999309	0.032186	0.004928	0.999866
101	feynman_III_17_37	RF	0.99973	0.056548	0.006815	0.999917
102	feynman_III_7_38	RF	0.999573	0.409599	0.552861	0.999868
103	feynman_III_8_54	RF	0.965408	0.039261	0.004317	0.97834
104	feynman_II_10_9	RF	0.999448	0.002955	0.000034	0.999874
105	feynman_II_11_28	RF	0.999992	0.000481	0.000001	0.999997
106	feynman_II_13_23	RF	0.999951	0.004556	0.000073	0.99998
107	feynman_II_13_34	RF	0.999861	0.015029	0.000616	0.999954
108	feynman_II_15_4	RF	0.999696	0.062073	0.008304	0.999894

	Dataset Name	Algorithm	R^2 Mean \uparrow	MAE \downarrow	MSE \downarrow	Spearman coeff. \uparrow
109	feynman.II_15_5	RF	0.999697	0.062022	0.00828	0.999894
110	feynman.II_24_17	RF	0.999885	0.006752	0.000086	0.999944
111	feynman.II_27_16	RF	0.9971	0.891547	2.322599	0.999906
112	feynman.II_27_18	RF	0.999992	0.044954	0.005057	0.999997
113	feynman.II_34_2	RF	0.999737	0.104984	0.024754	0.999887
114	feynman.II_34_29a	RF	0.999531	0.002667	0.000025	0.999868
115	feynman.II_34_2a	RF	0.999604	0.005112	0.000083	0.999869
116	feynman.II_37_1	RF	0.999754	0.250366	0.135856	0.999893
117	feynman.II_38_14	RF	0.999991	0.000411	0.0	0.999996
118	feynman.II_3_24	RF	0.999981	0.000101	0.0	0.999997
119	feynman.II_4_23	RF	0.999287	0.000406	0.000001	0.999869
120	feynman.II_8_31	RF	0.999993	0.02147	0.001142	0.999997
121	feynman.II_8_7	RF	0.999148	0.001033	0.000007	0.999891
122	feynman.I_10_7	RF	0.99995	0.00454	0.000073	0.999981
123	feynman.I_12_1	RF	0.999994	0.009182	0.000162	0.999997
124	feynman.I_12_4	RF	0.999006	0.000286	0.000001	0.999896
125	feynman.I_12_5	RF	0.999994	0.009267	0.000166	0.999997
126	feynman.I_14_3	RF	0.999739	0.209379	0.097592	0.999884
127	feynman.I_14_4	RF	0.999993	0.02161	0.001161	0.999997
128	feynman.I_15_10	RF	0.999872	0.01471	0.000571	0.999957
129	feynman.I_16_6	RF	0.999897	0.007634	0.000133	0.999946
130	feynman.I_18_12	RF	0.9998	0.073355	0.010974	0.999927
131	feynman.I_25_13	RF	0.999987	0.001564	0.000008	0.999996
132	feynman.I_26_2	RF	0.999993	0.00082	0.000002	0.999998
133	feynman.I_27_6	RF	0.999747	0.003801	0.000032	0.999894
134	feynman.I_29_4	RF	0.999979	0.00267	0.000038	0.999995
135	feynman.I_30_3	RF	0.997875	0.07419	0.014129	0.998623
136	feynman.I_30_5	RF	0.999473	0.001381	0.000008	0.999891
137	feynman.I_34_1	RF	0.999739	0.015217	0.000829	0.999932
138	feynman.I_34_14	RF	0.999841	0.012027	0.000418	0.99995
139	feynman.I_34_27	RF	0.999993	0.001505	0.000004	0.999997
140	feynman.I_37_4	RF	0.999741	0.030484	0.002131	0.999903
141	feynman.I_39_1	RF	0.999993	0.014017	0.000382	0.999997
142	feynman.I_39_11	RF	0.999621	0.034505	0.003542	0.999879
143	feynman.I_43_31	RF	0.999744	0.209035	0.096614	0.999887
144	feynman.I_47_23	RF	0.999705	0.007894	0.000134	0.999871
145	feynman.I_48_2	RF	0.999949	0.5204	0.529267	0.999975
146	feynman.I_6_2	RF	0.99999	0.000082	0.0	0.999996
147	feynman.I_6_2b	RF	0.999608	0.000729	0.000001	0.999819
148	nikuradse.1	RF	0.998261	0.004636	0.000043	0.990062
149	strogatz_bacres1	RF	0.99768	0.051648	0.014431	0.971473
150	strogatz_bacres2	RF	0.993031	0.050096	0.031067	0.99526
151	strogatz_barmag1	RF	0.959565	0.01236	0.00262	0.995512
152	strogatz_barmag2	RF	0.990584	0.009236	0.000698	0.991259
153	strogatz_glider1	RF	0.971766	0.088604	0.017235	0.986356
154	strogatz_glider2	RF	0.950929	0.114753	0.043182	0.969765
155	strogatz_lv1	RF	0.600604	0.217083	8.024616	0.993335
156	strogatz_lv2	RF	0.596278	0.089651	0.526566	0.971766
157	strogatz_predprey1	RF	0.926847	0.148677	0.806437	0.989732
158	strogatz_predprey2	RF	0.984844	0.08214	0.036595	0.993528
159	strogatz_shearflow1	RF	0.954483	0.026438	0.012076	0.992629
160	strogatz_shearflow2	RF	0.978411	0.010467	0.00115	0.995866
161	strogatz_vdp1	RF	0.877137	0.162954	0.317669	0.937715
162	strogatz_vdp2	RF	0.999721	0.000652	0.000002	0.999759

	Dataset Name	Algorithm	R^2 Mean \uparrow	MAE \downarrow	MSE \downarrow	Spearman coeff. \uparrow
1	1027_ESL	LGBM	0.844445	0.413833	0.305865	0.931222
2	1028_SWD	LGBM	0.359984	0.506554	0.413474	0.609287
3	1029_LEV	LGBM	0.524891	0.490583	0.429172	0.728595
4	1030_ERA	LGBM	0.346505	1.262428	2.504109	0.552466
5	1089_USCrime	LGBM	-0.160501	36.23973	1727.36776	NaN
6	1096_FacultySalaries	LGBM	-0.103898	3.356827	20.915339	0.760385
7	1199_BNG_echoMonths	LGBM	0.476546	8.791663	130.713328	0.666369
8	192_vineyard	LGBM	-0.063398	3.319048	19.168705	0.715896
9	197_cpu_act	LGBM	0.98535	1.555198	4.839184	0.966604
10	210_cloud	LGBM	0.607391	0.401731	0.409442	0.873838
11	225_puma8NH	LGBM	0.667638	2.499582	10.564509	0.810515
12	227_cpu_small	LGBM	0.979111	1.856602	6.902363	0.954275
13	228_elusage	LGBM	0.536545	10.575459	245.965478	0.658258
14	229_pwLinear	LGBM	0.849223	1.3139	2.845389	0.923151
15	294_satellite_image	LGBM	0.901703	0.366712	0.479844	0.947657
16	4544_GeographicalOriginalofMusic	LGBM	0.725209	0.382052	0.281681	0.84111
17	503_wind	LGBM	0.794789	2.322967	9.178021	0.891768
18	505_tecator	LGBM	0.980731	1.27209	4.103341	0.987641
19	519_vinnie	LGBM	0.703883	1.31389	2.669673	0.839341
20	522_pm10	LGBM	0.452875	0.509969	0.419688	0.684123
21	523_analcatdata_neavote	LGBM	0.913691	0.620019	1.24188	0.870881
22	529_pollen	LGBM	0.7574	1.215903	2.369972	0.862246
23	547_no2	LGBM	0.589485	0.373971	0.228427	0.753452
24	560_bodyfat	LGBM	0.95801	0.896907	2.929498	0.988279
25	562_cpu_small	LGBM	0.979111	1.856602	6.902363	0.954275
26	573_cpu_act	LGBM	0.98535	1.555198	4.839184	0.966604
27	579_fri_c0_250_5	LGBM	0.817921	0.310909	0.168316	0.899617
28	581_fri_c3_500_25	LGBM	0.895226	0.245636	0.104176	0.93901
29	582_fri_c1_500_25	LGBM	0.889654	0.254534	0.110448	0.941618
30	583_fri_c1_1000_50	LGBM	0.919194	0.21828	0.080416	0.956086
31	584_fri_c4_500_25	LGBM	0.879668	0.256692	0.118972	0.929843
32	586_fri_c3_1000_25	LGBM	0.929915	0.200981	0.069801	0.959121
33	588_fri_c4_1000_100	LGBM	0.911337	0.223146	0.089196	0.945709
34	589_fri_c2_1000_25	LGBM	0.918465	0.219992	0.080058	0.956587
35	590_fri_c0_1000_50	LGBM	0.874126	0.277299	0.121789	0.932544
36	591_fri_c1_100_10	LGBM	0.472097	0.570042	0.512804	0.684612
37	592_fri_c4_1000_25	LGBM	0.917119	0.215887	0.081934	0.951337
38	593_fri_c1_1000_10	LGBM	0.937294	0.190624	0.062492	0.962283
39	594_fri_c2_100_5	LGBM	0.486797	0.518448	0.468199	0.732305
40	595_fri_c0_1000_10	LGBM	0.893363	0.255197	0.106264	0.943872
41	596_fri_c2_250_5	LGBM	0.849539	0.284548	0.142847	0.908598
42	597_fri_c2_500_5	LGBM	0.925056	0.207562	0.074506	0.948969
43	598_fri_c0_1000_25	LGBM	0.899637	0.24992	0.099142	0.9502
44	599_fri_c2_1000_5	LGBM	0.943596	0.179893	0.056196	0.962465
45	601_fri_c1_250_5	LGBM	0.885572	0.246478	0.106492	0.933273
46	602_fri_c3_250_10	LGBM	0.796471	0.306398	0.194118	0.908101
47	603_fri_c0_250_50	LGBM	0.805041	0.338462	0.185065	0.903421
48	604_fri_c4_500_10	LGBM	0.911491	0.224825	0.087365	0.943372
49	605_fri_c2_250_25	LGBM	0.801806	0.329571	0.193584	0.889578
50	606_fri_c2_1000_10	LGBM	0.933535	0.196463	0.0653	0.959411
51	607_fri_c4_1000_50	LGBM	0.915084	0.213321	0.082569	0.950092
52	608_fri_c3_1000_10	LGBM	0.923461	0.201144	0.074706	0.958283
53	609_fri_c0_1000_5	LGBM	0.919816	0.225162	0.081722	0.957937
54	611_fri_c3_100_5	LGBM	0.608191	0.465827	0.340244	0.739156

	Dataset Name	Algorithm	R^2 Mean \uparrow	MAE \downarrow	MSE \downarrow	Spearman coeff. \uparrow
55	612_fri.c1_1000_5	LGBM	0.943877	0.178135	0.053381	0.969261
56	613_fri.c3_250_5	LGBM	0.854812	0.281067	0.147232	0.91031
57	615_fri.c4_250_10	LGBM	0.815332	0.309522	0.188706	0.895958
58	616_fri.c4_500_50	LGBM	0.856199	0.277982	0.140655	0.908752
59	617_fri.c3_500_5	LGBM	0.895849	0.225265	0.102203	0.944819
60	618_fri.c3_1000_50	LGBM	0.915046	0.217885	0.081729	0.942882
61	620_fri.c1_1000_25	LGBM	0.928287	0.209569	0.072189	0.959867
62	621_fri.c0_100_10	LGBM	0.725334	0.374063	0.235699	0.849173
63	622_fri.c2_1000_50	LGBM	0.915263	0.222149	0.08352	0.946356
64	623_fri.c4_1000_10	LGBM	0.9176	0.206872	0.079421	0.946893
65	624_fri.c0_100_5	LGBM	0.663385	0.414732	0.279963	0.807866
66	626_fri.c2_500_50	LGBM	0.881852	0.262801	0.116937	0.927061
67	627_fri.c2_500_10	LGBM	0.895066	0.229627	0.097222	0.937239
68	628_fri.c3_1000_5	LGBM	0.939786	0.185646	0.060039	0.96369
69	631_fri.c1_500_5	LGBM	0.894575	0.235954	0.103217	0.94264
70	633_fri.c0_500_25	LGBM	0.867758	0.28009	0.128961	0.928568
71	634_fri.c2_100_10	LGBM	0.554713	0.489593	0.412479	0.755689
72	635_fri.c0_250_10	LGBM	0.808018	0.325511	0.173748	0.888413
73	637_fri.c1_500_50	LGBM	0.88029	0.262	0.117988	0.935986
74	641_fri.c1_500_10	LGBM	0.920707	0.21553	0.079372	0.957008
75	643_fri.c2_500_25	LGBM	0.886997	0.256788	0.111016	0.929579
76	644_fri.c4_250_25	LGBM	0.763602	0.343271	0.229947	0.88179
77	645_fri.c3_500_50	LGBM	0.861184	0.269186	0.134287	0.910007
78	646_fri.c3_500_10	LGBM	0.895953	0.229111	0.101617	0.938216
79	647_fri.c1_250_10	LGBM	0.871382	0.272282	0.12434	0.920986
80	648_fri.c1_250_50	LGBM	0.826962	0.309924	0.169927	0.896567
81	649_fri.c0_500_5	LGBM	0.894272	0.251709	0.104998	0.946873
82	650_fri.c0_500_50	LGBM	0.847083	0.302548	0.150672	0.923984
83	651_fri.c0_100_25	LGBM	0.553901	0.551767	0.477772	0.769774
84	653_fri.c0_250_25	LGBM	0.790537	0.34996	0.201084	0.879091
85	654_fri.c0_500_10	LGBM	0.871514	0.272861	0.125055	0.934404
86	656_fri.c1_100_5	LGBM	0.523393	0.464672	0.378993	0.794858
87	657_fri.c2_250_10	LGBM	0.864705	0.273345	0.126912	0.894812
88	658_fri.c3_250_25	LGBM	0.768969	0.348552	0.235693	0.872487
89	663_rabe_266	LGBM	0.951179	8.545605	128.061611	0.970164
90	665_sleuth_case2002	LGBM	0.158356	6.037853	70.656119	0.396523
91	666_rmftsa.ladata	LGBM	0.427431	1.453889	4.351936	0.561823
92	678_visualizing_environmental	LGBM	0.192604	2.398792	9.545897	0.512608
93	687_sleuth_ex1605	LGBM	0.149332	10.431353	171.115995	0.501394
94	690_visualizing_galaxy	LGBM	0.970978	12.036517	261.18156	0.980453
95	695_chatfield.4	LGBM	0.816784	13.612425	379.114996	0.91925
96	712_chscase_geyser1	LGBM	0.719652	5.295068	44.129887	0.724247
97	feynman_III_12_43	LGBM	0.999807	0.008734	0.000126	0.999884
98	feynman_III_15_12	LGBM	0.943683	0.877025	1.478416	0.966702
99	feynman_III_15_14	LGBM	0.998361	0.000355	0.0	0.998577
100	feynman_III_15_27	LGBM	0.99867	0.063433	0.009479	0.999169
101	feynman_III_17_37	LGBM	0.998974	0.123542	0.025872	0.999485
102	feynman_III_7_38	LGBM	0.998856	0.857281	1.47939	0.999199
103	feynman_III_8_54	LGBM	0.55409	0.186592	0.055649	0.787142
104	feynman_II_10_9	LGBM	0.998836	0.005788	0.000071	0.999288
105	feynman_II_11_28	LGBM	0.99982	0.002903	0.000015	0.999845
106	feynman_II_13_23	LGBM	0.999909	0.008282	0.000135	0.999959
107	feynman_II_13_34	LGBM	0.99967	0.0289	0.001463	0.999854
108	feynman_II_15_4	LGBM	0.999007	0.123948	0.027096	0.99948

	Dataset Name	Algorithm	R^2 Mean \uparrow	MAE \downarrow	MSE \downarrow	Spearman coeff. \uparrow
109	feynman.II_15_5	LGBM	0.998989	0.125219	0.027641	0.999477
110	feynman.II_24_17	LGBM	0.999691	0.011978	0.00023	0.999832
111	feynman.II_27_16	LGBM	0.999096	1.917405	7.245248	0.999355
112	feynman.II_27_18	LGBM	0.999833	0.246181	0.109237	0.999893
113	feynman.II_34_2	LGBM	0.998982	0.234243	0.095705	0.999271
114	feynman.II_34_29a	LGBM	0.998847	0.005464	0.00006	0.999204
115	feynman.II_34_2a	LGBM	0.998851	0.010951	0.000242	0.999194
116	feynman.II_37_1	LGBM	0.999066	0.546615	0.515954	0.999381
117	feynman.II_38_14	LGBM	0.999788	0.002343	0.00001	0.999883
118	feynman.II_3_24	LGBM	0.999771	0.000514	0.000001	0.999797
119	feynman.II_4_23	LGBM	0.998652	0.0008	0.000002	0.999158
120	feynman.II_8_31	LGBM	0.999833	0.124132	0.027658	0.999891
121	feynman.II_8_7	LGBM	0.99865	0.001993	0.000011	0.999217
122	feynman.I_10_7	LGBM	0.999906	0.008359	0.000138	0.999958
123	feynman.I_12_1	LGBM	0.999805	0.054983	0.005011	0.999884
124	feynman.I_12_4	LGBM	0.998701	0.000526	0.000001	0.998989
125	feynman.I_12_5	LGBM	0.999803	0.055327	0.005072	0.999883
126	feynman.I_14_3	LGBM	0.99897	0.468719	0.384822	0.999263
127	feynman.I_14_4	LGBM	0.99983	0.123958	0.027743	0.999889
128	feynman.I_15_10	LGBM	0.999675	0.028835	0.00145	0.999852
129	feynman.I_16_6	LGBM	0.99934	0.021985	0.000856	0.999655
130	feynman.I_18_12	LGBM	0.999291	0.150274	0.038946	0.99961
131	feynman.I_25_13	LGBM	0.999774	0.008472	0.000139	0.999854
132	feynman.I_26_2	LGBM	0.999856	0.004474	0.000036	0.999931
133	feynman.I_27_6	LGBM	0.999205	0.007532	0.000102	0.999539
134	feynman.I_29_4	LGBM	0.999725	0.013899	0.000482	0.999811
135	feynman.I_30_3	LGBM	0.970219	0.332563	0.197979	0.965192
136	feynman.I_30_5	LGBM	0.99902	0.00253	0.000014	0.999463
137	feynman.I_34_1	LGBM	0.999405	0.029987	0.00189	0.999756
138	feynman.I_34_14	LGBM	0.999609	0.022975	0.001025	0.999836
139	feynman.I_34_27	LGBM	0.999808	0.008736	0.000126	0.999886
140	feynman.I_37_4	LGBM	0.999146	0.06299	0.007028	0.999475
141	feynman.I_39_1	LGBM	0.999804	0.083128	0.011441	0.999882
142	feynman.I_39_11	LGBM	0.998859	0.074227	0.010657	0.999252
143	feynman.I_43_31	LGBM	0.998984	0.468055	0.382724	0.999274
144	feynman.I_47_23	LGBM	0.998968	0.016486	0.000469	0.999409
145	feynman.I_48_2	LGBM	0.999779	1.147807	2.279839	0.999849
146	feynman.I_6_2	LGBM	0.99978	0.000467	0.0	0.999882
147	feynman.I_6_2b	LGBM	0.997631	0.00187	0.000009	0.998732
148	nikuradse.1	LGBM	0.992314	0.008647	0.000192	0.984635
149	strogatz_bacres1	LGBM	0.978434	0.139073	0.138135	0.918411
150	strogatz_bacres2	LGBM	0.980091	0.086343	0.089204	0.985652
151	strogatz_barmag1	LGBM	0.945527	0.017393	0.003195	0.98347
152	strogatz_barmag2	LGBM	0.774422	0.034429	0.017593	0.930467
153	strogatz_glider1	LGBM	0.935193	0.132137	0.039287	0.962894
154	strogatz_glider2	LGBM	0.908837	0.1514	0.07748	0.939587
155	strogatz_lv1	LGBM	-2.331265	0.39982	8.297826	0.445691
156	strogatz_lv2	LGBM	-0.336276	0.170791	0.591586	0.795204
157	strogatz_predprey1	LGBM	0.711828	0.340823	2.44352	0.93433
158	strogatz_predprey2	LGBM	0.983054	0.096986	0.041181	0.991001
159	strogatz_shearflow1	LGBM	0.812026	0.085183	0.059188	0.909604
160	strogatz_shearflow2	LGBM	0.946065	0.023819	0.002921	0.978591
161	strogatz_vdp1	LGBM	0.759776	0.291957	0.62354	0.852349
162	strogatz_vdp2	LGBM	0.998405	0.001758	0.000013	0.999232

G. Detailed Results for Anomaly Detection

Our method Familiarity Conviction (FC) and Similarity conviction (SC) is compared with six other popular methods for carrying out anomaly detection. DeepSVDD was trained on 20 epochs with the inlier set of training data. Picking a conviction level of 0.7 for all datasets (without choosing it in a dataset specific manner), our method achieves the highest $F1$ scores in 12 of the 20 datasets.

Table 4. Information of the 20 ODDS dataset used for anomaly detection

Dataset	Dataset Size	% Anomalies
wine.mat	[129, 13]	7.70%
wbc.mat	[278, 30]	5.60%
vowels.mat	[456, 12]	3.40%
vertebral.mat	[240, 6]	12.50%
thyroid.mat	[3772, 6]	2.50%
speech.mat	[3686, 400]	1.65%
shuttle.mat	[49097, 9]	7%
satimage-2.mat	[5803, 36]	1.20%
satellite.mat	[6435, 36]	32%
pima.mat	[768, 8]	35%
optdigits.mat	[5216, 64]	3%
musk.mat	[3062, 166]	3.20%
mnist.mat	[7603, 100]	9.20%
lympho.mat	[148, 18]	4.10%
letter.mat	[1600, 32]	6.25%
ionosphere.mat	[351, 33]	36%
glass.mat	[214, 9]	4.20%
cardio.mat	[1831, 21]	9.60%
breastw.mat	[683, 9]	35%
arrhythmia.mat	[452, 274]	15 %

Table 5. F1 scores of Anomaly Detection on ODDS datasets.

(Blue values indicate the best performance; Brown values indicate the second-best performance)

Dataset	Ours (FC)	Ours (SC)	OCSVM	IForest	CBLOF	LOF	ECOD	DeepSVDD
wine	0.44	0.18	0.31	0.1	0.87	0.95	0.24	0.53
wbc	0.57	0.65	0.54	0.61	0.51	0.40	0.44	0.49
vowels	0.20	0.75	0.21	0.21	0.37	0.10	0.17	0.42
vertebral	0.28	0.19	0.05	0.04	0.04	0.00	0.14	0.05
thyroid	0.26	0.64	0.29	0.54	0.30	0.19	0.56	0.33
speech	0.06	0.10	0.02	0.00	0.03	0.00	0.06	0.06
shuttle	0.26	0.60	0.33	0.89	0.82	0.10	0.75	0.60
satimage-2	0.10	0.94	0.39	0.41	0.22	0.14	0.34	0.26
satellite	0.58	0.75	0.14	0.51	0.48	0.04	0.29	0.66
pima	0.52	0.01	0.12	0.29	0.25	0.06	0.22	0.52
optdigits	0.10	0.00	0.03	0.08	0.18	0.00	0.03	0.26
musk	0.22	0.78	0.14	0.71	0.48	0.00	0.20	0.48
mnist	0.34	0.24	0.19	0.39	0.34	0.01	0.20	0.43
lympho	0.35	0.73	0.38	0.36	0.29	0.00	0.09	0.26
letter	0.17	0.43	0.18	0.10	0.22	0.08	0.13	0.31
ionosphere	0.59	0.85	0.27	0.67	0.43	0.78	0.32	0.90
glass	0.20	0.14	0.13	0.14	0.13	0.30	0.19	0.30
cardio	0.35	0.51	0.24	0.44	0.54	0.10	0.48	0.61
breastw	0.33	0.86	0.17	0.90	0.42	0.09	0.32	0.94
arrhythmia	0.47	0.51	0.23	0.11	0.41	0.37	0.43	0.51